

ปฏิกิริยาไฮโดรจีเนชันของคาร์บอนไดออกไซด์บนตัวเร่งปฏิกิริยาโคบอลต์บนอะลูมินาที่ปรับปรุง  
ด้วยเบสออกไซด์



นางสาวพรวิ สมเกื้อ

จุฬาลงกรณ์มหาวิทยาลัย

CHULALONGKORN UNIVERSITY

วิทยานิพนธ์นี้เป็นส่วนหนึ่งของการศึกษาตามหลักสูตรปริญญาวิศวกรรมศาสตรมหาบัณฑิต

สาขาวิชาวิศวกรรมเคมี ภาควิชาวิศวกรรมเคมี

คณะวิศวกรรมศาสตร์ จุฬาลงกรณ์มหาวิทยาลัย

ปีการศึกษา 2556

ลิขสิทธิ์ของจุฬาลงกรณ์มหาวิทยาลัย

บทคัดย่อและแฟ้มข้อมูลฉบับเต็มของวิทยานิพนธ์ตั้งแต่ปีการศึกษา 2554 ที่ให้บริการในคลังปัญญาจุฬาฯ (CUIR)

เป็นแฟ้มข้อมูลของนิสิตเจ้าของวิทยานิพนธ์ ที่ส่งผ่านทางบัณฑิตวิทยาลัย

The abstract and full text of theses from the academic year 2011 in Chulalongkorn University Intellectual Repository (CUIR) are the thesis authors' files submitted through the University Graduate School.

CO<sub>2</sub> HYDROGENATION OVER BASIC OXIDE-MODIFIED Al<sub>2</sub>O<sub>3</sub> SUPPORTED COBALT  
CATALYSTS



Miss Pornrawee Somkua

จุฬาลงกรณ์มหาวิทยาลัย  
**CHULALONGKORN UNIVERSITY**

A Thesis Submitted in Partial Fulfillment of the Requirements  
for the Degree of Master of Engineering Program in Chemical Engineering

Department of Chemical Engineering

Faculty of Engineering

Chulalongkorn University

Academic Year 2013

Copyright of Chulalongkorn University

Thesis Title	CO <sub>2</sub> HYDROGENATION OVER BASIC OXIDE-MODIFIED Al <sub>2</sub> O <sub>3</sub> SUPPORTED COBALT CATALYSTS
By	Miss Pornrawee Somkua
Field of Study	Chemical Engineering
Thesis Advisor	Associate Professor Joongjai Panpranot, Ph.D.

---

Accepted by the Faculty of Engineering, Chulalongkorn University in Partial Fulfillment of the Requirements for the Master's Degree

.....Dean of the Faculty of Engineering  
(Professor Bundhit Euaarporn, Ph.D.)

#### THESIS COMMITTEE

.....Chairman  
(Associate Professor Bunjerd Jongsomjit, Ph.D.)

.....Thesis Advisor  
(Associate Professor Joongjai Panpranot, Ph.D.)

.....Examiner  
(Assistant Professor Suphot Phatanasri, D.Eng.)

.....External Examiner  
(Assistant Professor Okorn Mekasuwandamrong, D.Eng.)

พรรวี สมเกื้อ : ปฏิริยาไฮโดรจิเนชันของคาร์บอนไดออกไซด์บนตัวเร่งปฏิริยาโคบอลต์บนอะลูมินาที่ปรับปรุงด้วยเบสออกไซด์. (CO<sub>2</sub> HYDROGENATION OVER BASIC OXIDE-MODIFIED Al<sub>2</sub>O<sub>3</sub> SUPPORTED COBALT CATALYSTS) อ.ที่ปริกาษาวิธานิพนธ์หลัก: รศ. ดร. จุงใจ ปั้นประณต, 105 หน้า.

งานวิจัยนี้ศึกษาคุณลักษณะและสมบัติของตัวเร่งปฏิริยาโคบอลต์บนอะลูมินาที่ปรับปรุงด้วยเบสออกไซด์ชนิดต่างๆได้แก่ แมกนีเซียมออกไซด์ แคลเซียมออกไซด์ และแลนทานัมออกไซด์ โดยเตรียมอะลูมินาที่ได้รับการปรับปรุงโดยวิธีการเคลือบฝัง หลังจากนั้นจึงนำไปเคลือบฝังอีกครั้งด้วยโคบอลต์ จากการวิเคราะห์ด้วยเทคนิคการกระเจิงรังสีเอ็กซ์ การวัดพื้นที่ผิวโดนวิธีการดูดซับทางกายภาพด้วยไนโตรเจน การส่องด้วยกล้องจุลทรรศน์อิเล็กตรอนแบบส่องกราดและส่องผ่าน วิเคราะห์ความเป็นกรดบนพื้นที่ผิวของตัวเร่งปฏิริยาโดยวิธีการดูดซับของแอมโมเนีย การรีดักชันแบบโปรแกรมอุณหภูมิ การดูดซับด้วยแก๊สไฮโดรเจน พบว่าการปรับปรุงตัวรองรับอะลูมินาด้วยแมกนีเซียม-อะลูมิเนียม และแลนทานัมมีผลต่อการรีดักชันของตัวเร่งปฏิริยาโคบอลต์ การปรับปรุงตัวรองรับอะลูมินาด้วยแมกนีเซียม-อะลูมิเนียม และแลนทานัมสามารถยับยั้งอันตรกิริยาที่แข็งแรงระหว่างโลหะโคบอลต์และตัวรองรับอะลูมินา ทำให้อุณหภูมิในการรีดิวซ์ของตัวเร่งปฏิริยาโคบอลต์ต่ำลงและให้ค่าความว่องไวที่สูงกว่าในปฏิริยาไฮโดรจิเนชันของคาร์บอนไดออกไซด์ อย่างไรก็ตามการปรับปรุงตัวรองรับอะลูมินาด้วยแมกนีเซียมที่มากเกินไปด้วยการเผาที่อุณหภูมิสูงจะนำไปสู่การเกิดผลึกของแมกนีเซียมอะลูมิเนต ซึ่งจะส่งผลให้คุณสมบัติการรีดิวซ์ของตัวเร่งปฏิริยาโคบอลต์ลดต่ำลง และทำให้ค่าความว่องไวในปฏิริยาไฮโดรจิเนชันของคาร์บอนไดออกไซด์ลดต่ำลง



จุฬาลงกรณ์มหาวิทยาลัย  
CHULALONGKORN UNIVERSITY

ภาควิชา วิศวกรรมเคมี

ลายมือชื่อนิสิต .....

สาขาวิชา วิศวกรรมเคมี

ลายมือชื่อ อ.ที่ปริกาษาวิธานิพนธ์หลัก .....

ปีการศึกษา 2556

# # 5570306421 : MAJOR CHEMICAL ENGINEERING

KEYWORDS: ALUMINA SUPPORTED COBALT CATALYSTS / MAGNESIUM  
MODIFICATION / LANTHANUM MODIFICATION / CALCIUM MODIFICATION / CARBON  
DIOXIDE HYDROGENATION

PORNRAWEE SOMKUA: CO<sub>2</sub> HYDROGENATION OVER BASIC OXIDE-  
MODIFIED AL<sub>2</sub>O<sub>3</sub> SUPPORTED COBALT CATALYSTS. ADVISOR: ASSOC.  
PROF. JOONGJAI PANPRANOT, Ph.D., 105 pp.

Basic oxides including MgO, CaO and La<sub>2</sub>O<sub>3</sub> oxides were used to modify the properties of Al<sub>2</sub>O<sub>3</sub> supported cobalt catalysts (15 wt% Co) in this study. The catalysts were prepared by the incipient wetness impregnation method of cobalt precursor onto the alumina supports. The catalysts were characterized by several techniques including XRD, BET, SEM, TEM, NH<sub>3</sub>-TPD, H<sub>2</sub>-TPR and H<sub>2</sub>-chemisorption. It was found that the reduction behaviors of cobalt species on the alumina supports were altered by the basic oxide modification. The TPR results showed that the addition of MgAl and La promoters could suppress the strong interaction between cobalt metal and the alumina support leading to the improvement of reducibility of the cobalt catalysts hence higher catalytic activity in CO<sub>2</sub> hydrogenation were obtained. However, the addition of excessive amount of Mg with high calcination temperature of the magnesium modified alumina support brought about the formation of magnesium aluminate spinel (MgAl<sub>2</sub>O<sub>4</sub>), which resulted in lower reducibility and lower catalytic activity in the CO<sub>2</sub> hydrogenation.

จุฬาลงกรณ์มหาวิทยาลัย

CHULALONGKORN UNIVERSITY

Department: Chemical Engineering      Student's Signature .....

Field of Study: Chemical Engineering      Advisor's Signature .....

Academic Year: 2013

## ACKNOWLEDGEMENTS

The author would like to express her sincere gratitude and appreciation to her advisor, Associate Professor Joongjai Panpranot, for her invaluable suggestions, encouragement during her study, and useful discussion throughout this study. In addition, I would be also grateful to thank to Associate Professor Bunjerd Jongsomjit who has been the chairman of the committee for this thesis, and Assistant Professor Suphot Phatanasri, Assistant Professor Okorn Mekasuwandamrong, members of thesis committee for their kind cooperation.

Moreover, TEM equipment from Stimulus Package 2 (SP2) of Minister of Education under the theme of Green Engineering for Green Society is acknowledged.

Most of all, the author would like to express his highest gratitude to her parents who always pay attention to her all the times for their suggestions and have provided support and encouragements. The most success of graduation is devoted to her parents.

Finally, the author wishes to thank all my friends and members of the Center of Excellent on Catalysis & Catalytic Reaction Engineering, Department of Chemical Engineering, Chulalongkorn University for their assistance and friendly encouragement. To the others, not specifically named, who have provided her with support and encouragement, please be assured that she thinks of you.

## CONTENTS

	Page
THAI ABSTRACT .....	iv
ENGLISH ABSTRACT .....	v
ACKNOWLEDGEMENTS .....	vi
CONTENTS .....	vii
LIST OF TABLES .....	xi
LIST OF FIGURES .....	xiii
CHAPTER I INTRODUCTION .....	1
1.1 Rationale.....	1
1.2 Objective .....	3
1.3 Research Scopes .....	3
1.4 Research Methodology.....	4
CHAPTER II THEORY .....	5
2.1 Carbon dioxide hydrogenation reaction.....	5
2.2 Aluminium Oxides or Alumina (Al <sub>2</sub> O <sub>3</sub> ) .....	12
2.3 Cobalt.....	14
2.3.1 General.....	14
2.3.2 Physical properties .....	15
2.3.3 Cobalt oxides .....	16
2.3.4 Cobalt catalyst.....	19
CHAPTER III LITERATURE REVIEW.....	20
3.1 Effect of basic oxide including calcium oxide, lanthanum oxide and magnesium oxide modified support in various reaction .....	20
3.1.1 Effect of calcium oxide modified support.....	21
3.1.2 Effect of lanthanum oxide modified support .....	22
3.1.3 Effect of magnesium oxide modified support.....	23
3.2 Effect of addition of mixture solution magnesium nitrate and aluminium nitrate into the alumina support in various reaction .....	25

3.3 Effect of alumina supports on the properties of Co/Al <sub>2</sub> O <sub>3</sub> catalysts in carbon dioxide hydrogenation and carbon monoxide hydrogenation. ....	27
CHAPTER IV EXPERIMENTAL .....	29
4.1 Chemicals .....	29
4.2 Materials preparation.....	29
4.2.1 Preparation of MgAl-modified Al <sub>2</sub> O <sub>3</sub> on the supported Co/ Al <sub>2</sub> O <sub>3</sub> catalysts .....	29
4.2.2 Preparation of basic oxides (MgO, CaO, and La <sub>2</sub> O <sub>3</sub> ) modified Al <sub>2</sub> O <sub>3</sub> on the supported Co/ Al <sub>2</sub> O <sub>3</sub> catalysts. ....	30
4.3 Catalysts characterization.....	30
4.3.1 X-ray diffraction (XRD) .....	30
4.3.2 N <sub>2</sub> -physisorption.....	31
4.3.3 Hydrogen chemisorption. ....	32
4.3.4 Hydrogen temperature program reduction (H <sub>2</sub> -TPR).....	32
4.3.5 Temperature-programmed desorption (NH <sub>3</sub> -TPD) .....	33
4.3.6 Scanning Electron Microscopy (SEM) .....	33
4.3.7 Transmission Electron Microscopy (TEM).....	34
4.4 Reaction study in CO <sub>2</sub> hydrogenation.....	34
4.4.1 Material .....	34
4.4.2 Apparatus .....	35
4.4.3 Procedures .....	38
CHAPTER V RESULTS AND DISCUSSION .....	40
5.1 Effect of MgAl- modified Al <sub>2</sub> O <sub>3</sub> supported Co/Al <sub>2</sub> O <sub>3</sub> catalysts .....	41
5.1.1 Characterization of the catalysts .....	41
5.1.1.1 X-ray diffraction (XRD).....	41
5.1.1.2 BET surface areas .....	44
5.1.1.3 Scanning electron microscopy .....	44
5.1.1.4 Temperature Programmed Reduction (TPR).....	46



	Page
5.1.1.5 Temperature-programmed desorption (NH <sub>3</sub> -TPD).....	48
5.1.1.6 Hydrogen Chemisorption.....	50
5.1.2 Reaction study in CO <sub>2</sub> hydrogenation.....	51
5.2 Effect of basic oxide (MgO, CaO, and La <sub>2</sub> O <sub>3</sub> ) modified Al <sub>2</sub> O <sub>3</sub> supported Co/Al <sub>2</sub> O <sub>3</sub> catalysts using calcination temperatures of modified support at 900 °C .....	54
5.2.1 Characterization of the catalysts .....	54
5.2.1.1 X-ray diffraction (XRD).....	54
5.2.1.2 BET surface areas .....	57
5.2.1.3 Scanning electron microscopy.....	58
5.2.1.4 Temperature Programmed Reduction (TPR).....	60
5.2.1.5 Temperature-programmed desorption (NH <sub>3</sub> -TPD).....	62
5.2.1.6 Hydrogen Chemisorption.....	64
5.2.2 Reaction study in CO <sub>2</sub> hydrogenation.....	65
5.3 Effect of basic oxide (MgO, CaO, and La <sub>2</sub> O <sub>3</sub> ) modified Al <sub>2</sub> O <sub>3</sub> supported Co/Al <sub>2</sub> O <sub>3</sub> catalysts using calcination temperature of modified support at 550 °C.....	69
5.3.1 Characterization of the catalysts .....	69
5.3.1.1 X-ray diffraction (XRD).....	69
5.3.1.2 BET surface areas .....	72
5.3.1.3 Scanning electron microscopy.....	72
5.3.1.4 Temperature Programmed Reduction (TPR).....	74
5.3.1.5 Temperature-programmed desorption (NH <sub>3</sub> -TPD).....	76
5.2.1.6 Hydrogen Chemisorption.....	78
5.3.1.7 Transmission Electron Microscopy (TEM) .....	79
5.3.2 Reaction study in CO <sub>2</sub> hydrogenation.....	81
CHAPTER VI CONCLUSIONS AND RECOMMENDATIONS .....	85
6.1Conclusions .....	85
6.2Recommendations.....	86
REFERENCES .....	87

	Page
APPENDIX A CALCULATION FOR CATALYST PREPARATION.....	92
APPENDIX B CALCULATION OF THE CRYSTALLITE SIZE .....	97
APPENDIX C CALCULATION FOR TOTAL H <sub>2</sub> CHEMISSORPTION .....	100
APPENDIX D CALIBRATION CURVES .....	101
APPENDIX E CALCULATION OF CO <sub>2</sub> CONVERSION AND SELECTIVITY .....	104
VITA.....	105



จุฬาลงกรณ์มหาวิทยาลัย  
CHULALONGKORN UNIVERSITY

## LIST OF TABLES

	Page
Table 2.1 Physical properties of cobalt .....	17
Table 4.1 Operating condition for gas chromatograph.....	37
Table 5.1 Average Co <sub>3</sub> O <sub>4</sub> crystallite size of alumina supported cobalt catalysts after calcination at 650 °C and BET surface area of the support.....	44
Table 5.2 H <sub>2</sub> consumption for the TPR profile calculation of MgAl- modified alumina supported cobalt catalysts.....	48
Table 5.3 The acidity of MgAl- modified alumina supports .....	49
Table 5.4 The total H <sub>2</sub> chemisorption of MgAl- modified alumina supported cobalt catalysts .....	51
Table 5.5 The conversion and product selectivity during CO <sub>2</sub> hydrogenation on MgAl- modified alumina supported cobalt catalysts.....	54
Table 5.6 Average Co <sub>3</sub> O <sub>4</sub> crystallite size and BET surface area of the support .....	57
Table 5.7 H <sub>2</sub> consumption for the TPR profile calculation of basic oxide modified alumina supported cobalt catalysts .....	62
Table 5.8 The acidity of the non-modified and basic oxide modified alumina support after calcination at 900 °C .....	63
Table 5.9 The total H <sub>2</sub> chemisorption of basic oxide modified alumina supported cobalt catalysts (calcination temperatures of modified support at 900 °C) .....	65
Table 5.10 The conversion and product selectivity during CO <sub>2</sub> hydrogenation on basic oxide modified alumina supported cobalt catalysts.....	68
Table 5.11 Average Co <sub>3</sub> O <sub>4</sub> crystallite size and BET surface area of the support .....	71
Table 5.12 H <sub>2</sub> consumption for the TPR profile calculation of basic oxide modified alumina supported cobalt catalysts .....	76
Table 5.13 The acidity of the non-modified and basic oxide modified alumina support after calcination at 550 °C .....	78
Table 5.14 The total H <sub>2</sub> chemisorption of basic oxide modified alumina supported cobalt catalysts (calcination temperatures of modified support at 550 °C) .....	79

Table 5.15 The conversion and product selectivity during CO <sub>2</sub> hydrogenation on basic oxide modified alumina supported cobalt catalysts.....	84
Table D.1 Conditions used in shimadzu model GC-8A.....	102



## LIST OF FIGURES

	Page
Figure 2.1 Catalytic routes for carbon dioxide activation in heterogeneous phase leading to fuels and chemicals .....	7
Figure 2.2 Simplified pathways of carbon dioxide hydrogenation on supported metal catalysts .....	8
Figure 2.3 Thermal transformation of sequence of aluminum hydroxides .....	14
Figure 4.1 Flow diagram of carbon dioxide hydrogenation system.....	39
Figure 5.1 The XRD patterns of the non-modified and MgAl- modified alumina support.....	43
Figure 5.2 The XRD patterns of MgAl- modified alumina supported cobalt catalysts.	43
Figure 5.3 SEM images of MgAl- modified alumina supported cobalt catalysts.....	45
Figure 5.4 TPR profile of MgAl- modified alumina supported cobalt catalysts .....	47
Figure 5.5 NH <sub>3</sub> -TPD profile of MgAl- modified alumina supports .....	49
Figure 5.6 Performances of catalysts with the various modified support in CO <sub>2</sub> hydrogenation. ....	553
Figure 5.7 The XRD patterns of the non-modified and basic oxide modified alumina support after calcination at 900 °C .....	56
Figure 5.8 The XRD patterns of non-modified and basic oxide modified Co/Al <sub>2</sub> O <sub>3</sub> catalysts.....	56
Figure 5.9 SEM images of basic oxide modified alumina supported cobalt catalysts (calcination temperatures of modified support at 900 °C).....	59
Figure 5.10 TPR profile of basic oxide modified alumina supported cobalt catalysts (calcination temperatures of modified support at 900 °C).....	61
Figure 5.11 NH <sub>3</sub> -TPD profile of the non-modified and basic oxide modified alumina support after calcination at 900 °C .....	63
Figure 5.12 Performances of catalysts with the various modified support in CO <sub>2</sub> hydrogenation. ....	68
Figure 5.13 The XRD patterns of the non-modified and basic oxide modified alumina support after calcination at 550 °C .....	70

Figure 5.14 The XRD patterns of non-modified and basic oxide modified Co/Al <sub>2</sub> O <sub>3</sub> catalysts.....	71
Figure 5.15 The SEM images of basic oxide modified alumina supported cobalt catalysts (calcination temperatures of modified support at 550 °C).....	773
Figure 5.16 TPR profile of basic oxide modified alumina supported cobalt catalysts (calcination temperatures of modified support at 550 °C).....	75
Figure 5.17 NH <sub>3</sub> -TPD profile of the non-modified and basic oxide modified alumina support after calcination at 550 °C .....	77
Figure 5.18 The TEM images of basic oxide modified alumina supported cobalt catalysts .....	80
Figure 5.19 Performances of catalysts with the various modified support in CO <sub>2</sub> hydrogenation. ....	883
Figure B.1 The measured peak of Co/Al <sub>2</sub> O <sub>3</sub> to calculate the crystallite size.....	99
Figure B.2 The plot indicating the value of line broadening due to the equipment... ..	99
Figure D.1 The calibration curves of carbon dioxide.....	102
Figure D.2 The calibration curves of methane. ....	103
Figure D.3 The calibration curves of carbon monoxide. ....	103

# CHAPTER I

## INTRODUCTION

### 1.1 Rationale

Producing methane by CO<sub>2</sub> hydrogenation has been focused as a renewable energy source. CO<sub>2</sub> hydrogenation has received considerable research interest because it can diminish the effect of carbon dioxide emission into the atmosphere and it is an alternative route to produce methane gas from renewable sources. The most widely used catalysts for CO<sub>2</sub> hydrogenation are supported cobalt catalysts due to their unique properties such as high activity, high selectivity for linear hydrocarbons, and low activity for the water gas shift reaction [3, 6, 28].

The major part of published studies regarding this reaction is based on cobalt species on various supports including alumina, silica, titania, magnesia, carbon, and zeolites. Among various supports used for preparation of cobalt catalysts, alumina (Al<sub>2</sub>O<sub>3</sub>) is one of the most common crystalline materials [8, 28, 34], because of its favorable mechanical properties and adjustable surface properties such as high surface area, high purity, high melting temperature (above 2000 °C), good absorbent, high chemical stability and high catalytic activity [3]. However, cobalt supported on alumina support has a limited reducibility [28, 31] due to the interaction between metal oxide and alumina supports are stronger than other supports such as silica and titania [3]. It is well known that the strong interaction between cobalt and alumina support brings about the formation of inactive CoAl<sub>2</sub>O<sub>4</sub> species [34] and often results in the relatively low reducibility and low catalytic activity. Although, alumina support has various crystalline phases including chi( $\chi$ ), kappa( $\kappa$ ), eta( $\eta$ ), theta( $\theta$ ), delta( $\delta$ ), alpha( $\alpha$ ) and gamma( $\gamma$ )-phase [21, 33] but it is well known that the gamma( $\gamma$ )-alumina form is usually used as catalyst support. Furthermore, gamma ( $\gamma$ )-alumina is an exceptionally good selection for catalytic application due to the  $\gamma$ -Al<sub>2</sub>O<sub>3</sub> shows a high surface area and  $\gamma$ -Al<sub>2</sub>O<sub>3</sub> provides high dispersion of active metal [21].

In the past decades, many research groups studied the effect of addition of metal oxide promoters such as silica ( $\text{SiO}_2$ ), zirconia ( $\text{ZrO}_2$ ), manganese oxide ( $\text{MnO}_x$ ), zinc oxide ( $\text{ZnO}$ ), lanthanum oxide ( $\text{La}_2\text{O}_3$ ), calcium oxide ( $\text{CaO}$ ) and magnesium oxide ( $\text{MgO}$ ) on the properties of alumina supported catalysts [3, 8, 14, 17, 33]. They found that the addition of metal oxide promoter had significant effects on cobalt and/or nickel catalysts for various reactions including Fischer-Tropsch synthesis,  $\text{CO}_2$ -reforming of methane, methanol steam reforming. Addition of some metal oxide promoters could modify the support texture, suppress the formation of cobalt-supported compounds, and increase metal dispersion and reducibility [3].

In the present work, the effects of basic oxides ( $\text{MgO}$ ,  $\text{CaO}$ , and  $\text{La}_2\text{O}_3$ ) modified  $\text{Al}_2\text{O}_3$  on the supported  $\text{Co}/\text{Al}_2\text{O}_3$  catalysts were investigated in the  $\text{CO}_2$  hydrogenation. The catalysts were prepared by incipient wetness impregnation method and characterized by X-ray diffraction (XRD), scanning electron microscope (SEM), Brunauer-Emmett-Teller (BET) surface area analysis, hydrogen chemisorption, temperature programmed reduction of hydrogen ( $\text{H}_2$ -TPR) and temperature programmed desorption of ammonia ( $\text{NH}_3$ -TPD). The catalytic properties of basic oxides modified alumina supported cobalt catalysts were investigated in the  $\text{CO}_2$  hydrogenation under methanation conditions.



## 1.2 Objective

The objective of this research is to prepare and investigate the properties of basic oxide-modified alumina supported cobalt catalysts with various amount of magnesium and aluminium nitrate loading into  $\gamma$ - $\text{Al}_2\text{O}_3$  modified support and various basic oxides including lanthanum oxide ( $\text{La}_2\text{O}_3$ ), calcium oxide ( $\text{CaO}$ ) and magnesium oxide ( $\text{MgO}$ ) modified  $\text{Al}_2\text{O}_3$  on the supported  $\text{Co}/\text{Al}_2\text{O}_3$  catalysts .

## 1.3 Research Scopes

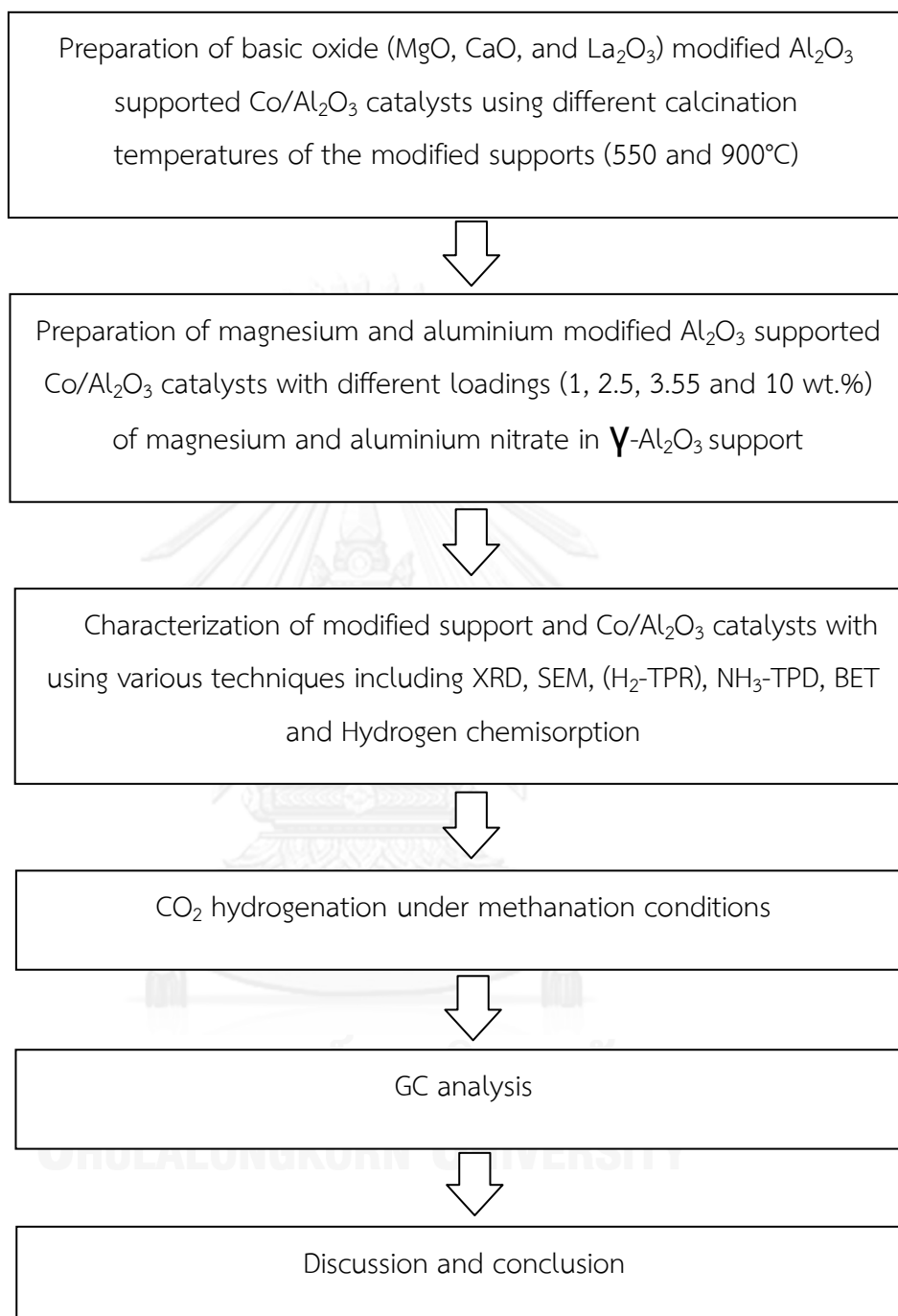
1.3.1 Preparation of basic oxide ( $\text{MgO}$ ,  $\text{CaO}$ , and  $\text{La}_2\text{O}_3$ ) modified  $\text{Al}_2\text{O}_3$  supported  $\text{Co}/\text{Al}_2\text{O}_3$  catalysts with various calcination temperatures of modified support (550 and 900 °C) and various amounts of magnesium and aluminium nitrate loading into  $\gamma$ - $\text{Al}_2\text{O}_3$  support.

1.3.2 Characterization of basic oxide ( $\text{MgO}$ ,  $\text{CaO}$ , and  $\text{La}_2\text{O}_3$ ) modified  $\text{Al}_2\text{O}_3$  support using X-ray diffraction (XRD), Brunauer-Emmett-Teller (BET) surface area analysis and temperature programmed desorption of ammonia ( $\text{NH}_3$ -TPD).

1.3.3 Characterization of  $\text{Co}/\text{Al}_2\text{O}_3$  catalysts with the various modified supported using X-ray diffraction (XRD), scanning electron microscope (SEM), hydrogen chemisorptions and temperature programmed reduction of hydrogen ( $\text{H}_2$ -TPR).

1.3.4 Investigation of catalytic activity of  $\text{Co}/\text{Al}_2\text{O}_3$  catalysts in the  $\text{CO}_2$  hydrogenation under methanation conditions at temperature 270 °C and pressure 1 atm and a feed gas  $\text{H}_2/\text{CO}_2$  ratio of 10/1.

## 1.4 Research Methodology



## CHAPTER II

### THEORY

#### 2.1 Carbon dioxide hydrogenation reaction

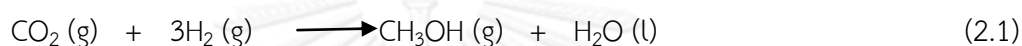
Due to an increasing rate of global energy demand bring about carbon dioxide emission into atmosphere, which was an important greenhouse gas and disadvantaging to the world and was exhausted gas. In addition, it is well known that the carbon dioxide emission into atmosphere is the cause of global warming, which was the cause of anthropogenic climate change in the world. Normally, in atmosphere have carbon dioxide around 0.038% result from human activities. For example, industrials revolution, transportation destruction of the rain forests and smoking even [2, 12, 18, 36].

The global warming cause by carbon dioxide emission into the atmosphere are of significant interest due to the burning of carbon-based fuels since the industrial revolution had been rapidly increased concentrations of atmospheric carbon dioxide. As the mention above, there are important sources of carbon dioxide emission into the atmosphere. Normally, the level of carbon dioxide into atmosphere was reduced by the natural such as algae, cyanobacteria and plant, which used for photosynthesize carbohydrate. However, photosynthesis cannot occur during darkness and at night some carbon dioxide is produced by plants during respiration. For this reason, carbon dioxide hydrogenation has received increasing research interest because it can diminish the effect of carbon dioxide emission into the atmosphere and it is an alternative route to produce methane gas from renewable sources [12, 24].

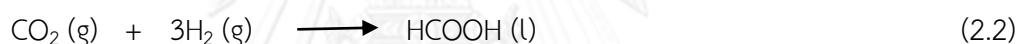
In recent years, the Fischer-Tropsch synthesis is known as carbon monoxide hydrogenation was attractively studied all over the world due to it is an important gas-to-liquids (GTL) technology [3], which hydrogenate carbon monoxide and hydrogen to liquid fuels. However, the production of fuels from carbon dioxide

hydrogenation has been attracting considerable attention as one of the applied technology for CO<sub>2</sub> capture and recycling.

Nowadays, there are many technologies involved in carbon dioxide capture and recycling of carbon dioxide. First of all, the catalytic synthesis of methanol from hydrogenation of carbon dioxide has been considerable an alternative, which produced methanol from carbon dioxide and hydrogen [13].



In addition, formic acid can produced by carbon dioxide hydrogenation reaction, which an important chemical with numerous application



Furthermore, the methane production from carbon dioxide reforming has been considered due to the simultaneous consumption of two major greenhouse gases.



In the past decades, the alternation of convert from carbon dioxide into the chemical products and fuels [13], which could be performed using the heterogeneous catalysts process were actively studied all over the world, which presented in Figure 2.1

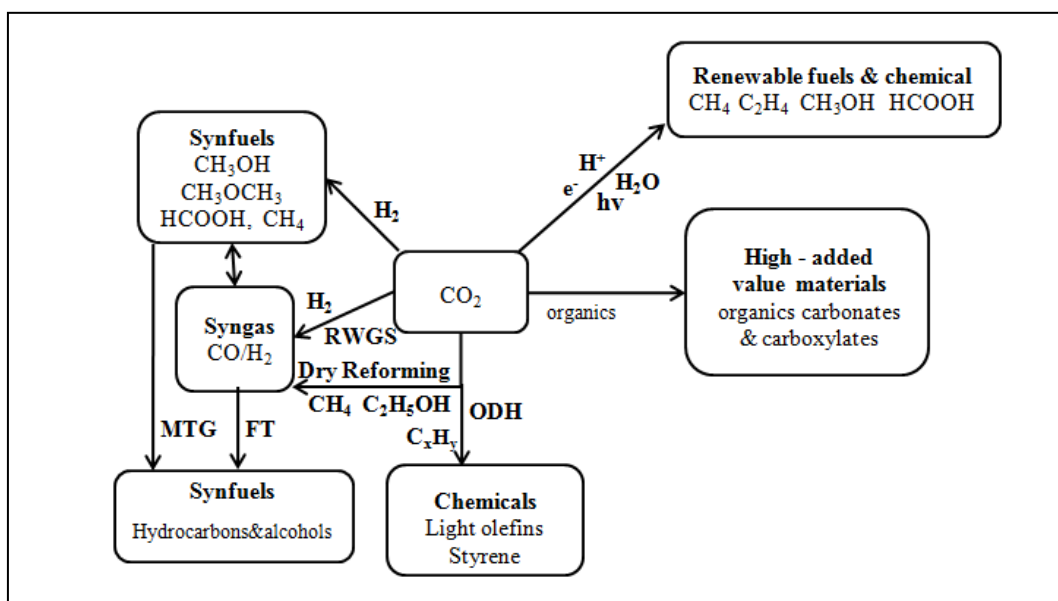


**Figure 2 1** Catalytic routes for carbon dioxide activation in heterogeneous phase leading to fuels and chemicals [13].

However, the most favored reaction in the series of  $\text{CO}_2$  hydrogenation reaction is the catalytic carbon dioxide hydrogenation to methane [13].



The convert carbon dioxide to methane need the transfer of eight electrons, which bring about significant kinetic restriction. The carbon dioxide hydrogenation reaction is highly exothermic [35] hence an important issue of carbon dioxide hydrogenation reactor is the removed of heat from reactor. Consequently, this process require the high-performance catalysts and adequate reactor in order to achieve gratifying rate and selectivity.

Application of carbon dioxide hydrogenation process under methanation condition consist of hydrogen purification from ammonia manufacture and can diminish or/and remove carbon dioxide from confined spaces. In addition, carbon

dioxide hydrogenation is an alternative route to produce methane gas, which was a way of recycling carbon dioxide in a natural gas power plant.

The widely used catalysts for carbon dioxide hydrogenation to methane are based on metals from group 8-10 species on various supports. The most of useful and studies systems regarding carbon dioxide methanation are supported nickel-based catalysts, cobalt-based catalysts and iron-based catalysts. The effects of the support on catalytic performance in carbon dioxide hydrogenation are an important topic for studied. At low temperatures, higher activities and stability were obtained over the noble metals such as Ru, Pd and Pt, which was better than that of the nickel-based catalysts. However, it has been reported that the various catalysts including iron (Fe), cobalt (Co) nickel (Ni) and group 8 metals shows the activity of the water-gas-shift reaction and carbon monoxide hydrogenation [35], indicating that the both reaction of carbon monoxide hydrogenation and carbon dioxide hydrogenation are using the same catalysts. However, the most widely used catalysts for carbon dioxide hydrogenation are supported cobalt catalysts due to their unique properties such as high activity, high selectivity for linear hydrocarbons, and low activity for the water gas shift reaction [13].

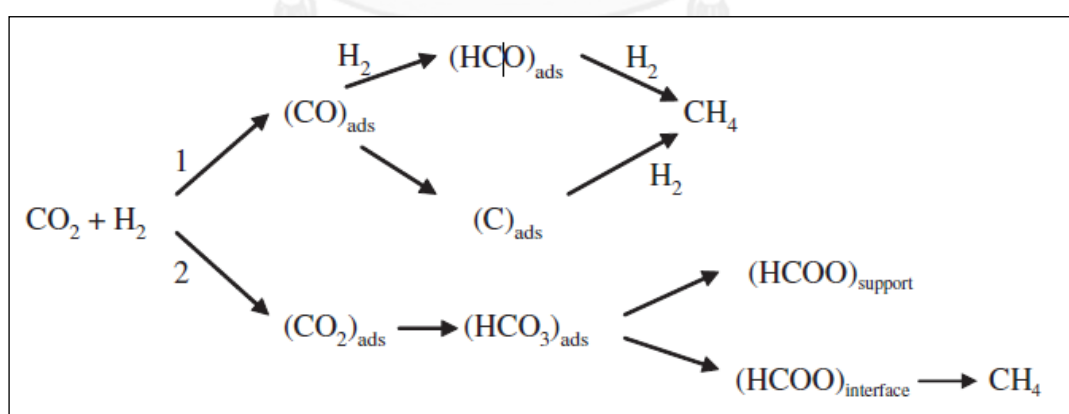


**Figure 2 2** Simplified pathways of carbon dioxide hydrogenation on supported metal catalysts [13].

Figure 2.2 shows the major mechanism of carbon dioxide hydrogenation under methanation conditions. There are two main mechanisms involved in methanation of carbon dioxide. First of all, carbon dioxide hydrogenation is hydrogenated with intermediate CO formation. Second, carbon dioxide hydrogenation is direct synthesis of methane from carbon dioxide without intermediate CO formation. In the first mechanism, formyl species  $(\text{HCO})_{\text{ads}}$  or surface carbon  $(\text{C}_{\text{ads}})$  species was adsorbed, which produces methane. In the second mechanism are the adsorbed hydrogen carbonate  $(\text{HCO}_3)_{\text{ads}}$  and formate  $(\text{HCOO})_{\text{ads}}$  surface species, which occur via possible intermediate. Furthermore, the stream adsorption on the metal-support interface investigated as the significant step in the production of methane through this mechanism.

In addition, Dorner et al. (2009) [30] studied the overall reaction for convert carbon dioxide in the  $\text{CO}_2$  hydrogenation reaction into hydrocarbons are illustrated in equation (2.1) and (2.2)



The carbon dioxide hydrogenation is an exothermic process that takes place according to the following global reaction:



When  $n=1$ , equation

However, the carbon dioxide can be reduced to carbon monoxide by the catalytic reverse water-gas shift reaction (RWGS) [29].

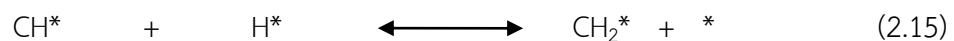
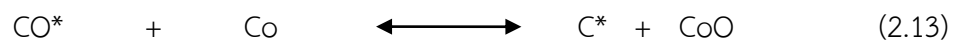
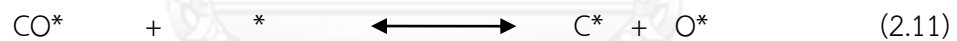


Then, methane was produced by the methanation of carbon monoxide

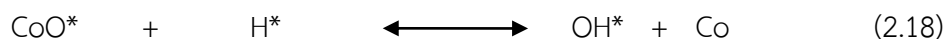
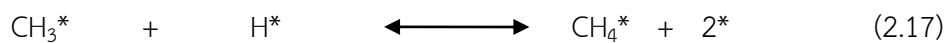
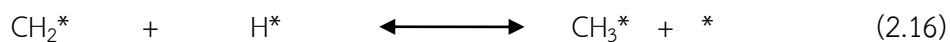


In recent year, Lahtinen et al (1994) [15] reported that the reaction mechanism for methane from carbon dioxide hydrogenation and carbon monoxide hydrogenation on the polycrystalline cobalt foils.

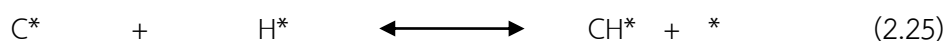
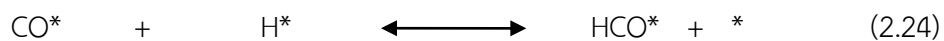
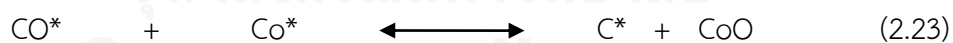
-Reaction mechanisms for carbon monoxide hydrogenation that takes place according to the following set of mechanism:

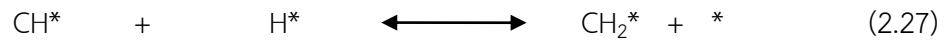
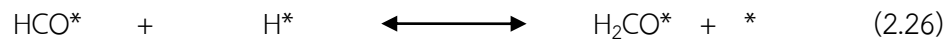






-Reaction mechanisms for carbon dioxide hydrogenation that takes place according to the following set of mechanism:





Equation (2.24), (2.26) and (2.28) are alternative reaction ways, which were equations (2.26) and (2.28) could be occurred by affecting from equation (2.24).

## 2.2 Aluminium Oxides or Alumina ( $\text{Al}_2\text{O}_3$ )

In the past decades, alumina is one of the most common crystalline materials due to it is a very appealing crystalline material with widely applicability including coating, adsorbent, ceramic tools, fillers, wear-resistant ceramics, catalysts and catalyst supports. As a result of their unique properties such as high surface area, fine particle size, high melting temperature (above 2000 °C), high purity, good adsorbent and high activity: they are used in a wide range of large-scale technological processes [8, 20, 28, 34].

It is well known that the term of aluminium oxides refers to alumina ( $\text{Al}_2\text{O}_3$ ), which has a number of crystalline phases. Normally, alumina can exist in many kinds metastable phase and it can transform to the stable phase of alumina. In addition, it is well known that the alpha( $\alpha$ )-alumina form or corundum form is the stable form of alumina. There are many principle phase involved in stable phase of alumina, which designated by the Greek symbols including chi( $\chi$ ), kappa( $\kappa$ ), eta( $\eta$ ), theta( $\theta$ ), delta( $\delta$ ), alpha( $\alpha$ ) and gamma( $\gamma$ )-phase [21].

Furthermore, the different types of starting materials such as gibbsite, boehmite and other can be transformation to six principle phases via many factors. There are many factors involved in phase transformation of alumina including calcination temperature, heating environment is known as heat treatment conditions, which presented in Figure 3.

In short, the route of direct phase transformation from gibbsite to alpha ( $\alpha$ )-alumina phase is divided to two routes. First of all, route one is phase transformation from gibbsite to chi( $\chi$ ) to kappa( $\kappa$ ) to alpha( $\alpha$ )-alumina. Second, route 2 is phase transformation from gibbsite to boehmite to gamma ( $\gamma$ ) to delta ( $\delta$ ) to theta ( $\theta$ ) to alpha ( $\alpha$ )-alumina. It is well known that the phase transformation depending on temperature, heating environment, particle size of starting material of gibbsite and heating rate, indicating that the calcinations temperature is an important factor for the phase transformation of alumina.

In fact, the phase transform could be occurred from fine gibbsite to rho-alumina (100-400°C), to eta ( $\eta$ ) (270-500 °C), to theta ( $\theta$ ) (870-1150 °C) to alpha ( $\alpha$ ) alumina (1150 °C). For instantaneous dehydration at 800 °C, gibbsite from eta( $\eta$ ), theta( $\theta$ ) and alpha( $\alpha$ ) alumina.

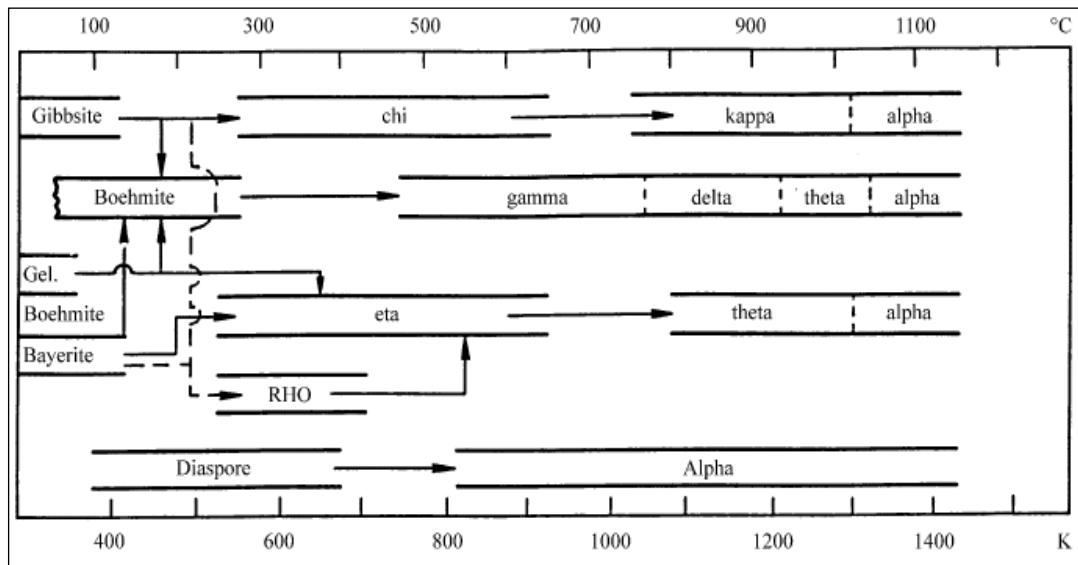


**Figure 2.3** Thermal transformation of sequence of aluminum hydroxides [27].

## 2.3 Cobalt.

### 2.3.1 General

Cobalt is a transition metal element with symbol Co, which have atomic number 27. Cobalt is similar to silver in appearance and lacquers. Cobalt and cobalt compounds have been used to make drying agents in paints for ground coat fits in pottery, animal and human nutrients, electroplating material. In addition, it also used to form alloys for make high temperature alloys, hard facing alloys, high speed tool, magnetic alloys and it also used in radiology. Moreover, Cobalt is an important catalyst for synthesis of heating fuel from crude oil in hydrocarbon refining [32].

### 2.3.2 Physical properties

The ground state electron configuration of cobalt is  $[\text{Ar}] 3d^7 4s^2$ . Cobalt presented in crystalline structure of  $\alpha$  (or  $\epsilon$ ) form at room temperature, which is close-packed hexagonal (cph) and their lattice parameters are  $a=0.2501$  nm and  $C=0.4066$  nm. The transition temperature to centered cubic (fcc) allotrope is an approximately  $417$  °C in crystalline structure of the  $\gamma$  (or  $\beta$ ) form and their lattice parameters are  $a=0.3554$  nm. Heating in air or oxygen at high temperature produces the scale formed on unalloyed cobalt, which is double-layered. In the range of  $300$  and  $900$  °C, the scale consists of a thin layer of mixed cobalt oxide, which is  $\text{Co}_3\text{O}_4$  on the outside and cobalt (II) oxide (CoO) layer next to metal. At temperatures below  $300$  °C, the cobalt species may be formed to cobalt (III) oxide ( $\text{Co}_2\text{O}_3$ ). Moreover, at temperature above  $900$  °C result in  $\text{Co}_3\text{O}_4$  decomposes and both layer, although of different appearance, are composed of CoO only. At temperature below  $600$  °C and above  $750$  °C, the scales formed appear to be stable to cracking on cooling, while those produced at the range of  $600$  to  $700$  °C crack and flake off the surface.

Cobalt is an importance chemical element for industrial. It is well known that the standard atomic weight is  $58.933$  and its appearance in transition series of Group 8 (VIII B). Number of isotope of cobalt is thirteen but only three isotopes are significant. In terms of isotopes of cobalt,  $^{59}\text{Co}$  is the only stable cobalt isotope and the only naturally occurring isotope while  $^{60}\text{Co}$  with a half life of  $5.3$  years is a common source of  $\gamma$ -source for Mössbauer spectroscopy.

The common oxidation states of cobalt compounds are the  $+2$  or  $+3$  valence states. Although multitude of cobalt compounds with oxidation states  $+3$  (cobalt (III)) are exists, but few stable simple salt are also known. In addition, the most common stereochemistry of cobalt (II) ion is octahedral stereochemistry and it as well as for cobalt (III). Octahedral or tetrahedral stereochemistry are the most form numerous simple compounds and complexes in nature. Cobalt (II) forms more tetrahedral complex than other transition – metal ions. On account of the small stability differences between tetrahedral and octahedral of cobalt (II), both complexes

can be found that the equilibrium for a number of complexes. Typically, the octahedral cobalt (II) salts and complexes are pink to brownish red. Moreover, the most of the tetrahedral cobalt (II) salts are blue. Physical properties of cobalt are show in Table 2.1.

### 2.3.3 Cobalt oxides

There are three kind formed of cobalt oxides including cobalt (II) oxide (CoO), cobalt (III) oxide (Co<sub>2</sub>O<sub>3</sub>) and cobalt (II, III) oxide (Co<sub>3</sub>O<sub>4</sub>). First of all, cobalt (II) oxide (CoO) or cobalt monoxide is an cubic crystalline material that appears as olive green. Cobalt (II) oxide is the final product formed, which transformation phase can occurred when the other oxides was calcined by sufficiently high temperature, preference in a neutral or slightly reducing atmosphere. In addition, pure cobalt (II) oxide is a difficult to prepare due to it readily takes up O<sub>2</sub> even at ambient temperature transform to a higher oxide. At temperature above 850 °C the cobalt (II) oxide form is stable. The product of trade is usually dark gray and contains 75 – 78 wt% cobalt. Cobalt (II) oxide can dissolve in water, ammonia solution and organic solvents but not in strong mineral acid. Cobalt (II) oxide has for centuries used in glass decorating, coloring agent and it is a precursor of cobalt chemical.

In addition, cobalt (III) oxide is an inorganic compound with the molecular formula Co<sub>2</sub>O<sub>3</sub>. Cobalt (III) oxide was prepared by heating at low temperature in excess of air. Some authorities told that the cobalt (III) oxide exists only in the hydrate form. Cobalt (III) oxide was appeared in black powder form by oxidizing neutral cobalt solution. At temperature above 265 °C, the Co<sub>2</sub>O<sub>3</sub> or Co<sub>2</sub>O<sub>3</sub>·H<sub>2</sub>O is completely converted to cobalt oxide (Co<sub>3</sub>O<sub>4</sub>) form. Co<sub>3</sub>O<sub>4</sub> will adsorption oxygen to correspond to the Co<sub>2</sub>O<sub>3</sub>.

Moreover, cobalt oxide (Co<sub>3</sub>O<sub>4</sub>) was occurred by carbonate or the hydrated sesquioxides are heating at temperatures above 265 °C in air and not exceeding 800 °C.

Table 2 1 Physical properties of cobalt [23].

Property	Value
Atomic number	27
Atomic weight	58.93
Transformation temperature, °C	417
Heat of transformation, J/g <sup>a</sup>	251
Melting point, °C	1493
Latent heat of fusion, $\Delta H_{\text{fus}}$ J/g <sup>a</sup>	395
Boiling point, °C	3100
Latent heat of vaporization at bp, $\Delta H_{\text{vap}}$ kJ/g <sup>a</sup>	6276
Specific heat, J/(g °C)	
15-100 °C	0.442
Molten metal	0.560
Coefficient of thermal expansion, °C <sup>-1</sup>	
cph at room temperature	12.5
fcc at 417 °C	14.2
Thermal conductivity at 25 °C, W/(mK)	69.16
Thermal neutron absorption, Bohr atom	34.8
Resistivity, at 20 °C <sup>b</sup> , 10 <sup>-8</sup> Ωm	6.24
Curie temperature, °C	1121
Saturation induction, 4πI <sub>s</sub> , T <sup>c</sup>	1.870
Permeability, μ	
initial	68
max	245

**Table 2.1** Physical properties of cobalt [23].

Property	Value		
Residual induction, T <sup>c</sup>	0.490		
Coercive force, A/m	708		
Young's modulus, Gpac	211		
Poisson's ratio	0.32		
Hardness <sup>f</sup> , diamond pyramid, of%Co	99.9	99.98 <sup>e</sup>	
at 20 °C	225	253	
at 300 °C	141	145	
at 600 °C	62	43	
at 900 °C	22	17	
Strength of 99.99%cobalt, MPa <sup>g</sup>	as cast	annealed	sintered
tensile	273	588	679
Tensile yield	138	193	302
compressive	841	808	
Compressive yield	291	387	

<sup>a</sup>To convert J to cal, divided by 4.184

<sup>b</sup>conductivity = 27.6 % of International Annealed Copper Standard

<sup>c</sup>To convert T to gauss, multiply by 10<sup>4</sup>

<sup>d</sup>To convert GPa to psi, multiply by 145,000

<sup>e</sup>Zone refined

<sup>f</sup>Vickers

<sup>g</sup>To convert MPa to psi, multiply by 145



### 2.3.4 Cobalt catalyst

The most widely used catalysts for the synthesis of hydrocarbons from natural gas such as carbon dioxide and carbon monoxide are supported cobalt catalysts due to their unique properties such as high activity, high selectivity for linear hydrocarbons, and low activity for the water gas shift reaction. Typical support material are alumina, silica, titania, magnesia, carbon, and zeolites due to their provides good mechanical properties and thermal stability under reaction condition.

The formed support is heat treated to modify the mechanical strength. The most an important factor of support is the controlling of the pore size result in the amount of cobalt dispersion on the support and catalytic performance. Moreover, the addition of promoter metal such as lanthanum, palladium, platinum, rhenium and ruthenium could be modified the support result in enhance the subsequent reduction step. It has been reported that addition of some metal such as lanthanum, rhenium and ruthenium could improved the effective to facilitate catalyst re-reduction. However, the promoters are not essential to produce the best supported cobalt catalyst. The effective reduction to metallic cobalt and the support geometry are an important factor for studied.

## CHAPTER III

### LITERATURE REVIEW

This chapter reviews the relating research. There are three sections involved in literature review in the research. The first sections review the research investigations on the effect of basic oxide including calcium oxide, lanthanum oxide and magnesium oxide modified support in various reaction. The second section review the research involved in the effect of addition of mixture solution magnesium nitrate and aluminium nitrate into the alumina support on the catalytic activity and stability in various reaction. The last section review the research involved in the effect of alumina supports on the properties of Co/Al<sub>2</sub>O<sub>3</sub> catalysts in carbon dioxide hydrogenation and carbon monoxide hydrogenation.

#### **3.1 Effect of basic oxide including calcium oxide, lanthanum oxide and magnesium oxide modified support in various reaction**

In recent years, the basic oxides including calcium oxide, lanthanum oxide and magnesium oxide modified were attractively studied all over the world in various reactions due to the cobalt supported on alumina support has a limited reducibility due to the interaction between metal oxide and alumina supports are stronger than other supports such as silica and titania (Bao et al., 2009) [3]. It is well known that the strong interaction between cobalt and alumina support brings about the formation of inactive CoAl<sub>2</sub>O<sub>4</sub> species and often results in the relatively low reducibility and low catalytic activity. They found that the addition of metal oxide promoter had significant effects on cobalt and/or nickel catalysts for various reactions.

### 3.1.1 Effect of calcium oxide modified support

Calcium oxide modified alumina support had significant effect to improve reducibility. It had been reported that calcium loading could suppress the strong interaction between metallic phase and support. Bao et al. (2009) [3] studied the effect of calcium oxide on Co/Al<sub>2</sub>O<sub>3</sub> catalysts for Fischer-Tropsch synthesis by preparing a series of calcium oxide modified alumina supported cobalt catalysts, with different calcium oxide loadings (0.5 and 1.0 wt%). The catalysts were prepared by incipient wetness impregnation method. N<sub>2</sub>-adsorption, X-ray diffraction (XRD), temperature programmed reduction (TPR), temperature programmed desorption and oxygen titration were used for studied the effect of calcium oxide on the cobalt dispersion, reducibility of catalyst and cobalt particle size. The catalytic activity for Fischer-Tropsch synthesis was evaluated in a continuous stirred tank reactor (CSTR). The result showed that the calcium oxide adjusted reducibility of the cobalt oxide, indicating that calcium oxide modification can suppress the strong interaction between cobalt oxide and support. In addition, the calcium oxide modified alumina-supported cobalt catalysts can improve the catalytic activity for Fischer-Tropsch synthesis. A positive correlation was observed between CO conversion, C<sub>5+</sub> selectivity and calcium oxide content. Furthermore, methane selectivity decreased with increasing calcium oxide content. However, high quantity of calcium oxide caused a decrease in methane selectivity, due probably to the improved reducibility that provides abundant active sites.

In addition, different contents of calcium oxide were investigated according to Dias and Assaf (2003) [9], in which the effect of calcium oxide promoted on Ni/Y-Al<sub>2</sub>O<sub>3</sub> catalysts for carbon dioxide reforming of methane was investigated. The variables studied were different contents of calcium oxide and the order of addition. The catalysts were prepared by impregnation of Ni and Ca into alumina supports. N<sub>2</sub>-adsorption, TPR and CO<sub>2</sub>-TPD were used for the characterization of the catalysts. The results showed that when nickel was added first followed by calcium, calcium, sintering of the alumina support occurred and it blocked the small pores. However, when calcium oxide was added first followed by nickel on alumina support, the

addition of calcium oxide led to the competing strong interaction between Ca and Ni with the alumina support. Moreover, when calcium oxide was added first followed by nickel on alumina support, higher reducibility of the catalysts was obtained, due to the competition between calcium and nickel for strong interaction with the alumina support. The formation of nickel species being more difficultly reducible could be avoided. In addition, the low amount of calcium can improve the catalytic activity for carbon dioxide reforming of methane, due probably to attraction effects between carbon dioxide and calcium oxide, but the high amount of calcium oxide resulted in lower catalytic activity, due to this effect being connected with the increase in electron density of the catalyst.

Furthermore, Quencoces et al (2001) [26] studied the effect of calcium oxide modified on Ni/Al<sub>2</sub>O<sub>3</sub> catalysts for carbon dioxide reforming of methane. The catalysts were prepared by impregnation method with difference calcium oxide loading (1 and 5 wt %) and characterized by different techniques such as BET surface area analysis, XRD, H<sub>2</sub>-chemisorptions and TPR. It was found that the addition of calcium oxide into alumina supported nickel catalysts resulted in the lower amount of carbon deposition during reaction time due probably to the increase of basicity, which favors the reaction CO<sub>2</sub> adsorption. In addition, the improved catalytic performance in carbon dioxide reforming of methane was obtained over the calcium oxide modified alumina supported nickel catalyst and addition of CaO showed improvement in the catalyst stability during 3 h time-on-stream.

### 3.1.2 Effect of lanthanum oxide modified support

Lanthanum oxide promoted on the various supports had shown significant impact to improve reducibility of the catalysts. According to Cai et al. (2010) [7], the effect of lanthanum oxide promoted on the Al<sub>2</sub>O<sub>3</sub> supported cobalt catalyst was investigated in the Fischer-Tropsch synthesis. The variables studied were different preparation methods between impregnation method and co-precipitation method. Nitrogen adsorption-desorption, XRD, TPR, TPD, DRIFTS and oxygen titration

were used for the characterization of the catalysts. It was found that the presence of lanthanum oxide had strong influence on the catalytic performance in Fischer-Tropsch synthesis significantly. The alumina was modified with lanthanum by co-precipitation showed better reducibility of the cobalt oxide, catalytic activity and product selectivity, due to the higher ratio of the octahedral to tetrahedral cobalt species of the synthesized catalysts by co-precipitation method relative to the synthesized catalysts by impregnation method.

It had been reported that lanthanum oxide loading can improve strong interaction between metallic phase and support. According to Zhi et al. (2011) [35], the effect of addition of lanthanum oxide modified Ni/SiC catalysts for methanation of carbon dioxide was investigated. The catalysts were prepared by impregnation method and characterized by difference technique such as XRD, H<sub>2</sub>-TPR and XPS. It was found that the addition of lanthanum oxide resulted in the highest catalytic activity and stability during the 70 h time-on-stream due to the addition of MgO into nickel catalyst improved the nickel oxide dispersion and it can improve the strong interaction between nickel oxide and support. In addition, lanthanum oxide doped on alumina support can modify the electron environment surrounding nickel atoms, hence reactant on nickel atoms can be activated more easily.

### 3.1.3 Effect of magnesium oxide modified support

According to the literature in this section, the presence of magnesium oxide on support could also improve catalytic performance and the effect of addition of magnesium oxide resulted in the formation of magnesium aluminate spinel. In addition, the formation of magnesium aluminate spinel depended on many factors such as calcination temperature and amount of magnesium loading on support. The different contents of magnesium oxide was investigated according to Penkova et al. (2011) [25]. The effect of magnesium oxide modified alumina supported on NiSn/Al<sub>2</sub>O<sub>3</sub> catalyst was studied in the hydrogen production by methanol steam reforming. The variables studied was the different contents of magnesium oxide (0, 5,

10 and 30 wt.%). The catalysts were prepared by incipient wetness impregnation method and characterized by BET surface area analysis, XRD and H<sub>2</sub>-TPR. The results showed that the addition of magnesium oxide resulted in magnesium aluminate spinel formation. Furthermore, surface acidity of alumina support decreased with increasing magnesium oxide content. In addition, formation of magnesium aluminate spinel can suppress the incorporation of Ni in the Al<sub>2</sub>O<sub>3</sub> phase resulting in an improved nickel dispersion. The catalysts modified by 30 wt.% MgO exhibited the highest H<sub>2</sub> yield with high stability.

In addition, Zhang et al.(2005) [34] studied the effect of magnesium oxide modified alumina supported cobalt catalysts for Fischer-Tropsch synthesis. The different contents of magnesium oxide (9 and 12 wt% of MgO) were prepared via two-step incipient wetness impregnation method and the catalysts were characterized by Nitrogen adsorption-desorption, XRD, TPR, TPD, LRS, XPS and oxygen titration. The results showed that the magnesium oxide modified alumina supported cobalt catalysts resulted in the lower of strong interaction between cobalt metal and alumina support, hence lower cobalt surface phase were obtained. In addition, the improved catalytic activity in Fischer-Tropsch synthesis was obtained over the low content of magnesium oxide. However, high content of magnesium oxide resulted in lower reducibility of the catalysts and lower catalytic activity due to the formation of magnesium oxide-cobalt oxide solid solution resulting in the formation of more difficult to reduce cobalt species, probably the MgO-CoO solid solution. However, all the cobalt catalysts modified by magnesium oxide showed the improved of CO<sub>2</sub> selectivity.

Furthermore, Dieuzeide et al.(2013) [11] studied the effect of magnesium oxide modified Ni/  $\gamma$ -Al<sub>2</sub>O<sub>3</sub> catalysts for glycerol steam reforming. The variables studied were different contents of magnesium oxide loading on Ni/  $\gamma$ -Al<sub>2</sub>O<sub>3</sub> catalysts. The catalysts were prepared by impregnation method and characterized by different techniques such as BET surface area analysis, XRD, SEM, H<sub>2</sub>-chemisorptions, H<sub>2</sub>-TPR, TPD and TPO. The results showed that the addition of magnesium oxide resulted in the formation of Mg<sub>1-x</sub> Al<sub>2</sub>O<sub>4-x</sub> spinel phase and improved the nickel metal

crystallite size, acidic-base properties and strong interaction between nickel oxide and alumina support. It was found that the highest catalytic activity in glycerol stream reforming was obtained over the Ni(10)Mg(3)Al catalyst while the lowest amount of carbon deposition on catalyst during reaction time was obtained over the Ni(10)Mg(15)Al catalyst. Although the unmodified Ni/  $\gamma$ -Al<sub>2</sub>O<sub>3</sub> catalysts showed good catalytic activity for glycerol stream reforming due to the increased amount of magnesium resulting in the basic properties, but the samples had the highest content of carbon deposition on the catalyst during reaction time. However, increasing amounts of magnesium caused to decrease in surface acidity on alumina support resulting in lower carbon deposition.

The different calcination temperatures over magnesium oxide modified alumina supported were investigated according to Dieuzeide et al.(2012) [10]. The effect of calcinations temperatures over magnesium oxide modified alumina supported nickel catalysts for stream reforming of glycerol as investigated. The variables studied were different calcination temperatures of the modified alumina supports (350, 600 and 900 °C) and different calcination temperatures of the catalysts (500, 700 and 800 °C). The catalysts were prepared by incipient wetness impregnation method and characterized by BET surface area analysis, XRD and H<sub>2</sub>-TPR. The best catalytic performance in stream reforming of glycerol was obtained over the catalyst calcined at 500 °C on the modified alumina supported calcined at 900 °C, due to the formation of magnesium aluminate spinel which favors the nickel metal dispersion result in improved of the catalytic activity.

### **3.2 Effect of addition of mixture solution magnesium nitrate and aluminium nitrate into the alumina support in various reaction**

In the past decades, the addition of mixture solution of magnesium nitrate and aluminium nitrate into alumina support is an objective of synthesis of the magnesium aluminate (MgAl<sub>2</sub>O<sub>4</sub>) support due to the MgAl<sub>2</sub>O<sub>4</sub> support had unique properties, such as good mechanical strength form room temperature to high

temperature and high resistance to chemical attack [5, 22]. Jiang et al. (2004) [16] studied the catalytic activity of palladium-lanthanum catalysts supported on  $\gamma$ - $\text{Al}_2\text{O}_3$  and  $\text{MgAl}_2\text{O}_4$  spinel for gas-phase amination reaction. The variables studied were different supports between  $\gamma$ - $\text{Al}_2\text{O}_3$  and modified alumina supports. The modified alumina supports were prepared by impregnating  $\gamma$ - $\text{Al}_2\text{O}_3$  with mixture solution of magnesium nitrate and aluminium nitrate, which were used for preparation of  $\text{MgAl}_2\text{O}_4$  spinel support. The catalysts were prepared by incipient wetness impregnation method and characterized by BET surface area analysis, XRD,  $\text{NH}_3$ -TPD, XPS and pyridine-IR techniques. The results showed that the addition of magnesium nitrate and aluminium nitrate modified alumina support palladium-lanthanum catalysts resulted in  $\text{MgAl}_2\text{O}_4$  spinel formation, which neutralized some strong acid sites and transformed it into relatively weaker acid sites. In addition, formation of  $\text{MgAl}_2\text{O}_4$  supported on Pd-La/  $\text{MgAl}_2\text{O}_4$  catalysts resulted in an improved reducibility of palladium oxide. Furthermore, the Pd-La/  $\text{MgAl}_2\text{O}_4$  catalysts exhibited highest conversion, selectivity and yield of 2-6DIPA after 200 h time-on-stream.

In addition, the different loadings of magnesium nitrate and aluminium nitrate were investigated in ethylene oxide hydration. Li et al (2005) [19] studied the effect of modified alumina supports with the mixture solution of magnesium nitrate and aluminium nitrate on  $\text{Nb}_2\text{O}_3/\alpha$ - $\text{Al}_2\text{O}_3$  catalyst for ethylene oxide hydration. The modified alumina supports were prepared by impregnating  $\alpha$ - $\text{Al}_2\text{O}_3$  with mixture solution of magnesium nitrate and aluminium nitrate and then calcined at 1400 °C. The catalyst were prepared by impregnating  $\text{MgAl}_2\text{O}_4/\alpha$ - $\text{Al}_2\text{O}_3$  with aqueous solution of niobic acid and characterized by BET surface area analysis, XRD,  $\text{CO}_2$ -TPD,  $\text{NH}_3$ -TPD and pyridine-IR techniques. It was found that the modified alumina supports with mixture solution of magnesium nitrate and aluminium nitrate resulted in the formation of  $\text{MgAl}_2\text{O}_4$  spinel and the modified alumina supports with  $\text{MgAl}_2\text{O}_4$  spinel brought about an increase in basicity and it could improve the mechanical strength of support. In addition, it was found that the addition of magnesium nitrate and aluminium nitrate on  $\text{Nb}_2\text{O}_3/\alpha$ - $\text{Al}_2\text{O}_3$  catalyst led to the decreased acidity of catalyst when the amount of  $\text{MgAl}_2\text{O}_4$  increased. The catalytic activity test showed that the EO



conversion decreased with increasing amount of  $\text{MgAl}_2\text{O}_4$  and selectivity to MEG exhibited a maximum at  $\text{MgAl}_2\text{O}_4$  loading of 2.23%. Furthermore, the addition of  $\text{MgAl}_2\text{O}_4$  loading of 2% on  $\text{Nb}_2\text{O}_5/\alpha\text{-Al}_2\text{O}_3$  catalyst exhibited excellent stability in 1000 h time-on-stream.

However, there are many methods involved in the synthesis of the magnesium aluminate ( $\text{MgAl}_2\text{O}_4$ ) support. Navaei et al. (2009) [1] studied the effect of application of mesoporous nano-crystalline  $\text{MgAl}_2\text{O}_4$  spinel as support for nickel catalyst in dry reforming reaction. The supports were prepared by co-precipitation method with the surfactant-assisted route using N-cetyl-N,N,N-trimethylammonium bromide as surfactant and characterized by nitrogen adsorption-desorption, XRD and TPO. The results showed that preparation of  $\text{MgAl}_2\text{O}_4$  spinel by co-precipitation method were obtain the  $\text{MgAl}_2\text{O}_4$  spinel formation and larger crystallite size of  $\text{MgAl}_2\text{O}_4$  spinel were obtain with the increase in the calcination temperature. Furthermore, the addition of N-cetyl-N,N,N-trimethylammonium bromide surfactant resulted in the increased specific surface area and at high calcination temperature with high thermal stability. In addition, it was found that the amount of carbon deposition increased when the nickel loading increased.

### 3.3 Effect of alumina supports on the properties of $\text{Co}/\text{Al}_2\text{O}_3$ catalysts in carbon dioxide hydrogenation and carbon monoxide hydrogenation.

It has been reported that the most widely used catalysts for the synthesis of hydrocarbons from natural gas such as carbon dioxide and carbon monoxide are supported cobalt catalysts due to their unique properties such as high activity, high selectivity for linear hydrocarbons, and low activity for the water gas shift reaction. According to Bechara et al. (2001) [4], the effect of different loadings of cobalt on the alumina supported cobalt catalysts for carbon monoxide hydrogenation was studied. The variables studied were different contents of cobalt (15-17 wt% cobalt). The catalysts were prepared by incipient wetness impregnation method and characterized by BET surface area analysis, XRD, XPS, magnetic measurements and TGA. It was

found that the improved catalytic activity and selectivity for light hydrocarbon product in carbon monoxide hydrogenation was obtained over the increasing in the reaction temperature. In addition, the results showed that the catalytic activity of the alumina supported cobalt catalysts at 15 wt.% cobalt on alumina decreased with the time on stream, indicating that the evolution of the catalyst such as partial re-oxidation and site blocking. However, the product distribution and by-product were not significantly changed with the time on stream. In addition, the increasing of the reduction temperature could improve the CO transformation rate and favor the production of higher hydrocarbons. Furthermore, high amount of cobalt resulted in improved reducibility of the metallic phase.

However, it is well known that the addition of noble metal could improve the catalytic activity in hydrogenation of carbon dioxide. Wan Bakar et al. (2012) [31] studied the effect of calcination temperatures and the effect of noble metals (ruthenium and platinum) loading on the alumina supported cobalt catalysts for carbon dioxide hydrogenation. The catalysts prepared by wet impregnation method, with variation of the ratios between cobalt and noble metal. It was found that the Pt/Co(10:90)/Al<sub>2</sub>O<sub>3</sub> catalysts calcined at 700 °C exhibited highest catalytic activity. In addition, the Pt/Co(10:90)/Al<sub>2</sub>O<sub>3</sub> catalysts showed small particle size with uniformly distributed. Furthermore, the formation of methane was expected to increase at higher reaction temperature because the carbon dioxide hydrogenation reaction is an exothermic reaction. The FT-IR and TGA-DTA analysis showed the presence of nitrates residual and hydroxyl ions on both of potential catalysts due to the incompletely remove all the nitrates and surface hydroxyl molecules at 700 °C calcination temperature.

## CHAPTER IV

### EXPERIMENTAL

#### 4.1 Chemicals

- 4.1.1  $\gamma$ - $\text{Al}_2\text{O}_3$  puralox SBa 200 available from SASOL Germany
- 4.1.2 Cobalt (II) nitrate hexahydrate 98% available from Aldrich
- 4.1.3 Magnesium (II) nitrate hexahydrate 99% available from Merck
- 4.1.4 Aluminium (III) nitrate nanohydrate 99% available from Merck
- 4.1.5 Calcium (II) nitrate tetrahydrate 99% available from Aldrich
- 4.1.6 Lanthanum (III) nitrate hexahydrate 99.99% available from Aldrich

#### 4.2 Materials preparation

##### 4.2.1 Preparation of MgAl-modified $\text{Al}_2\text{O}_3$ on the supported Co/ $\text{Al}_2\text{O}_3$ catalysts

The MgAl-modified alumina supports were prepared by impregnating  $\gamma$ - $\text{Al}_2\text{O}_3$  with mixture solution of  $\text{Al}(\text{NO}_3)_3 \cdot 9\text{H}_2\text{O}$  and  $\text{Mg}(\text{NO}_3)_2 \cdot 6\text{H}_2\text{O}$  with different loadings (1, 2.5, 3.55 and 10 wt%) of MgAl. The samples were dried at 120 °C over night, followed by the calcination in air at 900 °C for 6 h. The cobalt catalysts were prepared by the incipient wetness impregnation method using  $\text{Co}(\text{NO}_3)_2 \cdot 6\text{H}_2\text{O}$  with 15 wt% cobalt. The catalysts were dried at 120 °C overnight calcined in air at 650 °C at a rate of 10 °C/min for 5 h. Finally, the catalysts were cooled down to room temperature in  $\text{N}_2$  (75ml/min).

#### 4.2.2 Preparation of basic oxides (MgO, CaO, and La<sub>2</sub>O<sub>3</sub>) modified Al<sub>2</sub>O<sub>3</sub> on the supported Co/ Al<sub>2</sub>O<sub>3</sub> catalysts.

The modified alumina supports were prepared by impregnating  $\gamma$ -Al<sub>2</sub>O<sub>3</sub> with an aqueous solution of La(NO<sub>3</sub>)<sub>3</sub>.6H<sub>2</sub>O or Ca(NO<sub>3</sub>)<sub>3</sub>.4H<sub>2</sub>O to give 2.5 wt% of La and Ca. In addition, an aqueous solution of Mg(NO<sub>3</sub>)<sub>2</sub>.6H<sub>2</sub>O and the mixture of Al(NO<sub>3</sub>)<sub>3</sub>.9H<sub>2</sub>O and Mg(NO<sub>3</sub>)<sub>2</sub>.6H<sub>2</sub>O solution were also used for preparation of Mg- and MgAl- modified Al<sub>2</sub>O<sub>3</sub> supports at concentration of 2.5 wt% Mg and 2.5 wt% MgAl. After impregnation, the modified supports were dried in oven at 120 °C and calcined in air at different temperatures (550 °C and 900 °C) for 6 h.

The cobalt catalyst were prepared by the incipient wetness impregnation method using Co(NO<sub>3</sub>)<sub>3</sub>.6H<sub>2</sub>O with 15 wt% cobalt. The catalysts dried at 120 °C overnight and calcined in air at 650 °C for 5 h.

### 4.3 Catalysts characterization

#### 4.3.1 X-ray diffraction (XRD)

X-ray diffraction pattern and bulk phase of catalysts were determine by X-ray diffractometer (D8 Advance of Bruker AXS) connected with a computer with program diffract ZT version 3.3 for fully control of the XRD analyzer. by the XRD measurement were carried out Cu k $\alpha$  radiation with Ni filter. The spectra were scanned in the  $2\theta$  range from 10° to 80° degrees resolution 0.04°. The average crystallite size was calculated from line broadening using the Scherrer's equation.

### 4.3.2 N<sub>2</sub>-physisorption

BET equipment for the single point method.

Two feed lines gas of helium and nitrogen were use for the reaction apparatus of the BET surface area measurement and the fine-metering valve on the gas chromatograph were use for adjusted flow rate of these gas. The BET surface area measurements were performed in a U-shaped tubular glass reactor.

BET surface area measurement was carried out as follows 0.3 g of the modified alumina support material was placed in a U-shaped glass tube. Followed by the mixture gases of helium and nitrogen were flow passed through the system at the nitrogen relative 0.3. Then, the temperature was raised from ambient temperature about 25 °C up to 160 °C at a rate of 10 °C/min and kept at this temperature for 2 h. Next, the sample was cooled down to room temperature. Follow by their step was used for studied BET surface area. First, adsorption step the support that set in the U-shaped glass tube was dipped into liquid nitrogen temperature. The nitrogen gas that passed through the modified support was adsorbed on the surface of the support until equilibrium was obtained. Second, Desorption step: The U-tube cell with nitrogen gas -absorption support sample was dipped into the water at room temperature. In this case, the adsorbed nitrogen gas surface sample was desorbed from the surface sample. Desorption step was completed when the indicator line was in the position of base line. Finally, Calibration step: the nitrogen gas about 1 ml at 1 atm was injected passed calibration port on the gas chromatograph. The area of support sample was calculated from amount of N<sub>2</sub>.

### 4.3.3 Hydrogen chemisorption.

The number of reduce surface cobalt metal atoms and the overall cobalt dispersion were determined by H<sub>2</sub>-chemisorption technique. In this experimental, following the procedure described by Reuel and Bartholomew (1984) and using Micromeritics chemisorb 2750 (pulse chemisorption system) and ASAP 2101C V.3.00 software.

There are many step involved in Hydrogen chemisorption technique. First, 0.2 g of the cobalt catalyst sample was placed in U-type glass tube. Second, the catalysts were reduced in Hydrogen gas at a flow rate of 50 ml/min. Then, the temperature was raised from ambient temperature up to 350 °C at a rate of 10 °C/min and kept at this temperature for 3 h. Next, the sample was cooled down to ambient temperature in a He flow. Finally, the number of H<sub>2</sub>-chemisorbed was determined by thermal conductivity detector and injection was continued until no further the Hydrogen adsorption was observed.

### 4.3.4 Hydrogen temperature program reduction (H<sub>2</sub>-TPR).

The H<sub>2</sub>-TPR was performed to determine the reduction behavior of the supported cobalt catalysts using a Micromeritics chemisorb 2750. There are five steps involved in Hydrogen temperature program reduction technique. First, 0.1 g of the cobalt catalysts sample was placed in U-type glass tube. Second, the catalysts were heated in nitrogen gas at a flow rate of 10 °C/min from room temperature to 200 °C and kept at this temperature for 1 h. Then, the sample was cooled down to room temperature. Next, the catalysts were heated in the carrier gas (10%H<sub>2</sub>/Ar) at a flow rate of 10 cc/min from 35 °C up to 800 °C at a rate 10 °C/min and a cold trap was used for remove water produced. Finally, the number of hydrogen consumption was determined by a thermal conductivity detector (TCD).

#### 4.3.5 Temperature-programmed desorption (NH<sub>3</sub>-TPD)

Acidity of the catalysts was determined using temperature programmed desorption of ammonia (NH<sub>3</sub>-TPD)

Temperature-programmed desorption of alumina (NH<sub>3</sub>-TPD) was performed to determine the acidity of the catalysts using a Micromeritics Chemisorb 2750. There are many steps involved in NH<sub>3</sub>-TPD technique. First, 0.1 g of the sample was placed in glass tube. Second, the sample was heated in helium gas at a flow rate 10 °C/min from room temperature to 550 °C to remove the water from the support sample and kept at this temperature for 1 h. Then, the sample was cooled down to 100 °C followed by the ammonia gas was flowed through the sample at a rate of 25 ml/min for 30 min. The ammonia gas that passed through the sample was adsorbed on the surface of sample. Next, the sample was heated from 100 °C to 550 °C in the carrier gas (He) at a flow rate 25 cc/min. In this the adsorbed ammonia gas on surface sample was desorbed from the surface sample. Finally, the amount of acidity was determined by a thermal conductivity detector (TCD).

#### 4.3.6 Scanning Electron Microscopy (SEM)

SEM was performed to study the morphologies of the catalysts sample using JEOL mode JSM-5800L V. scanning electron microscopy.

### 4.3.7 Transmission Electron Microscopy (TEM)

Transmission electron microscopy was performed to study the morphologies of the catalysts sample, crystallite size and size distribution of supported metals operated at 160 kV, using TEM equipment from Stimulus Package 2 (SP2) of Minister of Education under the theme of Green Engineering for Green Society, Chulalongkorn University.

## 4.4 Reaction study in CO<sub>2</sub> hydrogenation

### 4.4.1 Material

The feed gas used for the catalyst activity tests was the mixture gases of carbon and hydrogen gas as supplied by Thai Industrial Gas Limited (TIG).

CO<sub>2</sub> hydrogenation reaction was performed in a fixed bed reactor using 0.2 g of catalyst packed in center of a tubular glass reactor. which is placed in the furnace .The reactant feed gas H<sub>2</sub>/CO<sub>2</sub> ratio of 10/1 was flowed through the sample at a total flow rate of 30 ml/min. Activation of the cobalt catalyst involved reductive treatment with hydrogen at 350 °C for 3 h. The CO<sub>2</sub> hydrogenation was carried out at 270 °C and atmosphere pressure. The effluent gases from the reactor were analyzed by gas chromatograph equipped with a thermal conductivity detector (TCD) with molecular sieve 5 Å were used for separation of carbon monoxide (CO), Carbon dioxide (CO<sub>2</sub>), and light hydrocarbon such as methane (CH<sub>4</sub>), ethane (C<sub>2</sub>H<sub>6</sub>) and propane (C<sub>3</sub>H<sub>8</sub>)



## 4.4.2 Apparatus

Fig 4.1 shows flow diagram of CO<sub>2</sub> hydrogenation system. The CO<sub>2</sub> hydrogenation system compose of a Fixed-bed reactor, an electrical furnace, a temperature controller, a gas system and gas chromatography.

### 4.4.2.1 Reactor

A fixed-based reactor was made from glass tube (O.D. 3/8"). The position of sampling points located at above and below the catalyst bed. The catalyst was placed above quartz wool layer.

### 4.4.2.2 Temperature Controller

Automation temperature controller consisted of a magnetic switch connected to electrical transformer and a solid-state relay temperature controller model connected to a thermocouple. The temperature in a Fixed-bed reactor was measured at the bottom of the catalyst bed.

### 4.4.2.3 Electrical Furnace

The electrical furnace is a type of heat producing equipment for carbon dioxide hydrogenation. The reactor could be operated from room temperature to 800 °C at the maximum voltage of 220 volt.

#### 4.4.2.4 Gas controlling system

Feed gas for the system was each provided controlled with a pressure regulator and on-off gas control valves and metering valves were use for adjusted the gas flow rates.

#### 4.4.2.5 Gas Chomatography

The composition of gas in the product stream from the reactor were analyzed by gas chromatograph equipped with a thermal conductivity detector (TCD), which used to analyze hydrogen and carbon dioxide in the reactant feed gas and product streams.

Table 4 1 Operating condition for gas chromatograph

Gas Chromatograph	SHIMADZU GC-8A
Detector	TCD
Column	Molecular sieve 5Å
-Column material	SUS
-Length	2 m
-Outer diameter	4mm
-Inner diameter	3mm
-Mesh range	60/80
Maximum	
Temperature	70°C
Carrier gas	He (99.999%)
Carrier gas flow	40 cc/min
Column gas	He (99.999%)
Column gas flow	40 cc/min
Column temperature	
-initial (°C)	70°C
-final (°C)	70°C
Injector temperature (°C)	100°C
Detector temperature (°C)	100°C
Current (mA)	80
Analyzed gas	Hydrocarbon C <sub>1</sub> -C <sub>4</sub> , CO,CO <sub>2</sub> ,H <sub>2</sub>

### 4.4.3 Procedures

**4.1.1.1** The 0.2 g of catalyst was placed above quartz wool layer which packed in the center of tubular glass reactor. The tubular glass reactor was placed in the electrical furnace

**4.1.1.2** A flow rate of Nitrogen = 8.8 cc/min, carbon dioxide in hydrogen = 21.3 cc/min and Hydrogen = 50 cc/min in a fixed-bed reactor. A relatively high H<sub>2</sub>/CO<sub>2</sub> ratio was used to minimize deactivation because carbon deposition during reaction

**4.1.1.3** Activation of cobalt catalyst involved reductive treatment with hydrogen at 350 °C for 3 h prior to CO<sub>2</sub> hydrogenation.

**4.1.1.4** The CO<sub>2</sub> hydrogenation was carried out at 270 °C at atmospheric pressure in a flow of 8.8% CO<sub>2</sub> in H<sub>2</sub>

**4.1.1.5** The effluent gases from the reactor were analyzed by gas chromatograph equipped with a thermal conductivity detector (TCD), which used to analyze hydrogen and carbon dioxide in the reactant feed gas product stream.

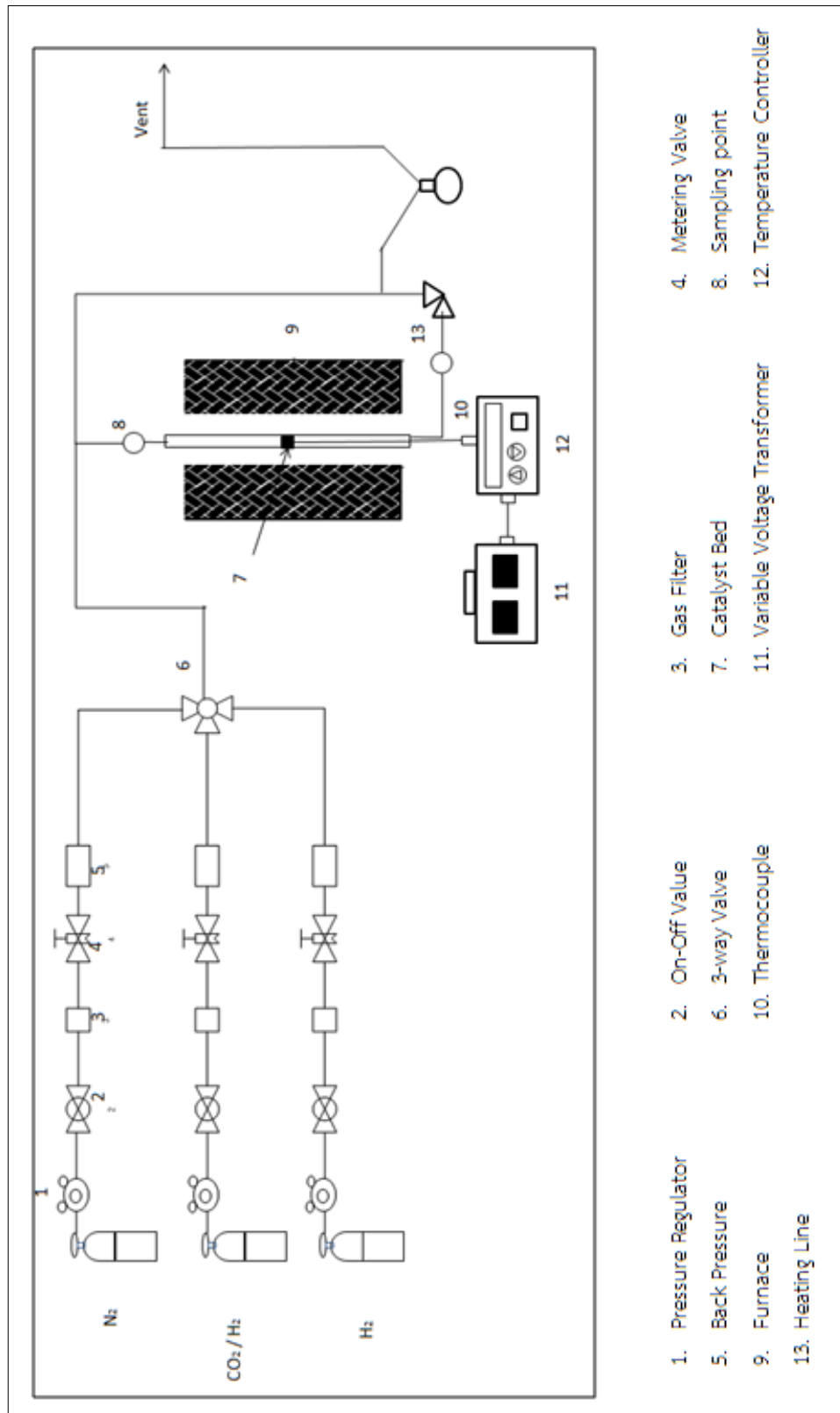


Figure 4. 1 Flow diagram of carbon dioxide hydrogenation system

## CHAPTER V

### RESULTS AND DISCUSSION

This chapter is divided into three main parts: part (5.1) describes the effect of magnesium and aluminium modified  $\text{Al}_2\text{O}_3$  supported  $\text{Co}/\text{Al}_2\text{O}_3$  catalysts with different loading (1, 2.5, 3.55 and 10 wt.%) of magnesium and aluminium nitrate in  $\gamma\text{-Al}_2\text{O}_3$  support, part (5.2) describes the effect of basic oxide ( $\text{MgO}$ ,  $\text{CaO}$ , and  $\text{La}_2\text{O}_3$ ) modified  $\text{Al}_2\text{O}_3$  supported  $\text{Co}/\text{Al}_2\text{O}_3$  catalysts using calcination temperatures of modified support at  $900\text{ }^\circ\text{C}$  and the last part describes the effect of basic oxide ( $\text{MgO}$ ,  $\text{CaO}$ , and  $\text{La}_2\text{O}_3$ ) modified  $\text{Co}/\text{Al}_2\text{O}_3$  catalysts (calcination temperatures of modified support at  $550\text{ }^\circ\text{C}$ ).

This chapter presents the catalyst characterization by several techniques including XRD, BET, SEM, TEM,  $\text{NH}_3\text{-TPD}$ ,  $\text{H}_2\text{-TPR}$  and  $\text{H}_2\text{-chemisorption}$ . For  $\text{CO}_2$  hydrogenation, the reaction was carried out at  $270\text{ }^\circ\text{C}$  and atmosphere pressure with the reactant feed gas  $\text{H}_2/\text{CO}_2$  ratio of 10/1

The nomenclature used for the basic oxide modified alumina supported cobalt catalysts in this study are as follows:

**x% MgAl** is referred to the modified alumina support prepared from impregnating  $\gamma\text{-Al}_2\text{O}_3$  with the mixture solution of  $\text{Al}(\text{NO}_3)_3 \cdot 9\text{H}_2\text{O}$  and  $\text{Mg}(\text{NO}_3)_2 \cdot 6\text{H}_2\text{O}$  based on the calculation for the preparation of the x% of  $\text{MgAl}_2\text{O}_4$  on  $\text{Al}_2\text{O}_3$  support.

**2.5% Mg** is referred to the modified alumina support prepared from impregnating  $\gamma\text{-Al}_2\text{O}_3$  with an aqueous solution of  $\text{Mg}(\text{NO}_3)_2 \cdot 6\text{H}_2\text{O}$  based on the calculation for the preparation of the 2.5% of Mg on  $\text{Al}_2\text{O}_3$  support.

**2.5% La** is referred to the modified alumina support prepared from impregnating  $\gamma$ - $\text{Al}_2\text{O}_3$  with an aqueous solution of  $\text{La}(\text{NO}_3)_3 \cdot 6\text{H}_2\text{O}$  based on the calculation for the preparation of the 2.5% of La on  $\text{Al}_2\text{O}_3$  support.

**2.5% Ca** is referred to the modified alumina support prepared from impregnating  $\gamma$ - $\text{Al}_2\text{O}_3$  with an aqueous solution of  $\text{Ca}(\text{NO}_3)_2 \cdot 4\text{H}_2\text{O}$  based on the calculation for the preparation of the 2.5% of Ca on  $\text{Al}_2\text{O}_3$  support.

## 5.1 Effect of MgAl- modified $\text{Al}_2\text{O}_3$ supported Co/ $\text{Al}_2\text{O}_3$ catalysts

### 5.1.1 Characterization of the catalysts

#### 5.1.1.1 X-ray diffraction (XRD)

The XRD patterns of the non-modified and MgAl- modified alumina support with different loadings (1, 2.5, 3.55 and 10 wt.%) of magnesium and aluminium nitrate in  $\gamma$ - $\text{Al}_2\text{O}_3$  support are presented in **Figure 5.1**. The patterns were recorded in the  $2\theta$  range of 10-80°. The non-modified alumina support shows the characteristic diffraction lines corresponding to the (440), (400), and (311) planes of the gamma phase of alumina at  $2\theta$  degrees 66.79°, 45.76° and 37.58°, respectively. For the  $\gamma$ - $\text{Al}_2\text{O}_3$  modified with MgAl contents ranging between 1-3.55 wt.% MgAl, the XRD peaks were also similar to the  $\gamma$ - $\text{Al}_2\text{O}_3$  pattern and there were no indication of the  $\text{MgAl}_2\text{O}_4$  formation. On the other hand, the diffraction patterns of  $\gamma$ - $\text{Al}_2\text{O}_3$  modified with the highest MgAl loading (10 wt.%) showed the characteristics of the  $\text{MgAl}_2\text{O}_4$  spinel formation. However, the  $\text{MgAl}_2\text{O}_4$  spinel and  $\gamma$ - $\text{Al}_2\text{O}_3$  diffraction patterns were very similar. A shift of diffraction line to lower  $2\theta$  degrees can be ascribed to the formation of a spinel [25], due probably to the high addition of MgAl contained an excess of magnesium in the relation to the required content to completely transform the alumina support into the spinel phase [25]. The characteristic reflection observed

for the 10 wt.% of magnesium and aluminium nitrate in  $\gamma$ - $\text{Al}_2\text{O}_3$ : might be attributed to a strong interaction between Mg and gamma alumina support related to the high amount being added.

The XRD patterns of MgAl- modified alumina supported cobalt catalysts with different loadings (1, 2.5, 3.55 and 10 wt.%) of magnesium and aluminium nitrate in  $\gamma$ - $\text{Al}_2\text{O}_3$  are presented in Figure 5.2. The spectra were recorded in the  $2\theta$  range of 10-80 degrees. The diffraction peaks at  $45.7^\circ$  and  $66.6^\circ$  were attributed to the  $\gamma$ - $\text{Al}_2\text{O}_3$  support and the peaks at  $31.4^\circ$ ,  $36.9^\circ$ ,  $45.0^\circ$ ,  $59.5^\circ$ , and  $65.5^\circ$  were assigned to the  $\text{Co}_3\text{O}_4$  phase [7], which existed on all the catalysts.

It was found that the non-modified  $\text{Co}/\text{Al}_2\text{O}_3$  catalysts exhibited lower intensity XRD patterns than the magnesium and aluminium nitrate modified  $\text{Co}/\text{Al}_2\text{O}_3$  catalysts, due probably to the average crystalline size of  $\text{Co}_3\text{O}_4$  were smaller than magnesium and aluminium nitrate modified  $\text{Co}/\text{Al}_2\text{O}_3$  catalysts. The average crystallite size of  $\text{Co}_3\text{O}_4$ , calculated from line broadening of  $\text{Co}_3\text{O}_4$  at  $2\theta = 37^\circ$  diffraction peak using the Scherrer's equation are presented in **Table 5.1**. For the magnesium and aluminium nitrate modified  $\text{Co}/\text{Al}_2\text{O}_3$  catalysts, the crystallite size of  $\text{Co}_3\text{O}_4$  decreased with increasing amount of magnesium and aluminium nitrate. The crystallite size obtained from MgAl-modified  $\text{Al}_2\text{O}_3$  support were 15.0-17.5 nm whereas the average crystalline size of  $\text{Co}_3\text{O}_4$  particles obtained from non-modified  $\text{Co}/\text{Al}_2\text{O}_3$  catalysts was 11.7 nm.



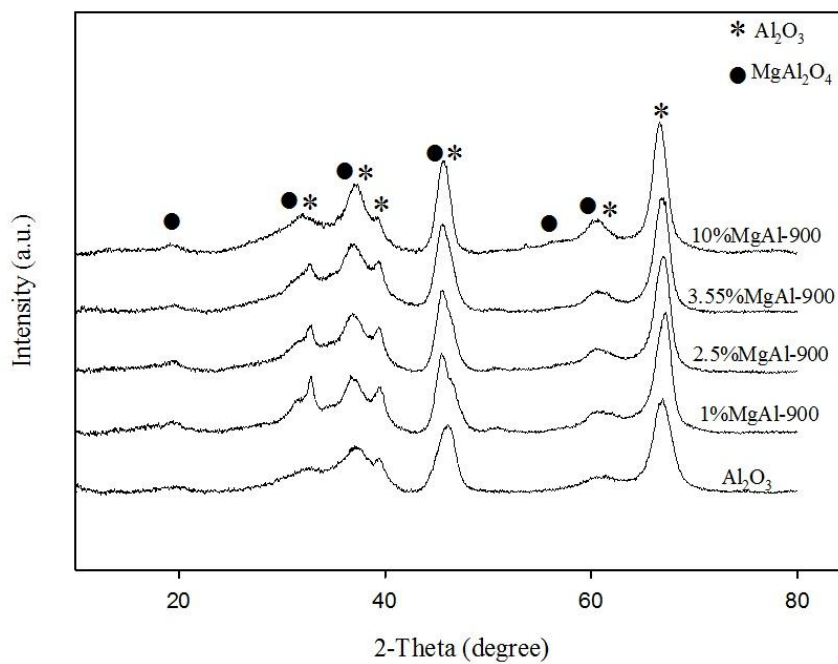


Figure 5. 1 The XRD patterns of the non-modified and MgAl- modified alumina support.

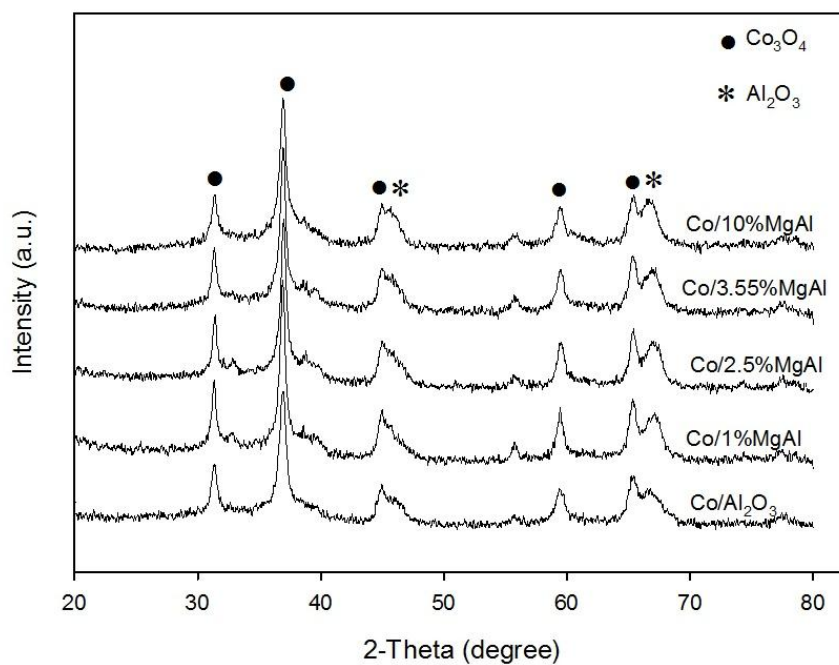


Figure 5. 2 The XRD patterns of MgAl- modified alumina supported cobalt catalysts

Table 5. 1 Average  $\text{Co}_3\text{O}_4$  crystallite size of alumina supported cobalt catalysts after calcination at 650 °C and BET surface area of the support.

Samples	Average $\text{Co}_3\text{O}_4$ crystallite size from XRD (nm)	BET surface area ( $\text{m}^2/\text{g}$ )
10%MgAl	15.0	81
3.55%MgAl	15.5	104
2.5%MgAl	16.2	81
1%MgAl	17.5	105
$\text{Al}_2\text{O}_3$	11.7	125

#### 5.1.1.2 BET surface areas

The textural properties of the modified alumina support were determined by BET, which is the most common method for determining surface area of solid by using adsorption and condensation of  $\text{N}_2$  at liquid nitrogen temperature.

BET surface area of the non-modified and MgAl-modified  $\gamma\text{-Al}_2\text{O}_3$  supports are compared in **Table 5.1**. The non-modified  $\gamma\text{-Al}_2\text{O}_3$  support had the BET specific surface area of 125  $\text{m}^2/\text{g}$  whereas lower surface areas (81-105  $\text{m}^2/\text{g}$ ) were obtained on MgAl-modified alumina support. There were no significant differences between surface area of MgAl-modified  $\gamma\text{-Al}_2\text{O}_3$  supports with different loadings (1, 2.5, 3.55 and 10 wt.%) of magnesium and aluminium nitrate in  $\gamma\text{-Al}_2\text{O}_3$  support and the support surface area was not directly related to the catalytic activity in this study.

#### 5.1.1.3 Scanning electron microscopy

The morphologies of  $\text{Co}/\text{Al}_2\text{O}_3$  catalysts with different loading (1, 2.5, 3.55 and 10 wt.%) of MgAl after calcinations were investigated by SEM. The particle

morphologies of the magnesium and aluminium modified  $\text{Al}_2\text{O}_3$  supported  $\text{Co}/\text{Al}_2\text{O}_3$  catalysts with different loading (1, 2.5, 3.55 and 10 wt.%) of magnesium and aluminium nitrate in  $\gamma\text{-Al}_2\text{O}_3$  supports are shown in **Figure 5.3**. The magnesium and aluminium modified  $\text{Al}_2\text{O}_3$  supported  $\text{Co}/\text{Al}_2\text{O}_3$  catalysts micrographs showed spherical shape particles with diameter around 10-20  $\mu\text{m}$ . There were no significant differences between particle morphologies of different catalysts.

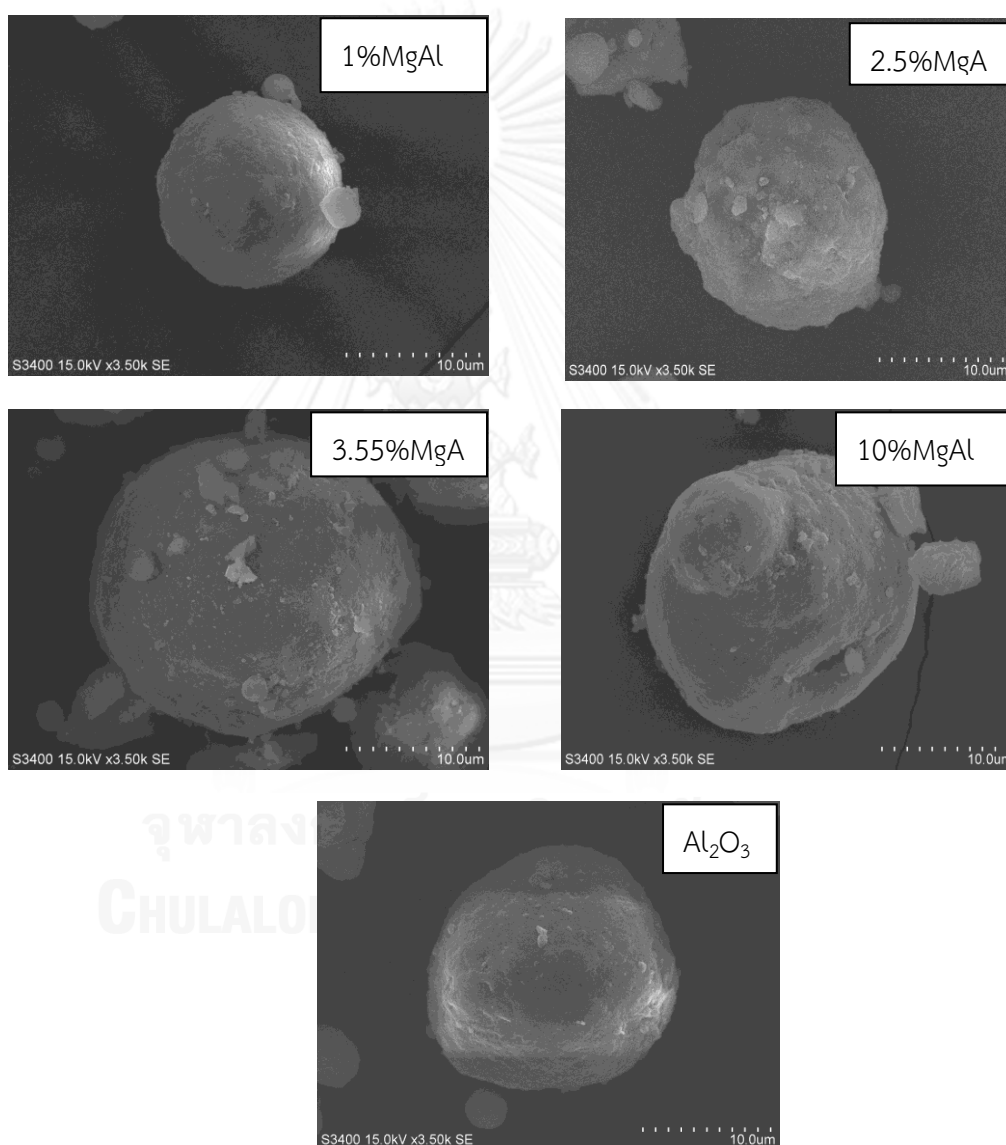


**Figure 5. 3** SEM images of MgAl- modified alumina supported cobalt catalysts

#### 5.1.1.4 Temperature Programmed Reduction (TPR)

The TPR profiles for all the magnesium and aluminium nitrate modified alumina supported cobalt catalysts are shown in **Figure 5.4**. The H<sub>2</sub>-consumption values calculated from TPR peak of all the catalysts are presented in **Table 5.2**. The H<sub>2</sub>-TPR was performed to determine the reduction behavior of the supported cobalt catalysts. All the catalysts exhibited two major reduction peaks. The occurrence of multiple reduction peaks indicates the presence of a number of reducible cobalt species in the precursor samples. Co<sub>3</sub>O<sub>4</sub> can be reduced by hydrogen to form Co via a two-step reduction of Co<sub>3</sub>O<sub>4</sub> to CoO and then to Co<sup>0</sup> [36]. The first peak could be assigned to the reduction of Co<sub>3</sub>O<sub>4</sub> to CoO [7]. The second peak is ascribed to the subsequent reduction of CoO to Co<sup>0</sup>. For the non-modified Co/Al<sub>2</sub>O<sub>3</sub> catalysts, the first peak centered at around 485°C, while the second broad peak distributed from 510°C to 770°C (centered at 610°C). Besides these two main reduction peaks, a small peak appeared at about 250°C. This peak could be attributed to the reduction of the residual cobalt nitrate [7], which usually decomposed completely above 400°C [3]. For the 1%MgAl-modified Co/Al<sub>2</sub>O<sub>3</sub> catalysts, the sharp peak at low temperature zone slightly shifted from 485 °C for non-modified Co/Al<sub>2</sub>O<sub>3</sub> catalyst to higher temperature 520°C for 1%MgAl-modified Co/Al<sub>2</sub>O<sub>3</sub> catalyst and a second reduction peak with maximum at about 590°C. Furthermore, Co/Al<sub>2</sub>O<sub>3</sub>-1%MgAl catalyst had higher H<sub>2</sub> consumption than the non-modified Co/Al<sub>2</sub>O<sub>3</sub> catalysts. On the other hand, for the Co/Al<sub>2</sub>O<sub>3</sub>-2.5%MgAl catalyst, both reduction peaks were shifted to lower temperature, with the first peak centered at around 430°C and the second peak at around 600°C. Moreover, Co/Al<sub>2</sub>O<sub>3</sub>-2.5%MgAl catalyst had higher H<sub>2</sub> consumption than the non-modified Co/Al<sub>2</sub>O<sub>3</sub> catalysts. It is suggested that the 2.5%MgAl- modified Co/Al<sub>2</sub>O<sub>3</sub> catalyst resulted in an increase in reducibility of the modified catalysts. For the 3.55%MgAl -modified Co/Al<sub>2</sub>O<sub>3</sub> catalyst, the sharp peak at low temperature zone shifted to 470 °C, while the second peak similar to the non-modified Co/Al<sub>2</sub>O<sub>3</sub> catalysts. However, 3.55%MgAl -modified Co/Al<sub>2</sub>O<sub>3</sub> catalyst had lower H<sub>2</sub>-consumption than the non-modified Co/Al<sub>2</sub>O<sub>3</sub> catalysts. For 10%MgAl-modified Co/Al<sub>2</sub>O<sub>3</sub> catalyst, the reduction peak occurred as a shoulder and one major peak, which located at

480 °C and 570°C, respectively. In addition, the 10%MgAl-modified Co/Al<sub>2</sub>O<sub>3</sub> catalyst had lower H<sub>2</sub>-consumption than the non-modified Co/Al<sub>2</sub>O<sub>3</sub> catalysts. As can be seen, the amount of H<sub>2</sub>-consumption for MgAl- modified Co/Al<sub>2</sub>O<sub>3</sub> catalysts slightly decreased when larger amounts of MgAl were added to the Co/Al<sub>2</sub>O<sub>3</sub> catalysts.

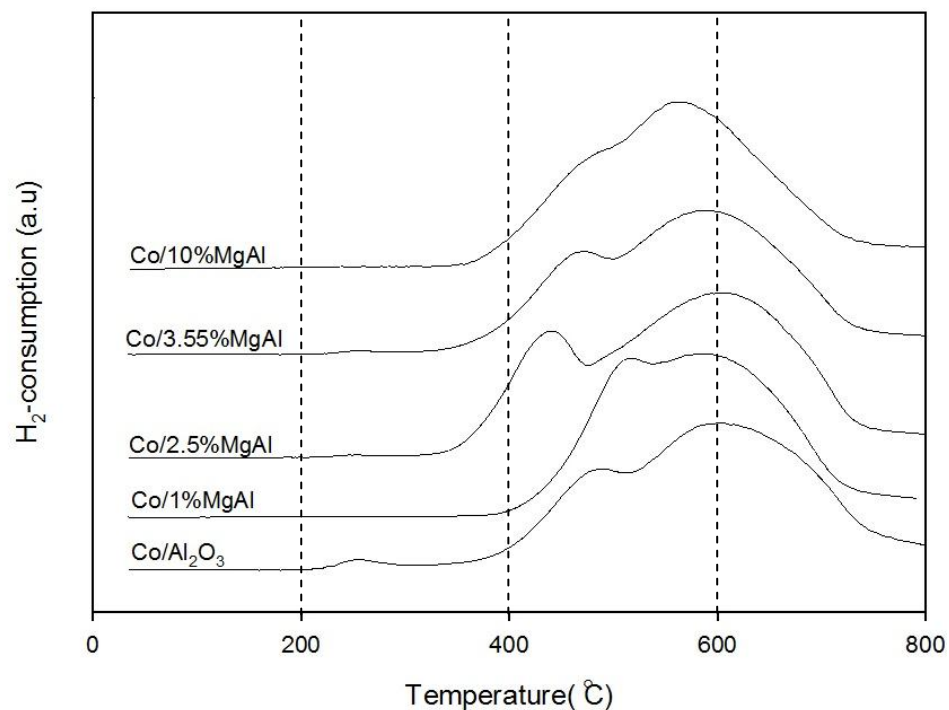


Figure 5. 4 TPR profile of MgAl- modified alumina supported cobalt catalysts

Table 5. 2 H<sub>2</sub> consumption for the TPR profile calculation of MgAl- modified alumina supported cobalt catalysts

Samples	H <sub>2</sub> -Consumption (mmol/g <sub>cat</sub> )
10%MgAl	151
3.55%MgAl	145
2.5%MgAl	189
1%MgAl	160
Al <sub>2</sub> O <sub>3</sub>	154

#### 5.1.1.5 Temperature-programmed desorption (NH<sub>3</sub>-TPD)

NH<sub>3</sub>-temperature program desorption was a commonly used technique for titration of surface acid sites. The strength of an acid site could be related to the corresponding desorption temperature, while the total amount of ammonia desorption after saturation coverage permits quantification of the number of acid sites at the surface[21]. The NH<sub>3</sub>-TPD profiles for the non-modified and magnesium and aluminium modified Al<sub>2</sub>O<sub>3</sub> supported Co/Al<sub>2</sub>O<sub>3</sub> catalysts with different loadings (1, 2.5, 3.55 and 10 wt.%) of MgAl in  $\gamma$ -Al<sub>2</sub>O<sub>3</sub> supports are shown in **Figure 5.5** and the acidity values calculated from TPD peak of all supports are presented in **Table 5.3**. It was found that the non-modified  $\gamma$ -Al<sub>2</sub>O<sub>3</sub> support exhibited two major desorption peak. The occurrence of multiple desorption peaks corresponded to the different of acid site in non-modified  $\gamma$ -Al<sub>2</sub>O<sub>3</sub> support, which are weak acid sites (occurring at low temperatures) and strong acid sites (occurring at high temperatures). The MgAl-modified Al<sub>2</sub>O<sub>3</sub> supports with different loadings (1, 2.5, 3.55 and 10 wt.%) of MgAl exhibited lower desorption peak area than the non-modified Al<sub>2</sub>O<sub>3</sub> support. It is suggested that MgAl-modified alumina supports resulted in a decrease in surface

acidity of  $\gamma$ - $\text{Al}_2\text{O}_3$  especially the strong acid sites. The decrement of the surface acidity of  $\gamma$ - $\text{Al}_2\text{O}_3$  modified with MgAl may be due to the basic nature of magnesium nitrate.

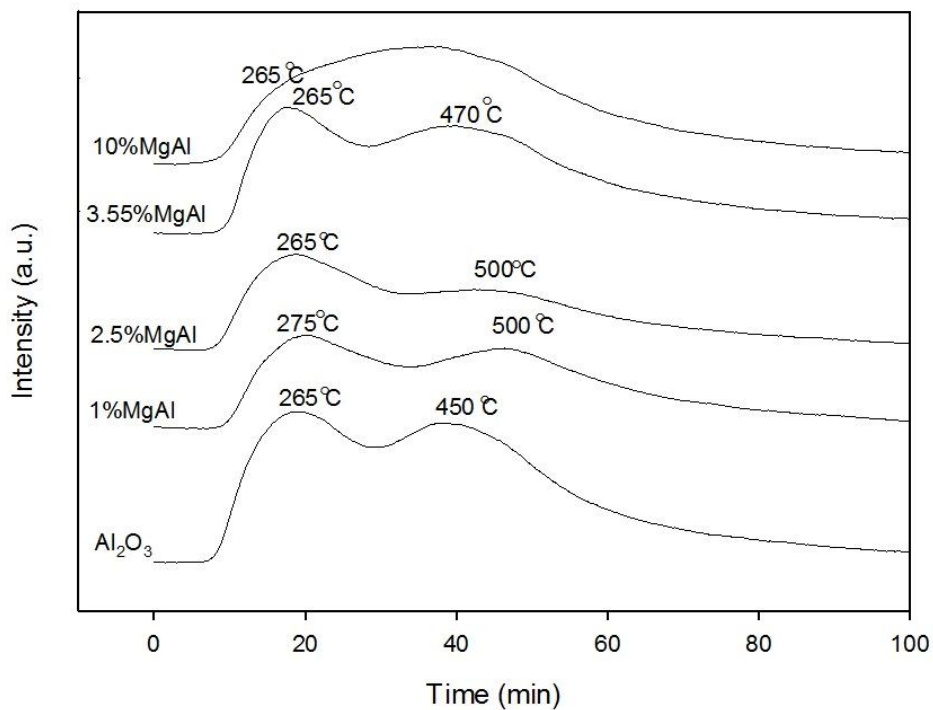


Figure 5. 5  $\text{NH}_3$ -TPD profile of MgAl- modified alumina supports

Table 5. 3 The acidity of MgAl- modified alumina supports

Samples	Total acid site ( $\text{mmol/g}_{\text{cat}}$ )
10%MgAl	4.5
3.55%MgAl	4.1
2.5%MgAl	3.7
1%MgAl	3.6
$\text{Al}_2\text{O}_3$	5.4

### 5.1.1.6 Hydrogen Chemisorption

The hydrogen chemisorption was a commonly used technique for determining the amount of active sites of catalyst.

The amount of H<sub>2</sub> uptake and overall Co dispersion on the non-modified and magnesium and aluminium modified Al<sub>2</sub>O<sub>3</sub> supported Co/Al<sub>2</sub>O<sub>3</sub> catalysts with different loading (1, 2.5, 3.55 and 10 wt.%) of MgAl in  $\gamma$ -Al<sub>2</sub>O<sub>3</sub> supports are shown in **Table 5.4**. The amount of H<sub>2</sub> uptake on MgAl-modified Co/Al<sub>2</sub>O<sub>3</sub> catalysts with different loadings (1, 2.5, 3.55 and 10 wt.%) of MgAl in  $\gamma$ -Al<sub>2</sub>O<sub>3</sub> supports were ranging between 8.9-22.3  $\mu$ mol H<sub>2</sub>/g of catalysts. It was found that the magnesium and aluminium nitrate modified Co/Al<sub>2</sub>O<sub>3</sub> catalysts exhibited higher amount of H<sub>2</sub> uptake on catalytic phase than non-modified Co/Al<sub>2</sub>O<sub>3</sub> catalysts, except 10%MgAl-modified Co/Al<sub>2</sub>O<sub>3</sub> catalysts. As can be seen, the amounts of H<sub>2</sub> chemisorption slightly increased when the amounts of MgAl increased indicating that the cobalt active sites increased when MgAl were added to the catalysts. In addition, the amount of H<sub>2</sub> uptake on catalytic phase of 3.55%MgAl- and 2.5%MgAl- modified Co/Al<sub>2</sub>O<sub>3</sub> catalysts increased from 15.1  $\mu$ mol H<sub>2</sub>/g of catalysts for the original Co/Al<sub>2</sub>O<sub>3</sub> catalysts to 22.3 and 19.5  $\mu$ mol H<sub>2</sub>/g of catalysts for 3.55%MgAl and 2.5%MgAl modified Co/Al<sub>2</sub>O<sub>3</sub> catalysts, respectively. Moreover, 3.55%MgAl- and 2.5%MgAl- modified Co/Al<sub>2</sub>O<sub>3</sub> catalysts exhibited higher overall cobalt dispersion. It is suggested that MgAl-modified alumina support cobalt catalysts resulted in an increase in cobalt dispersion on surface of the alumina supports. The addition of MgAl promoter could suppress the strong interaction between cobalt metal and the support hence the reducibility of the catalysts was improved. However, the amount of H<sub>2</sub> uptake and overall cobalt dispersion decreased significantly when large amounts of MgAl were added to the catalysts. In this case, the decrement of reducible cobalt species may be due to the formation of magnesium aluminate on the support and/or the interaction between cobalt oxide and magnesia was stronger resulted in the formation of CoO-MgO solid solution [34], in agreement with the results published by [34]. The H<sub>2</sub> chemisorption results are in good agreement with results from XRD and TPR experiments.



Table 5. 4 The total H<sub>2</sub> chemisorption of MgAl- modified alumina supported cobalt catalysts

Samples	Total H <sub>2</sub> chemisorption ( $\mu\text{mol H}_2/\text{g}_{\text{cat}}$ )	%Cobalt Dispersion
10%MgAl	8.9	3.5
3.55%MgAl	22.3	8.8
2.5%MgAl	19.5	7.7
1%MgAl	16.4	6.4
Al <sub>2</sub> O <sub>3</sub>	15.1	5.9

### 5.1.2 Reaction study in CO<sub>2</sub> hydrogenation

The reaction study was carried out in carbon dioxide hydrogenation to determine catalytic activity of the MgAl-modified Co/Al<sub>2</sub>O<sub>3</sub> catalysts. Activation of the cobalt catalyst involved reductive treatment with hydrogen at 350 °C for 3 h. The CO<sub>2</sub> hydrogenation was carried out at 270 °C and atmosphere pressure. The reactant feed gas H<sub>2</sub>/CO<sub>2</sub> ratio of 10/1 was flowed through the sample at a total flow rate of 30 ml/min.

The carbon dioxide conversion and product selectivity during carbon dioxide hydrogenation reaction are presented in **Table 5.5** and **Figure 5.6**. The catalytic activity for CO<sub>2</sub> hydrogenation on non-modified alumina support cobalt catalyst obviously changed when adding MgAl on alumina support cobalt catalyst. The steady state CO<sub>2</sub> conversion of non-modified and MgAl-modified alumina support cobalt catalysts were ranging between 37.6-61.8% in the order: 2.5%MgAl > Al<sub>2</sub>O<sub>3</sub> > 1%MgAl > 3.55%MgAl > 10%MgAl. The catalyst modified by 2.5%MgAl and 1%MgAl exhibited higher catalytic activity than the corresponding non-modified and the 3.55%MgAl- and 10%MgAl-modified Al<sub>2</sub>O<sub>3</sub> supported ones. Although the unmodified Co/Al<sub>2</sub>O<sub>3</sub> catalyst showed the highest initial CO<sub>2</sub> conversion at 61.2% but the sample was gradually deactivated with time on stream and reached the steady-state conversion at 55.2%.

The steady-state CO<sub>2</sub> conversion for the 2.5%MgAl- and 1%MgAl- modified Co/Al<sub>2</sub>O<sub>3</sub> catalyst were 61.8% and 57.5%, respectively and the CH<sub>4</sub> selectivity were 100%. The catalytic activity and catalyst stability were greatly improved by addition of small amount of MgAl. It is well known that the strong interaction between cobalt and alumina support bring about the formation of inactive CoAl<sub>2</sub>O<sub>4</sub> species relative to the low reducibility and low catalytic activity. The interaction of the reducible species (cobalt) with alumina support is more important in this study. It was found that the addition of 2.5%MgAl- modified Co/Al<sub>2</sub>O<sub>3</sub> catalyst could suppress the interaction between cobalt metal and alumina support. The TPR result also indicated that the addition of 2.5% MgAl result in the shift of reduction peaks to lower temperature, meaning that the interaction between reducible species (cobalt) and alumina support were weaker, suggesting that in this case, the quantity of reducible cobalt species was higher than other supported cobalt catalysts. The H<sub>2</sub>-chemisorption results also indicated that the addition of small amount of MgAl exhibited higher amount of H<sub>2</sub>-chemisorption and overall cobalt dispersion, which is related to the increasing of Co<sup>0</sup> sites (active sites). Therefore, the small amount of MgAl modification increased not only the reducibility of cobalt catalysts but also the catalytic activity in carbon dioxide hydrogenation under methanation condition. On the other hand, addition of larger amount of MgAl showed an opposite trend in which the activity for CO<sub>2</sub> hydrogenation decreased. As can be seen from TPR result, the amount of H<sub>2</sub>-consumption for MgAl-modified Co/Al<sub>2</sub>O<sub>3</sub> catalysts slightly decreased when larger amounts of MgAl were added to the Co/Al<sub>2</sub>O<sub>3</sub> catalysts. In this case, the quantity of reducible cobalt species may be lower. According to H<sub>2</sub>-chemisorption analyses, amount of H<sub>2</sub> uptake and overall cobalt dispersion decreased significantly when large amounts of MgAl were added to the catalysts. Therefore, the lower activities were obtained. According to XRD analyses, high addition of MgAl resulted in the formation of MgAl<sub>2</sub>O<sub>4</sub>. In this case, the decrement of reducible cobalt species may be due to the formation of magnesium aluminate on the support and/or the interaction between cobalt oxide and magnesia was stronger resulted in the formation of CoO-MgO solid solution and/or very weak interaction between metal and support. Normally, the metal-support interaction may also be divided into three categories: (1) very weak

interaction between metal and support (2) formation of solid solution, for example CoO-MgO-Al<sub>2</sub>O<sub>3</sub> system (3) strong between metal and support or metal-support compound formation [34]. In this study (alumina supported cobalt catalysts), the reducibility of the Co species often depends on the interaction between cobalt metal and alumina support.

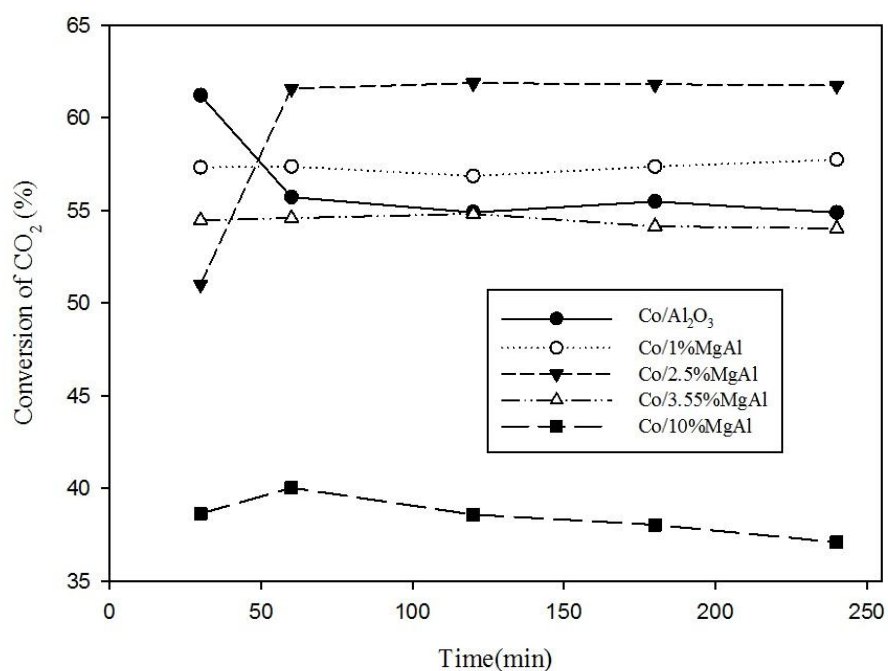


Figure 5. 6 Performances of catalysts with the various modified support in CO<sub>2</sub> hydrogenation.

Table 5. 5 The conversion and product selectivity during CO<sub>2</sub> hydrogenation on MgAl- modified alumina supported cobalt catalysts

Samples	Conversion		Product Selectivity (%)	
	Initial	Steady state	CH <sub>4</sub>	CO
10%MgAl	38.6	37.6	100	0
3.55%MgAl	54.5	54.1	100	0
2.5%MgAl	51.0	61.8	100	0
1%MgAl	57.3	57.5	100	0
Al <sub>2</sub> O <sub>3</sub>	61.2	55.2	100	0

## 5.2 Effect of basic oxide (MgO, CaO, and La<sub>2</sub>O<sub>3</sub>) modified Al<sub>2</sub>O<sub>3</sub> supported Co/Al<sub>2</sub>O<sub>3</sub> catalysts using calcination temperatures of modified support at 900 °C

### 5.2.1 Characterization of the catalysts

#### 5.2.1.1 X-ray diffraction (XRD)

The XRD patterns of basic oxide (MgO, CaO, and La<sub>2</sub>O<sub>3</sub>) modified Al<sub>2</sub>O<sub>3</sub> supported using calcination temperatures of modified support at 900 °C are presented in **Figure 5.7**. The patterns were recorded in the  $2\theta$  range of 10-80°. The non-modified alumina support shows the characteristic diffraction lines corresponding to the (440), (400), and (311) planes of the gamma phase of alumina at  $2\theta$  degrees 66.79°, 45.76° and 37.58°, respectively. For the La and Ca modified  $\gamma$ -Al<sub>2</sub>O<sub>3</sub>, the diffraction lines were similar to the  $\gamma$ -Al<sub>2</sub>O<sub>3</sub> pattern and the diffraction patterns of La<sub>2</sub>O<sub>3</sub> and CaO phase were not detected, due probably to the high dispersion of these oxides or the relatively low amount being added [7]. For the  $\gamma$ -Al<sub>2</sub>O<sub>3</sub> modified with magnesium and aluminium nitrate calcined at 900°C, the XRD peaks were also

similar to the  $\gamma$ - $\text{Al}_2\text{O}_3$  pattern and there was no indication of the  $\text{MgAl}_2\text{O}_4$  formation. On the other hand, the diffraction patterns of  $\gamma$ - $\text{Al}_2\text{O}_3$  modified with magnesium nitrate and calcined at  $900^\circ\text{C}$  showed the characteristics of the  $\text{MgAl}_2\text{O}_4$  spinel formation [10]. A shift of diffraction line to lower  $2\theta$  degrees can be ascribed to the formation of a spinel [25]. In this case, the formation of  $\text{MgAl}_2\text{O}_4$  spinel may be due to the high amount of magnesium nitrate being added.

The XRD patterns of the basic oxide ( $\text{MgO}$ ,  $\text{CaO}$ , and  $\text{La}_2\text{O}_3$ ) modified  $\text{Al}_2\text{O}_3$  (calcinations temperature at  $900^\circ\text{C}$ ) supported  $\text{Co}/\text{Al}_2\text{O}_3$  catalysts are presented in Figure 5.8. The patterns were recorded in the  $2\theta$  range of  $10$ - $80$  degrees. The diffraction peaks at  $45.7^\circ$  and  $66.6^\circ$  were attributed to the  $\gamma$ - $\text{Al}_2\text{O}_3$  support and the peaks at  $31.4^\circ$ ,  $36.9^\circ$ ,  $45.0^\circ$ ,  $59.5^\circ$ , and  $65.5^\circ$  were assigned to the  $\text{Co}_3\text{O}_4$  phase [7], which existed on all the catalysts.

The average crystallite size of  $\text{Co}_3\text{O}_4$ , calculated from line broadening of  $\text{Co}_3\text{O}_4$  at  $2\theta = 37^\circ$  diffraction peak using the Scherrer's equation are presented in Table 5.6. It was found that the crystallite size of  $\text{Co}_3\text{O}_4$  obtained from the addition of Ca, Mg and MgAl- modified  $\text{Al}_2\text{O}_3$  supported  $\text{Co}/\text{Al}_2\text{O}_3$  catalysts were  $12.8$ - $16.2$  nm whereas that the average crystalline size of  $\text{Co}_3\text{O}_4$  particles obtained from non-modified  $\text{Co}/\text{Al}_2\text{O}_3$  catalysts was  $11.7$  nm. In addition, the average crystalline size of  $\text{Co}_3\text{O}_4$  particles obtained from MgAl- and La- modified  $\text{Al}_2\text{O}_3$  supported  $\text{Co}/\text{Al}_2\text{O}_3$  catalysts were  $16.2$  and  $15.0$  nm, respectively. It is suggested that basic oxide modified  $\text{Al}_2\text{O}_3$  supported  $\text{Co}/\text{Al}_2\text{O}_3$  catalysts resulted in increased average crystallite size of  $\text{Co}_3\text{O}_4$  particle.

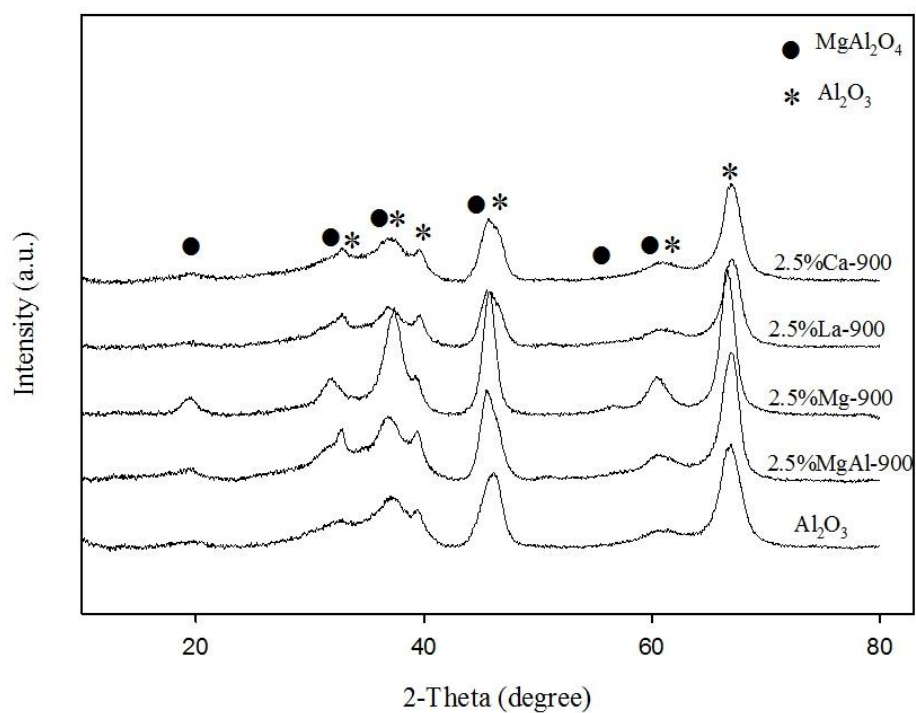


Figure 5. 7 The XRD patterns of the non-modified and basic oxide modified alumina support after calcination at 900 °C

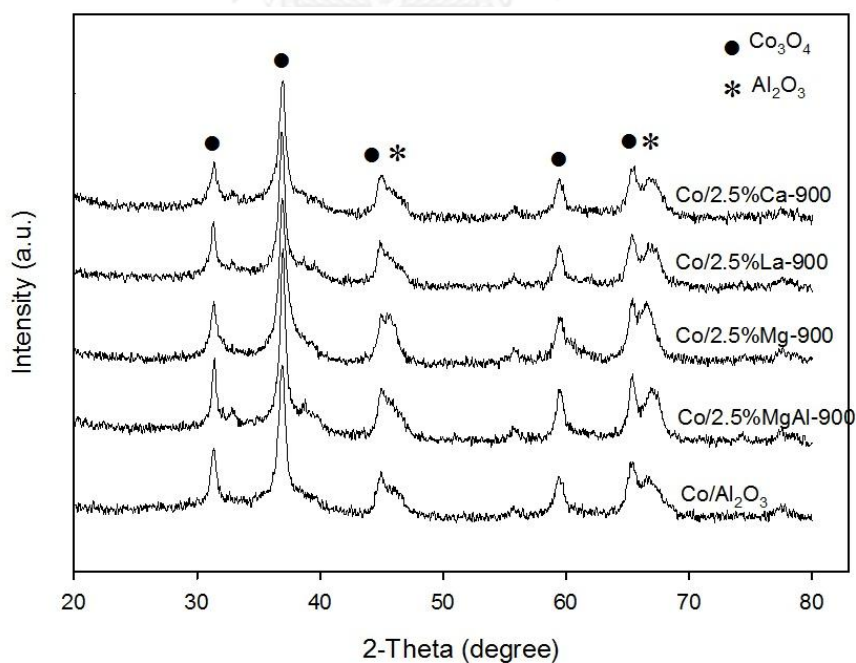


Figure 5. 8 The XRD patterns of non-modified and basic oxide modified Co/ $\text{Al}_2\text{O}_3$  catalysts.

Table 5. 6 Average  $\text{Co}_3\text{O}_4$  crystallite size and BET surface area of the support

Samples	Average $\text{Co}_3\text{O}_4$ crystallite size from XRD (nm)	BET surface area ( $\text{m}^2/\text{g}$ )
2.5%Ca-900	13.1	118
2.5%La-900	15.0	115
2.5%Mg-900	12.8	102
2.5%MgAl-900	16.2	81
$\text{Al}_2\text{O}_3$	11.7	125

#### 5.2.1.2 BET surface areas

BET surface area of non-modified and basic oxide ( $\text{MgO}$ ,  $\text{CaO}$ , and  $\text{La}_2\text{O}_3$ ) modified  $\text{Al}_2\text{O}_3$  supported using calcinations temperatures of modified support at 900 °C are compared in **Table 5.7**. The non-modified  $\gamma\text{-Al}_2\text{O}_3$  support had the BET specific surface area of 125  $\text{m}^2/\text{g}$  whereas the lower surface areas (81-118  $\text{m}^2/\text{g}$ ) were obtained on basic oxide ( $\text{MgO}$ ,  $\text{CaO}$ , and  $\text{La}_2\text{O}_3$ ) modified  $\text{Al}_2\text{O}_3$  supported using calcination temperatures of modified support at 900 °C. There were no significant differences between surface area of non-modified and basic oxide ( $\text{MgO}$ ,  $\text{CaO}$ , and  $\text{La}_2\text{O}_3$ ) modified  $\text{Al}_2\text{O}_3$  supported using calcination temperatures of modified support at 900 °C and the support surface area was not directly related to the catalytic activity in this study.

### 5.2.1.3 Scanning electron microscopy

The morphologies of Co/Al<sub>2</sub>O<sub>3</sub> catalysts with different basic oxide (MgO, CaO, and La<sub>2</sub>O<sub>3</sub>) modified Al<sub>2</sub>O<sub>3</sub> support using calcination temperatures of modified support at 900 °C were investigated by SEM. The particle morphologies of the basic oxide (MgO, CaO, and La<sub>2</sub>O<sub>3</sub>) modified Al<sub>2</sub>O<sub>3</sub> supported cobalt catalysts are shown in **Figure 5.9**. In all of the basic oxide (MgO, CaO, and La<sub>2</sub>O<sub>3</sub>) modified Al<sub>2</sub>O<sub>3</sub> supported Co/Al<sub>2</sub>O<sub>3</sub> catalysts micrographs spherical shape particles with diameter around 15 μm can be seen. There were no significant differences between particle morphologies of different catalysts.



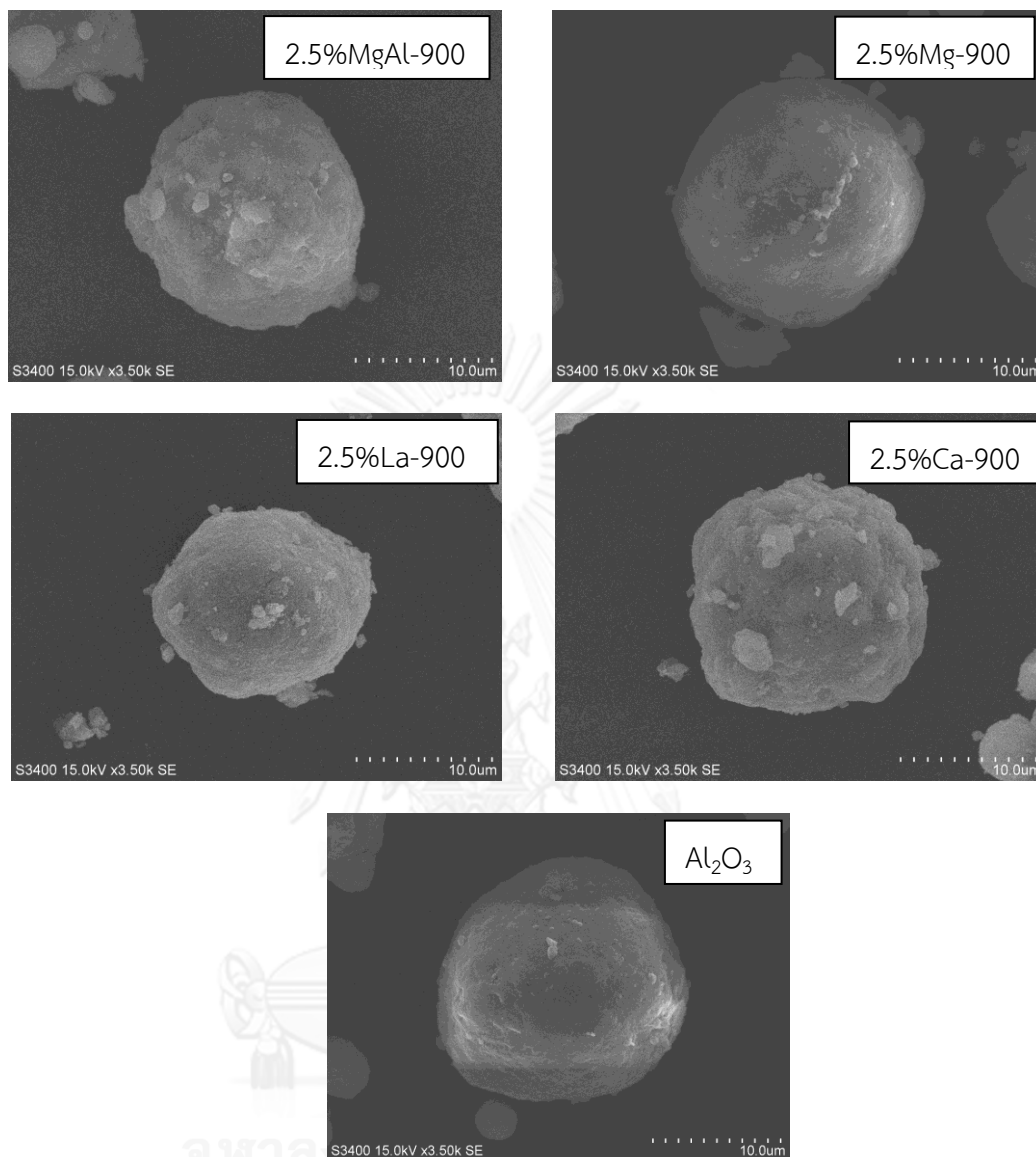


**Figure 5. 9** SEM images of basic oxide modified alumina supported cobalt catalysts (calcination temperatures of modified support at 900 °C).

#### 5.2.1.4 Temperature Programmed Reduction (TPR)

The TPR profiles for all Co/Al<sub>2</sub>O<sub>3</sub> catalysts with different basic oxide (MgO, CaO, and La<sub>2</sub>O<sub>3</sub>) modified Al<sub>2</sub>O<sub>3</sub> supported using calcination temperatures of modified support at 900 °C are shown in **Figure 5.10** and the H<sub>2</sub>-consumption values calculated from TPR peak of all catalysts are presented in **Table 5.7**. The H<sub>2</sub>-TPR was performed to determine the reduction behavior of the supported cobalt catalysts. All the catalysts exhibited two major reduction peaks. The first peak could be assigned to the reduction of Co<sub>3</sub>O<sub>4</sub> to CoO [7]. The second peak is ascribed to the subsequent reduction of CoO to Co<sup>0</sup>. For the non-modified Co/Al<sub>2</sub>O<sub>3</sub> catalysts, the first peak centered at around 485°C, while the second broad peak distributed from 510°C to 770°C (centered at 610°C). Besides these two main reduction peaks, a small peak appeared at about 250°C. This peak could be attributed to the reduction of the residual cobalt nitrate [7], which usually decomposed completely above 400°C [3]. For the MgAl-modified Co/Al<sub>2</sub>O<sub>3</sub> catalyst, both reduction peaks were shifted to lower temperature, with the first peak centered at around 430°C and the second peak at around 600°C. Moreover, Co/Al<sub>2</sub>O<sub>3</sub>-2.5%MgAl catalyst had higher H<sub>2</sub> consumption than the non-modified Co/Al<sub>2</sub>O<sub>3</sub> catalysts. In this case, the promotion of 2.5%MgAl caused changes in reduction behavior of the cobalt catalysts. The shift of reduction peak to lower temperature can be ascribed to the lower strength of interaction between cobalt metal and alumina support. On the other hand, there were also two major peaks for the Mg-modified Co/Al<sub>2</sub>O<sub>3</sub> catalyst located at 520°C and 680°C. The shift of reduction peaks towards higher temperature may be due to the formation of magnesium aluminate, which could be interacting with cobalt metal resulted in the formation of inactive CoAl<sub>2</sub>O<sub>4</sub> species bring about the reduction of cobalt metal at much higher reduction temperature. Moreover, Mg-modified Co/Al<sub>2</sub>O<sub>3</sub> catalyst had lower H<sub>2</sub> consumption than the non-modified Co/Al<sub>2</sub>O<sub>3</sub> catalysts. For the La-modified Co/Al<sub>2</sub>O<sub>3</sub> catalyst, the sharp peak at low temperature zone shifted from 485°C for the non-modified Co/Al<sub>2</sub>O<sub>3</sub> catalysts to 420°C for La-modified Co/Al<sub>2</sub>O<sub>3</sub> catalyst, while the second broad peak distributed from 450°C to 745°C (centered at 580°C). Moreover, Co/Al<sub>2</sub>O<sub>3</sub>-2.5%La catalyst had higher H<sub>2</sub> consumption than the non-modified Co/Al<sub>2</sub>O<sub>3</sub>

catalysts), indicating that La-modified cobalt catalysts increased catalysts reducibility. For the Ca-modified  $\text{Co}/\text{Al}_2\text{O}_3$  catalyst, the sharp peak at low temperature zone shifted to  $415^\circ\text{C}$ , while the second peak shift to higher temperature around  $725^\circ\text{C}$  with lower intensity. In this case, the quantity of reducible cobalt species may be lower and/or the interaction with the support was stronger. Moreover,  $\text{Co}/\text{Al}_2\text{O}_3\text{-}2.5\%\text{Ca}$  catalyst had the lowest  $\text{H}_2$  consumption.

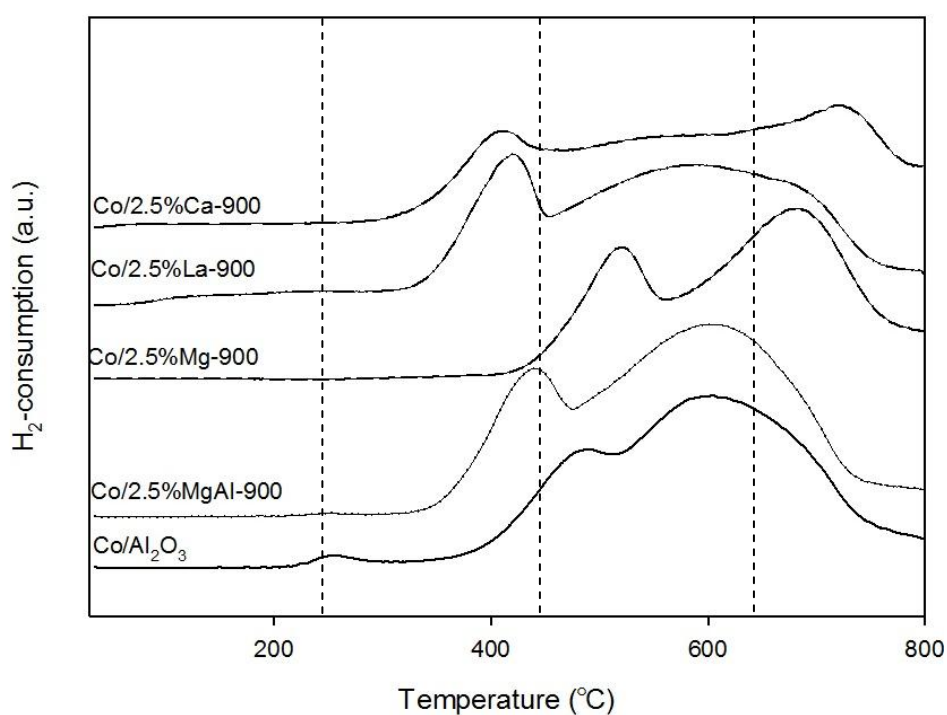


Figure 5. 10 TPR profile of basic oxide modified alumina supported cobalt catalysts (calcination temperatures of modified support at  $900^\circ\text{C}$ )

Table 5. 7 H<sub>2</sub> consumption for the TPR profile calculation of basic oxide modified alumina supported cobalt catalysts

Samples	H <sub>2</sub> -Consumption (mmol/g <sub>cat</sub> )
2.5%Ca-900	105
2.5%La-900	164
2.5%Mg-900	113
2.5%MgAl-900	189
Al <sub>2</sub> O <sub>3</sub>	154

#### 5.2.1.5 Temperature-programmed desorption (NH<sub>3</sub>-TPD)

The NH<sub>3</sub>-TPD profiles for the non-modified and basic oxide (MgO, CaO, and La<sub>2</sub>O<sub>3</sub>) modified Al<sub>2</sub>O<sub>3</sub> support using calcinations temperatures of modified support at 900 °C are shown in **Figure 5.11** and the acidity values calculated from TPD peak of all supports are presented in **Table 5.8**. It was found that the non-modified  $\gamma$ -Al<sub>2</sub>O<sub>3</sub> support exhibited two major desorption peak. The occurrence of multiple desorption peaks corresponding to the different of acid site on non-modified  $\gamma$ -Al<sub>2</sub>O<sub>3</sub> support, there are weak acid sites (occurring at low temperatures) and strong acid sites (occurring at high temperatures). However, the basic oxide (MgO, CaO, and La<sub>2</sub>O<sub>3</sub>) modified Al<sub>2</sub>O<sub>3</sub> support exhibited lower desorption peak area than the non-modified Al<sub>2</sub>O<sub>3</sub> support. It is suggested that basic oxide modified alumina supports resulted in a decrease in surface acidity of  $\gamma$ -Al<sub>2</sub>O<sub>3</sub> especially the strong acid sites. The decrement of the surface acidity of  $\gamma$ -Al<sub>2</sub>O<sub>3</sub> modified with basic oxide including MgO, CaO and La<sub>2</sub>O<sub>3</sub> may be due to the basic nature of basic oxide.

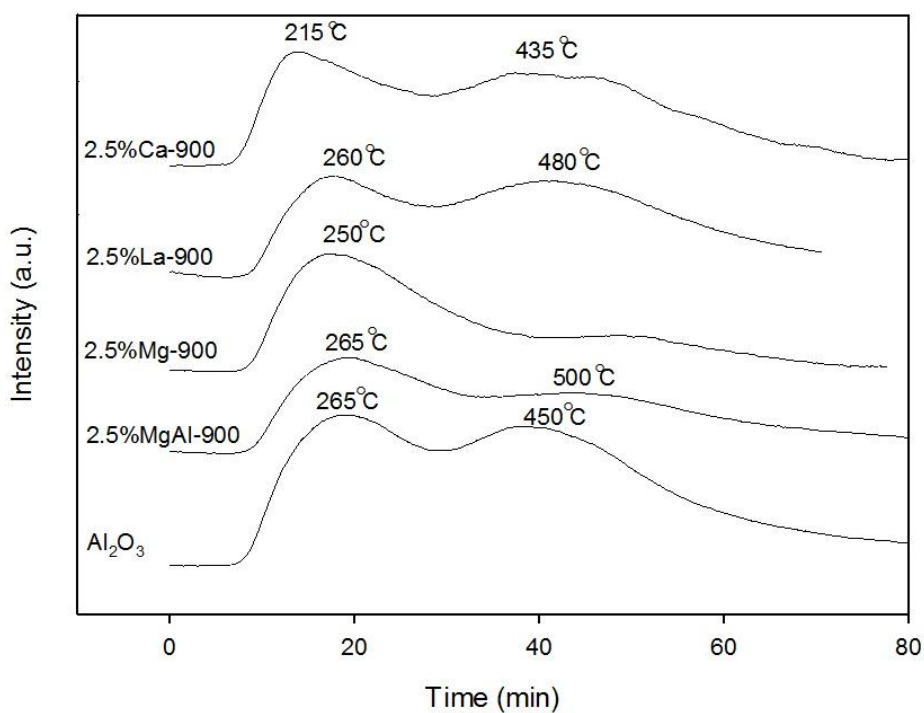


Figure 5. 11  $\text{NH}_3$ -TPD profile of the non-modified and basic oxide modified alumina support after calcination at 900 °C

Table 5. 8 The acidity of the non-modified and basic oxide modified alumina support after calcination at 900 °C

Samples	Total acid site ( $\text{mmol/g}_{\text{cat}}$ )
2.5%Ca-900	4.1
2.5%La-900	3.0
2.5%Mg-900	2.6
2.5%MgAl-900	3.7
$\text{Al}_2\text{O}_3$	5.4

### 5.2.1.6 Hydrogen Chemisorption

The amount of H<sub>2</sub> uptake and overall Co dispersion on the non-modified and basic oxide (MgO, CaO, and La<sub>2</sub>O<sub>3</sub>) modified alumina supported cobalt catalysts (calcinations temperatures of modified support at 900 °C) are shown in **Table 5.9**. The amount of H<sub>2</sub> uptake on MgAl-modified Co/Al<sub>2</sub>O<sub>3</sub> catalysts with different basic oxides (MgO, CaO, and La<sub>2</sub>O<sub>3</sub>) modified alumina supported cobalt catalysts were ranging between 12.0-24.6 μmol H<sub>2</sub>/g of catalysts. It was found that the 2.5%La- and 2.5%MgAl- modified Co/Al<sub>2</sub>O<sub>3</sub> catalysts exhibited higher amount of H<sub>2</sub> uptake on catalytic phase than non-modified Co/Al<sub>2</sub>O<sub>3</sub> catalysts. As can be seen, the amount of H<sub>2</sub> uptake on catalytic phase of 2.5%La- and 2.5%MgAl- modified Co/Al<sub>2</sub>O<sub>3</sub> catalysts increased from 15.1 μmol H<sub>2</sub>/g of catalysts for the original Co/Al<sub>2</sub>O<sub>3</sub> catalysts to 24.6 and 19.5 μmol H<sub>2</sub>/g of catalysts for 2.5%La- and 2.5%MgAl- modified Co/Al<sub>2</sub>O<sub>3</sub> catalysts, respectively. Moreover, 2.5%La- and 2.5%MgAl- modified Co/Al<sub>2</sub>O<sub>3</sub> catalysts exhibited higher overall cobalt dispersion. It is suggested that basic oxide (La and MgAl) modified alumina support cobalt catalysts resulted in increase in cobalt dispersion on surface of alumina supports. The result from this part indicates that the lanthanum modified alumina supported cobalt catalysts also improve the cobalt dispersion. On the other hand, the 2.5%Mg- modified Co/Al<sub>2</sub>O<sub>3</sub> catalysts resulted in a decrease in cobalt dispersion and amount of H<sub>2</sub> uptake on catalytic phase. In this case, the decrement of reducible cobalt species may be due to the formation of magnesium aluminate on the support (as can be seen from XRD result) and/or the interaction between cobalt oxide and magnesia was stronger resulted in the formation of CoO-MgO solid solution [34], in agreement with the results published by [34]. This result has also been related to result from XRD and TPR experiments.

Table 5. 9 The total H<sub>2</sub> chemisorption of basic oxide modified alumina supported cobalt catalysts (calcination temperatures of modified support at 900 °C)

Samples	Total H <sub>2</sub> chemisorption ( $\mu\text{mol H}_2/\text{g}_{\text{cat}}$ )	%Cobalt Dispersion
2.5%Ca-900	12.2	4.8
2.5%La-900	24.6	9.7
2.5%Mg-900	12.0	4.7
2.5%MgAl-900	19.5	7.7
Al <sub>2</sub> O <sub>3</sub>	15.1	5.9

### 5.2.2 Reaction study in CO<sub>2</sub> hydrogenation

The reaction study was carried out in carbon dioxide hydrogenation to determine catalytic activity of the basic oxide modified Co/Al<sub>2</sub>O<sub>3</sub> catalysts. Activation of the cobalt catalyst involved reductive treatment with hydrogen at 350 °C for 3 h. The CO<sub>2</sub> hydrogenation was carried out at 270 °C and atmosphere pressure. The reactant feed gas H<sub>2</sub>/CO<sub>2</sub> ratio of 10/1 was flowed through the sample at a total flow rate of 30 ml/min.

The carbon dioxide conversion and product selectivity during carbon dioxide hydrogenation reaction are presented in **Table 5.10** and **Figure 5.12**. The catalytic activity for CO<sub>2</sub> hydrogenation on non-modified alumina support cobalt catalyst obviously changed when adding MgAl on alumina support cobalt catalyst. The steady state CO<sub>2</sub> conversion of non-modified and MgAl-modified alumina support cobalt catalysts were ranging between 32.7-61.8% in the order: 2.5%MgAl-900 > Al<sub>2</sub>O<sub>3</sub> > 2.5%La-900 > 2.5%Ca-900 > 2.5%Mg-900. The catalyst modified by 2.5%MgAl exhibited higher catalytic activity than the corresponding non-modified and the La-,

Ca- and Mg-modified  $\text{Al}_2\text{O}_3$  supported ones. Although the unmodified  $\text{Co}/\text{Al}_2\text{O}_3$  catalyst showed the highest initial  $\text{CO}_2$  conversion at 61.2% but the sample was gradually deactivated with time on stream and reached the steady-state conversion at 55.2%. The steady-state  $\text{CO}_2$  conversion for the 2.5%MgAl- modified  $\text{Co}/\text{Al}_2\text{O}_3$  catalyst was 61.8% and the  $\text{CH}_4$  selectivity were 100%. The catalytic activity and catalyst stability were greatly improved by addition of MgAl. It is well known that the strong interaction between cobalt and alumina support bring about the formation of inactive  $\text{CoAl}_2\text{O}_4$  species relative to the low reducibility and low catalytic activity. The interaction of the reducible species (cobalt) with alumina support is more important in this study. It was found that the addition of 2.5%MgAl- modified  $\text{Co}/\text{Al}_2\text{O}_3$  catalyst could suppress the interaction between cobalt metal and alumina support. The TPR result also indicated that the addition of 2.5% MgAl result in the shift of reduction peaks to lower temperature, meaning that the interaction between reducible species (cobalt) and alumina support were weaker, suggesting that in this case, the quantity of reducible cobalt species is higher than other supported cobalt catalysts. The  $\text{H}_2$ -chemisorption results also indicated that the addition of 2.5% MgAl exhibited higher amount of  $\text{H}_2$ -chemisorption and overall cobalt dispersion, which is related to the increasing of  $\text{Co}^0$  sites (active sites). Therefore, the 2.5%MgAl modification increased not only the reducibility of cobalt catalysts but also the catalytic activity in carbon dioxide hydrogenation under methanation conditions.

Moreover, the 2.5%La modified  $\text{Co}/\text{Al}_2\text{O}_3$  catalyst exhibited higher  $\text{CO}_2$  conversion than the unmodified  $\text{Co}/\text{Al}_2\text{O}_3$  catalyst but the sample was gradually deactivated with time on stream and reached the steady-state conversion at 53.6%. According to TPR result, the addition of 2.5%La resulted in the shift of reduction peaks to lower temperature, meaning that the interaction between reducible species (cobalt) and alumina support were weaker, suggesting that in this case, the quantity of reducible cobalt species was higher than the other supported cobalt catalysts. The  $\text{H}_2$ -chemisorption results also indicated that the addition of 2.5% La exhibited the highest amount of  $\text{H}_2$ -chemisorption and overall cobalt dispersion, which is related to the increasing of  $\text{Co}^0$  sites (active sites). Therefore, the 2.5%La modification increased not only the reducibility of cobalt catalysts but also the catalytic activity in carbon



dioxide hydrogenation although the sample was gradually deactivated with time on stream.

On the other hand, addition of Ca- and Mg-modified Co/Al<sub>2</sub>O<sub>3</sub> catalysts showed an opposite trend in which the activity for CO<sub>2</sub> hydrogenation decreased. From TPR results, the addition of 2.5%Mg and 2.5%Ca resulted in the formation of more difficult to reduce cobalt species. As can be seen from TPR result, the addition of 2.5% Mg result in the shift of reduction peaks to higher temperature, meaning that the interaction between reducible species (cobalt) and alumina support were stronger, suggesting that in this case, the quantity of reducible cobalt species is lower than other supported cobalt catalysts. According to XRD analyses, the addition of Mg resulted in the formation of MgAl<sub>2</sub>O<sub>4</sub>. In this case, the decrement of reducible cobalt species may be due to the formation of magnesium aluminate on the support and/or the interaction between cobalt oxide and magnesia was stronger resulted in the formation of CoO-MgO solid solution and/or very weak interaction between metal and support [34]. From TPR result of the Ca-modified Co/Al<sub>2</sub>O<sub>3</sub> catalyst, the second peak presented a broad reduction zone with lower intensity. In this case, the quantity of reducible cobalt species may be lower and/or the interaction with the support was stronger. The H<sub>2</sub>-chemisorption results also indicated that the addition of Mg and Ca exhibited lower H<sub>2</sub>-chemisorption and overall cobalt dispersion than non-modified catalysts, which is related to the decreasing of Co<sup>0</sup> sites (active sites). Therefore, the Mg and Ca modification decreased not only the reducibility of cobalt catalysts but also the catalytic activity in carbon dioxide hydrogenation.

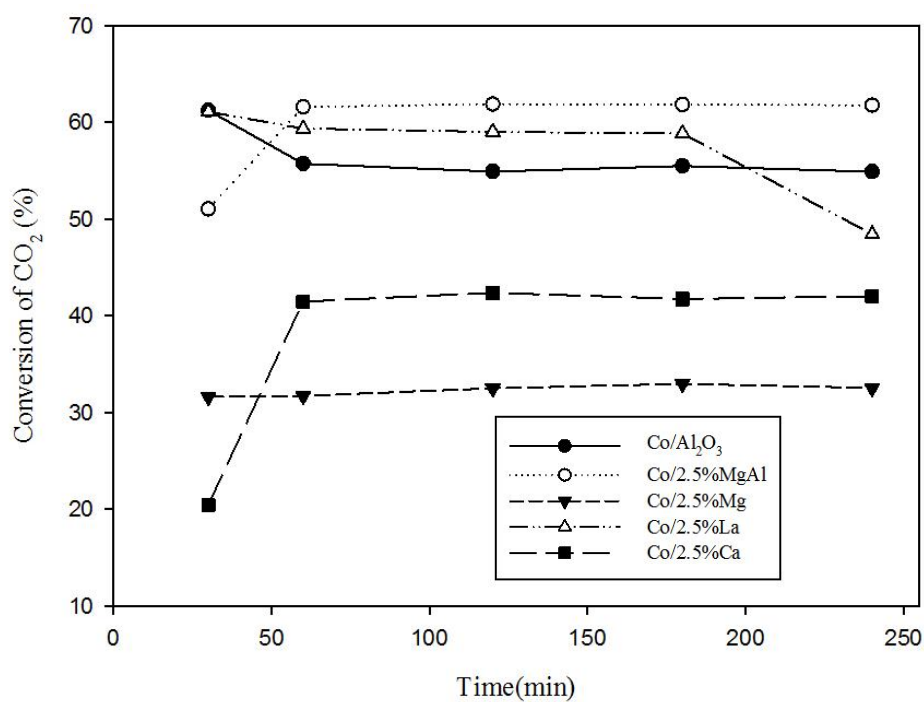


Figure 5. 12 Performances of catalysts with the various modified support in CO<sub>2</sub> hydrogenation.

Table 5. 10 The conversion and product selectivity during CO<sub>2</sub> hydrogenation on basic oxide modified alumina supported cobalt catalysts

Samples	Conversion		Product Selectivity (%)	
	Initial	Steady state	CH <sub>4</sub>	CO
2.5%Ca-900	20.4	41.8	100	0
2.5%La-900	61.1	53.6	100	0
2.5%Mg-900	31.6	32.7	100	0
2.5%MgAl-900	51.0	61.8	100	0
Al <sub>2</sub> O <sub>3</sub>	61.2	55.2	100	0

### 5.3 Effect of basic oxide (MgO, CaO, and La<sub>2</sub>O<sub>3</sub>) modified Al<sub>2</sub>O<sub>3</sub> supported Co/Al<sub>2</sub>O<sub>3</sub> catalysts using calcination temperature of modified support at 550 °C

#### 5.3.1 Characterization of the catalysts

##### 5.3.1.1 X-ray diffraction (XRD)

The XRD patterns of basic oxide (MgO, CaO, and La<sub>2</sub>O<sub>3</sub>) modified Al<sub>2</sub>O<sub>3</sub> support calcinations temperatures of modified support after calcinations at 550 °C are presented in **Figure 5.13**. The patterns were recorded in the  $2\theta$  range of 10-80°. The non-modified alumina support shows the characteristic diffraction lines corresponding to the (440), (400), and (311) planes of the gamma phase of alumina at  $2\theta$  degrees 66.79°, 45.76° and 37.58°, respectively. For the La and Ca modified  $\gamma$ -Al<sub>2</sub>O<sub>3</sub>, the diffraction lines were similar to the  $\gamma$ -Al<sub>2</sub>O<sub>3</sub> pattern and the diffraction patterns of La<sub>2</sub>O<sub>3</sub> and CaO phase were not detected, due probably to the high dispersion of these oxides or the relatively low amount being added [7]. For the  $\gamma$ -Al<sub>2</sub>O<sub>3</sub> modified with magnesium and aluminium nitrate calcinations at 550°C, the XRD peaks were also similar to the  $\gamma$ -Al<sub>2</sub>O<sub>3</sub> pattern and there was no indication of the MgAl<sub>2</sub>O<sub>4</sub> formation. In addition, the diffraction patterns of  $\gamma$ -Al<sub>2</sub>O<sub>3</sub> modified with magnesium nitrate and calcinations at 550°C also showed the patterns similar to the  $\gamma$ -Al<sub>2</sub>O<sub>3</sub> diffraction patterns and there was no indication of the MgAl<sub>2</sub>O<sub>4</sub> formation. The result of this part is in contrast with the results of  $\gamma$ -Al<sub>2</sub>O<sub>3</sub> modified with magnesium nitrate and calcinations at 900°C, due probably to a strong interaction between magnesium and gamma alumina support related to the high calcination temperature; in agreement with the results published by [10].

The XRD patterns of the basic oxide (MgO, CaO, and La<sub>2</sub>O<sub>3</sub>) modified Al<sub>2</sub>O<sub>3</sub> (calcinations temperature at 550 °C) supported Co/Al<sub>2</sub>O<sub>3</sub> catalysts are presented in **Figure 5.14**. The patterns were recorded in the  $2\theta$  range of 10-80 degrees. The diffraction peaks at 45.7° and 66.6° were attributed to the  $\gamma$ -Al<sub>2</sub>O<sub>3</sub> support and the

peaks at  $31.4^\circ$ ,  $36.9^\circ$ ,  $45.0^\circ$ ,  $59.5^\circ$ , and  $65.5^\circ$  were assigned to the  $\text{Co}_3\text{O}_4$  phase [7], which existed on all the catalysts.

The average crystallite size of  $\text{Co}_3\text{O}_4$ , calculated from line broadening of  $\text{Co}_3\text{O}_4$  at  $2\theta = 37^\circ$  diffraction peak using the Scherrer's equation are presented in **Table 5.11**. It was found that the crystallite size of  $\text{Co}_3\text{O}_4$  obtained from the addition of Ca, La and Mg modified  $\text{Al}_2\text{O}_3$  (calcination temperature at  $550^\circ\text{C}$ ) supported  $\text{Co}/\text{Al}_2\text{O}_3$  catalysts were 13.1, 12.3 and 13.1 nm, respectively. For the MgAl-modified  $\gamma\text{-Al}_2\text{O}_3$  supported  $\text{Co}/\text{Al}_2\text{O}_3$  catalysts was 15.0 nm whereas that the average crystalline size of  $\text{Co}_3\text{O}_4$  particles obtained from non-modified  $\text{Co}/\text{Al}_2\text{O}_3$  catalysts was 11.7 nm. It is suggested that basic oxide modified  $\text{Al}_2\text{O}_3$  supported  $\text{Co}/\text{Al}_2\text{O}_3$  catalysts (support calcinations temperature at  $550^\circ\text{C}$ ) resulted in increase average crystallite size of  $\text{Co}_3\text{O}_4$  particle.

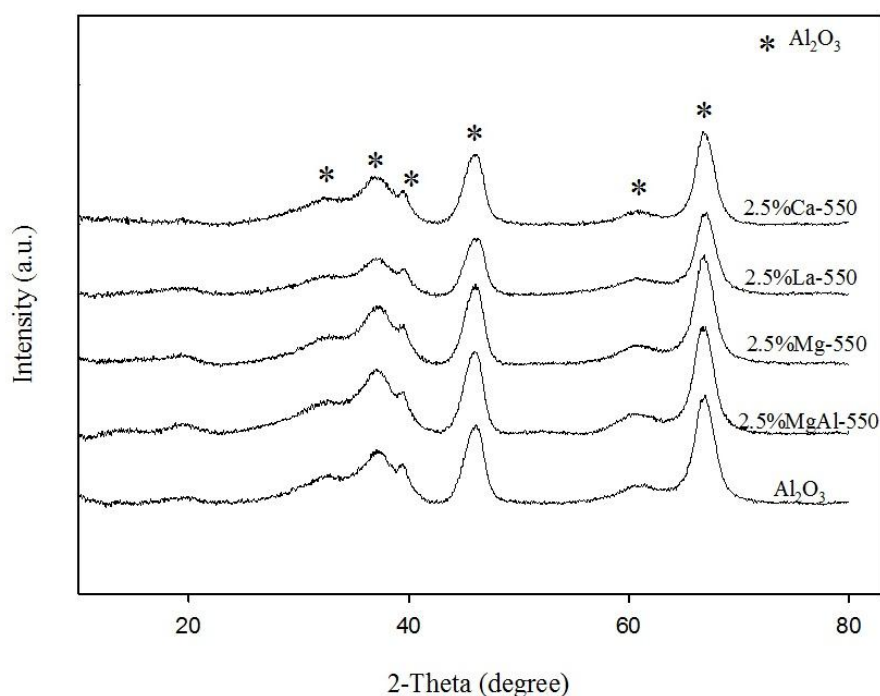


**Figure 5. 13** The XRD patterns of the non-modified and basic oxide modified alumina support after calcination at  $550^\circ\text{C}$

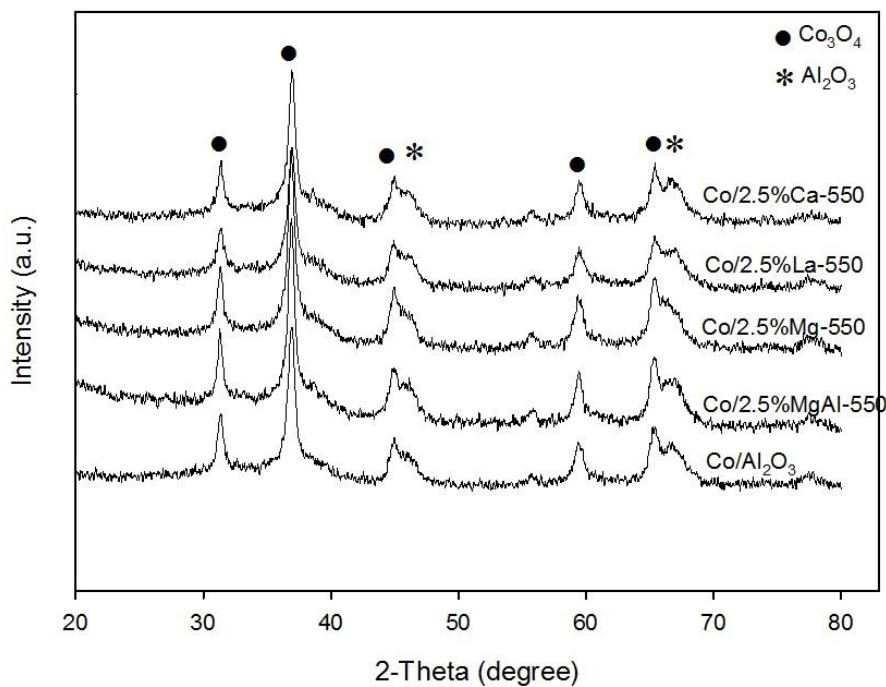


Figure 5. 14 The XRD patterns of non-modified and basic oxide modified Co/Al<sub>2</sub>O<sub>3</sub> catalysts.

Table 5. 11 Average Co<sub>3</sub>O<sub>4</sub> crystallite size and BET surface area of the support

Samples	Average Co <sub>3</sub> O <sub>4</sub> crystallite size from XRD (nm)	BET surface area (m <sup>2</sup> /g)
2.5%Ca-550	13.1	120
2.5%La-550	12.3	105
2.5%Mg-550	13.1	120
2.5%MgAl-550	15.0	118
Al <sub>2</sub> O <sub>3</sub>	11.7	125

### 5.3.1.2 BET surface areas

BET surface area of non-modified and basic oxide (MgO, CaO, and La<sub>2</sub>O<sub>3</sub>) modified Al<sub>2</sub>O<sub>3</sub> (calcinations temperature at 550 °C) supports are compared in **Table 5.11**. The BET specific surface area of basic oxide (MgO, CaO, and La<sub>2</sub>O<sub>3</sub>) modified Al<sub>2</sub>O<sub>3</sub> (calcinations temperature at 550 °C) supports decreased from 125 m<sup>2</sup>/g for the original Al<sub>2</sub>O<sub>3</sub> support to the lower surface areas (105-120 m<sup>2</sup>/g) for basic oxide (MgO, CaO, and La<sub>2</sub>O<sub>3</sub>) modified Al<sub>2</sub>O<sub>3</sub> (calcinations temperature at 550 °C) supports. It was found that the basic oxide (MgO, CaO, and La<sub>2</sub>O<sub>3</sub>) modified Al<sub>2</sub>O<sub>3</sub> (calcinations temperature at 550 °C) supports exhibited higher specific surface area than the basic oxide (MgO, CaO, and La<sub>2</sub>O<sub>3</sub>) modified Al<sub>2</sub>O<sub>3</sub> (calcinations temperature at 900 °C) supports, due probably to the lower calcinations temperature were used. However, the support surface area was not directly related to the catalytic activity in this study.

### 5.3.1.3 Scanning electron microscopy

The morphologies of Co/Al<sub>2</sub>O<sub>3</sub> catalysts with different basic oxide (MgO, CaO, and La<sub>2</sub>O<sub>3</sub>) modified Al<sub>2</sub>O<sub>3</sub> supported using calcinations temperatures of modified support at 550 °C were investigated by SEM. The particle morphologies of the basic oxide (MgO, CaO, and La<sub>2</sub>O<sub>3</sub>) modified Al<sub>2</sub>O<sub>3</sub> supported cobalt catalysts are shown in **Figure 5.15**. In all of the basic oxide (MgO, CaO, and La<sub>2</sub>O<sub>3</sub>) modified Al<sub>2</sub>O<sub>3</sub> supported Co/Al<sub>2</sub>O<sub>3</sub> catalysts micrographs spherical shape particles with diameter around 20 μm can be seen. There were no significant differences between particle morphologies of different catalysts.

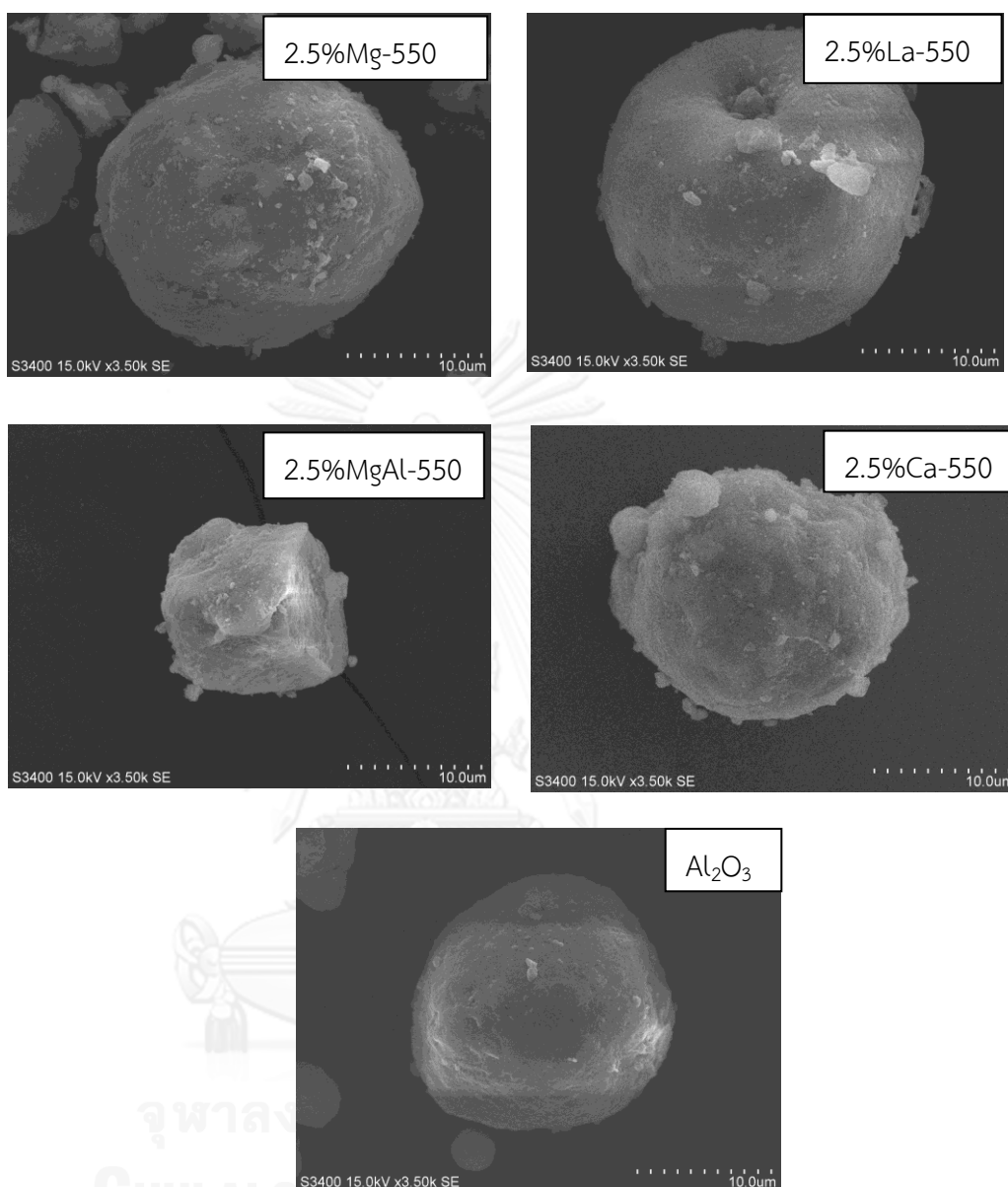


**Figure 5. 15** The SEM images of basic oxide modified alumina supported cobalt catalysts (calcination temperatures of modified support at 550 °C)

#### 5.3.1.4 Temperature Programmed Reduction (TPR)

The TPR profiles of all the Co/Al<sub>2</sub>O<sub>3</sub> catalysts with different basic oxides (MgO, CaO, and La<sub>2</sub>O<sub>3</sub>) modified Al<sub>2</sub>O<sub>3</sub> supported using calcination temperatures of modified support at 550 °C are shown in **Figure 5.16** and the H<sub>2</sub>-consumption values calculated from TPR peak of all catalysts are presented in **Table 5.12**. The H<sub>2</sub>-TPR was performed to determine the reduction behavior of the supported cobalt catalysts. All the catalysts exhibited two major reduction peaks. The first peak could be assigned to the reduction of Co<sub>3</sub>O<sub>4</sub> to CoO [7]. The second peak is ascribed to the subsequent reduction of CoO to Co<sup>0</sup>. For the non-modified Co/Al<sub>2</sub>O<sub>3</sub> catalysts, the first peak centered at around 485°C, while the second broad peak distributed from 510°C to 770°C (centered at 610°C). Besides these two main reduction peaks, a small peak appeared at about 250°C. This peak could be attributed to the reduction of the residual cobalt nitrate [7], which usually decomposed completely above 400°C [3].

For the MgAl-modified Co/Al<sub>2</sub>O<sub>3</sub> catalyst, the sharp peak at low temperature zone shifted from 485°C for the non-modified Co/Al<sub>2</sub>O<sub>3</sub> catalysts to higher temperature 510°C for Co/Al<sub>2</sub>O<sub>3</sub>-MgAl catalyst and a second reduction peak with maximum at about 590-600°C. Moreover, Co/Al<sub>2</sub>O<sub>3</sub>-2.5%MgAl catalyst had lower H<sub>2</sub> consumption than the non-modified Co/Al<sub>2</sub>O<sub>3</sub> catalysts. In this case, the promotion of MgAl after calcinations at 550°C caused changes in reduction behavior of the cobalt catalysts. The result of this part is in contrast with the results of MgAl after calcinations at 900°C, due probably to the lower calcinations temperature were used. On the other hand, there were also two major peaks for the Mg-modified Co/Al<sub>2</sub>O<sub>3</sub> catalyst located at 530°C and 650°C. In this case, both reduction peaks were shifted to higher temperature may be due to the effect of strong interaction between cobalt metal and alumina support. Moreover, Mg-modified Co/Al<sub>2</sub>O<sub>3</sub> catalyst had lower H<sub>2</sub> consumption than the non-modified Co/Al<sub>2</sub>O<sub>3</sub> catalysts.

For the La-modified Co/Al<sub>2</sub>O<sub>3</sub> catalyst, the sharp peak at low temperature zone slightly shifted from 485°C for the non-modified Co/Al<sub>2</sub>O<sub>3</sub> catalysts to 455°C for Co/Al<sub>2</sub>O<sub>3</sub>-La catalyst and a second reduction peak with maximum at about 590-600°C.



Besides these two main reduction peaks, a small peak appeared at about 250°C. Moreover, Co/Al<sub>2</sub>O<sub>3</sub>-2.5%La catalyst had higher H<sub>2</sub> consumption than the non-modified Co/Al<sub>2</sub>O<sub>3</sub> catalysts), indicating that La-modified cobalt catalysts increased catalysts reducibility. For the Ca-modified Co/Al<sub>2</sub>O<sub>3</sub> catalyst, the sharp peak at low temperature zone shifted to 425°C, while the second peak presented a broad reduction zone between 470°C and 760°C with lower intensity. In this case, the quantity of reducible cobalt species may be lower and/or the interaction with the support was stronger. Moreover, Co/Al<sub>2</sub>O<sub>3</sub>-2.5%Ca catalyst had lowest H<sub>2</sub> consumption.

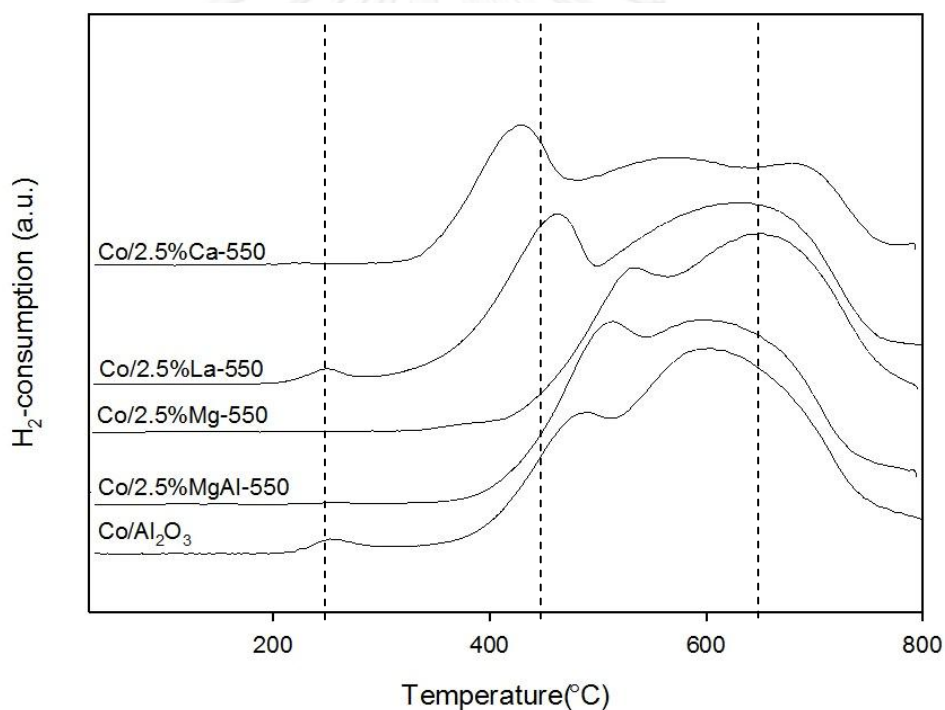


**Figure 5. 16** TPR profile of basic oxide modified alumina supported cobalt catalysts (calcination temperatures of modified support at 550 °C)

Table 5. 12 H<sub>2</sub> consumption for the TPR profile calculation of basic oxide modified alumina supported cobalt catalysts

Samples	H <sub>2</sub> -Consumption (mmol/g <sub>cat</sub> )
2.5%Ca-550	116
2.5%La-550	159
2.5%Mg-550	135
2.5%MgAl-550	142
Al <sub>2</sub> O <sub>3</sub>	154

#### 5.3.1.5 Temperature-programmed desorption (NH<sub>3</sub>-TPD)

NH<sub>3</sub>-TPD profiles of the non-modified and basic oxide (MgO, CaO, and La<sub>2</sub>O<sub>3</sub>) modified Al<sub>2</sub>O<sub>3</sub> supports using calcination temperatures of modified support at 550 °C are shown in **Figure 5.17** and the acidity values calculated from TPD peak of all supports are presented in **Table 5.13**. It was found that the non-modified  $\gamma$ -Al<sub>2</sub>O<sub>3</sub> support exhibited two major desorption peak. The occurrence of multiple desorption peaks corresponding to the different of acid site in non-modified  $\gamma$ -Al<sub>2</sub>O<sub>3</sub> support, there are weak acid sites (occurring at low temperatures) and strong acid sites (occurring at high temperatures). Only one broad desorption peak was observed in all basic oxide (MgO, CaO and La<sub>2</sub>O<sub>3</sub>) modified alumina support after calcinations at 550 °C. The desorption peak of all basic oxide modified catalysts occurring at low temperatures. Moreover, the basic oxide (MgO, CaO and La<sub>2</sub>O<sub>3</sub>) modified alumina support after calcinations at 550 °C exhibited lower desorption peak area than the non-modified Al<sub>2</sub>O<sub>3</sub> support. It is suggested that basic oxide modified alumina supports resulted in a decrease in surface acidity of  $\gamma$ -Al<sub>2</sub>O<sub>3</sub> especially the strong acid sites. The decrement of the surface acidity of  $\gamma$ -Al<sub>2</sub>O<sub>3</sub> modified with basic oxide including MgO, CaO and La<sub>2</sub>O<sub>3</sub> may be due to the basic nature of basic oxide. It was found that the temperature of desorption peak shifted from 265°C for the non-

modified  $\text{Al}_2\text{O}_3$  support to 230-250°C for basic oxide modified alumina support, except the La-modified alumina support. This result suggesting that the mainly weak acidic sites existed on the basic oxide modified alumina support and the strong acid sites decreased when the basic oxide were added.

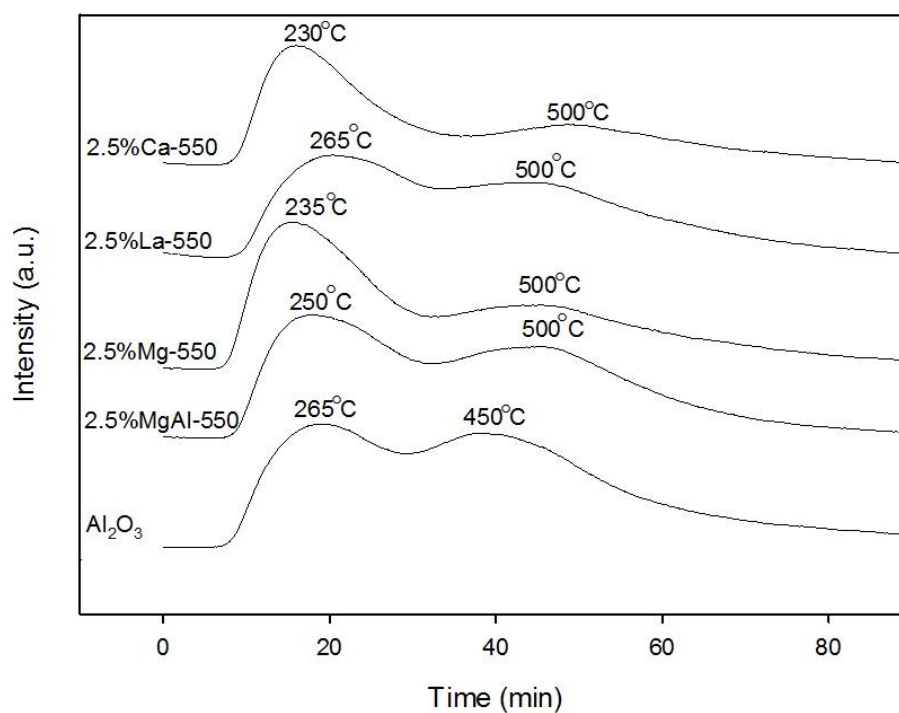


**Figure 5. 17**  $\text{NH}_3$ -TPD profile of the non-modified and basic oxide modified alumina support after calcination at 550 °C

Table 5. 13 The acidity of the non-modified and basic oxide modified alumina support after calcination at 550 °C

Samples	Total acid site (mmol/g <sub>cat</sub> )
2.5%Ca-550	2.8
2.5%La-550	4.1
2.5%Mg-550	4.0
2.5%MgAl-550	4.4
Al <sub>2</sub> O <sub>3</sub>	5.4

#### 5.2.1.6 Hydrogen Chemisorption

The amount of H<sub>2</sub> uptake, the percentages of cobalt dispersion and the average Co metal particle sizes determined from H<sub>2</sub> chemisorption on the non-modified and basic oxide (MgO, CaO, and La<sub>2</sub>O<sub>3</sub>) modified alumina supported cobalt catalysts (calcinations temperatures of modified support at 550 °C) are shown in **Table 5.14**. The amount of H<sub>2</sub> uptake on basic oxide (MgO, CaO, and La<sub>2</sub>O<sub>3</sub>) modified alumina supported cobalt catalysts (calcinations temperatures of modified support at 550 °C) were ranging between 10.9-15.6 μmol H<sub>2</sub>/g of catalysts. It was found that the amount of H<sub>2</sub> uptake and the overall dispersion of reduced Co on basic oxide (MgO, CaO, and La<sub>2</sub>O<sub>3</sub>) modified alumina supported cobalt catalysts (calcinations temperatures of modified support at 550 °C) were no significant changed with basic oxide modification, except 2.5%Mg. The result from this part is in contrast with the results of La- and MgAl- modified Co/Al<sub>2</sub>O<sub>3</sub> catalysts with calcinations support at 900°C indicates that the improvement of overall dispersion of reduced Co related to the high calcinations temperature of the La- and MgAl- modified alumina support. For the

2.5%Mg modified Co/Al<sub>2</sub>O<sub>3</sub> catalysts, the amount of H<sub>2</sub> uptake on catalytic phase decreased from 15.1  $\mu\text{mol H}_2/\text{g}$  of catalysts for the original Co/Al<sub>2</sub>O<sub>3</sub> catalysts to 10.9  $\mu\text{mol H}_2/\text{g}$  of catalysts for 2.5%Mg- modified Co/Al<sub>2</sub>O<sub>3</sub> catalysts. Moreover, 2.5%Mg- modified Co/Al<sub>2</sub>O<sub>3</sub> catalysts exhibited lower overall cobalt dispersion, which similar to the result from the addition of Mg- into Co/Al<sub>2</sub>O<sub>3</sub> catalysts with calcination of support at 900 °C.

**Table 5. 14** The total H<sub>2</sub> chemisorption of basic oxide modified alumina supported cobalt catalysts (calcination temperatures of modified support at 550 °C)

Samples	Total H <sub>2</sub> chemisorption ( $\mu\text{mol H}_2/\text{g}_{\text{cat}}$ )	%Cobalt Dispersion
2.5%Ca-550	14.8	5.8
2.5%La-550	15.1	6.0
2.5%Mg-550	10.9	4.3
2.5%MgAl-550	15.6	6.1
Al <sub>2</sub> O <sub>3</sub>	15.1	5.9

### 5.3.1.7 Transmission Electron Microscopy (TEM)

TEM micrographs of basic oxide modified alumina supported cobalt catalysts are shown in Figure 5.18. Transmission electron microscopy was performed to study the morphologies of the catalysts sample, crystallite size and size distribution of supported metals. As can be seen in this figure, the dark spots represented cobalt metals particles dispersed on the surface of the basic oxide modified alumina support after calcinations at 650 °C. The images obtained from all of catalysts showed a high dispersion of cobalt particles on the surface of the alumina support. For the non-modified Co/Al<sub>2</sub>O<sub>3</sub> catalysts and basic oxide modified Co/Al<sub>2</sub>O<sub>3</sub> catalysts were composed of very small particles.

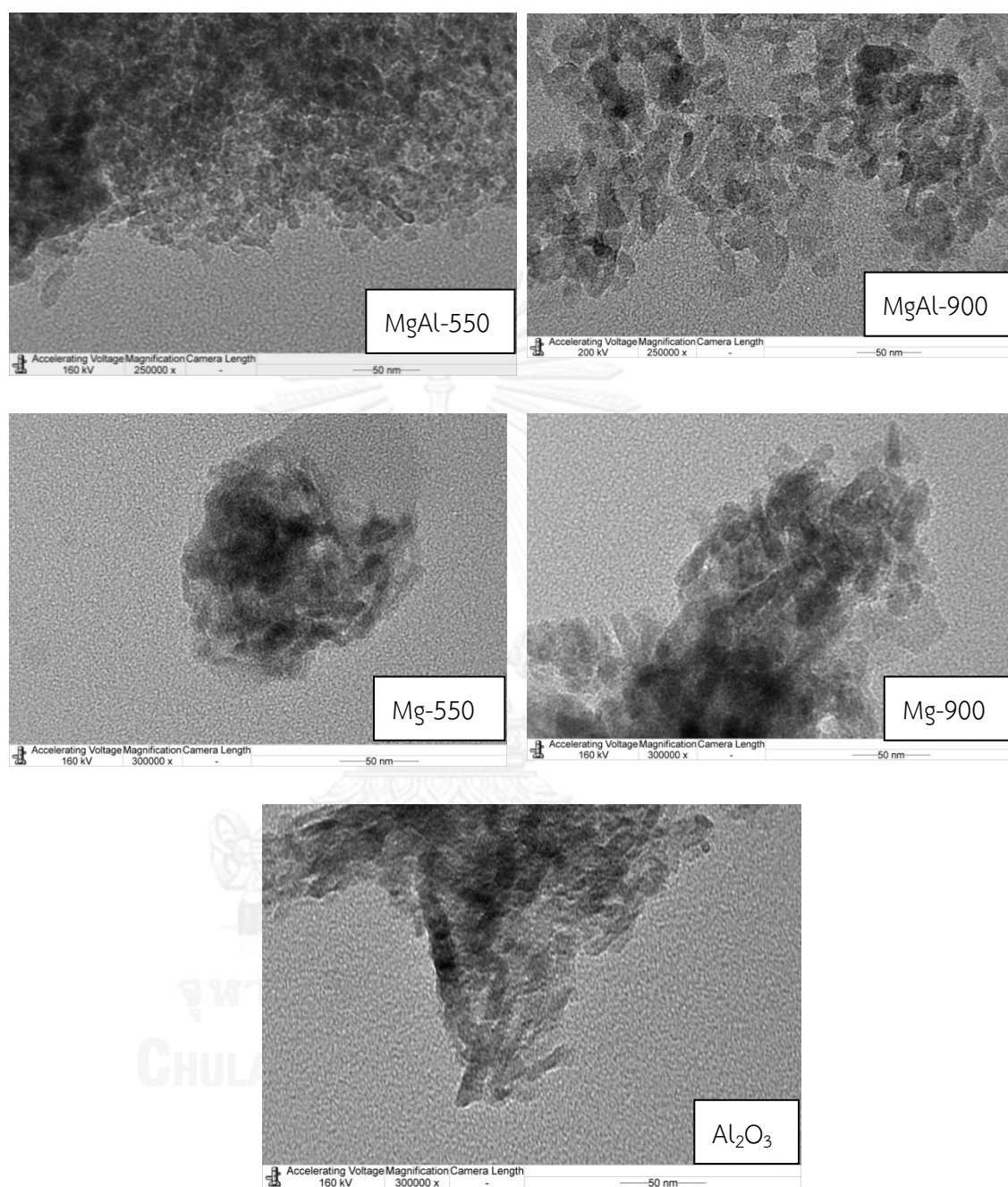


Figure 5. 18 The TEM images of basic oxide modified alumina supported cobalt catalysts

### 5.3.2 Reaction study in CO<sub>2</sub> hydrogenation

The reaction study was carried out in carbon dioxide hydrogenation to determine catalytic activity of the basic oxide modified Co/Al<sub>2</sub>O<sub>3</sub> catalysts. Activation of the cobalt catalyst involved reductive treatment with hydrogen at 350 °C for 3 h. The CO<sub>2</sub> hydrogenation was carried out at 270 °C and atmosphere pressure. The reactant feed gas H<sub>2</sub>/CO<sub>2</sub> ratio of 10/1 was flowed through the sample at a total flow rate of 30 ml/min.

The carbon dioxide conversion and product selectivity during carbon dioxide hydrogenation reaction are presented in **Table 5.15** and **Figure 5.19**. The catalytic activity for CO<sub>2</sub> hydrogenation on non-modified alumina support cobalt catalyst obviously changed when adding basic oxide on alumina support cobalt catalyst. The steady state CO<sub>2</sub> conversion of non-modified and basic oxide modified alumina support cobalt catalysts were ranging between 45.6-62.4% in the order: 2.5% La -550 > 2.5%MgAl-550 > Al<sub>2</sub>O<sub>3</sub> > 2.5%Mg-550 > 2.5%Ca-550. For the catalyst modified by 2.5%La and 2.5%MgAl exhibited higher catalytic activity than the corresponding non-modified and the La-, Ca- and Mg-modified Al<sub>2</sub>O<sub>3</sub> supported ones. Although the unmodified Co/Al<sub>2</sub>O<sub>3</sub> catalyst showed the higher initial CO<sub>2</sub> conversion at 61.2% but the sample was gradually deactivated with time on stream and reached the steady-state conversion at 55.2%. The steady-state CO<sub>2</sub> conversion for the 2.5%La-modified Co/Al<sub>2</sub>O<sub>3</sub> catalyst was 62.4% and the CH<sub>4</sub> selectivity were 100%. Moreover, the 2.5%MgAl modified Co/Al<sub>2</sub>O<sub>3</sub> catalyst also showed the higher steady-state CO<sub>2</sub> conversion (57.9%) than non-modified Co/Al<sub>2</sub>O<sub>3</sub> catalyst although TPR peak showed the shift of reduction peaks to higher temperature but the amount of total H<sub>2</sub> chemisorption and cobalt dispersion determined from H<sub>2</sub> chemisorption were higher than the non-modified Co/Al<sub>2</sub>O<sub>3</sub> catalyst.

The catalytic activity and catalyst stability were greatly improved by addition of La and MgAl (calcinations temperature at 550 °C). The result from this part similar to the result of basic oxide modified Co/Al<sub>2</sub>O<sub>3</sub> catalyst (calcinations temperature of support at 900 °C), which also showed the addition of La and MgAl can improved the

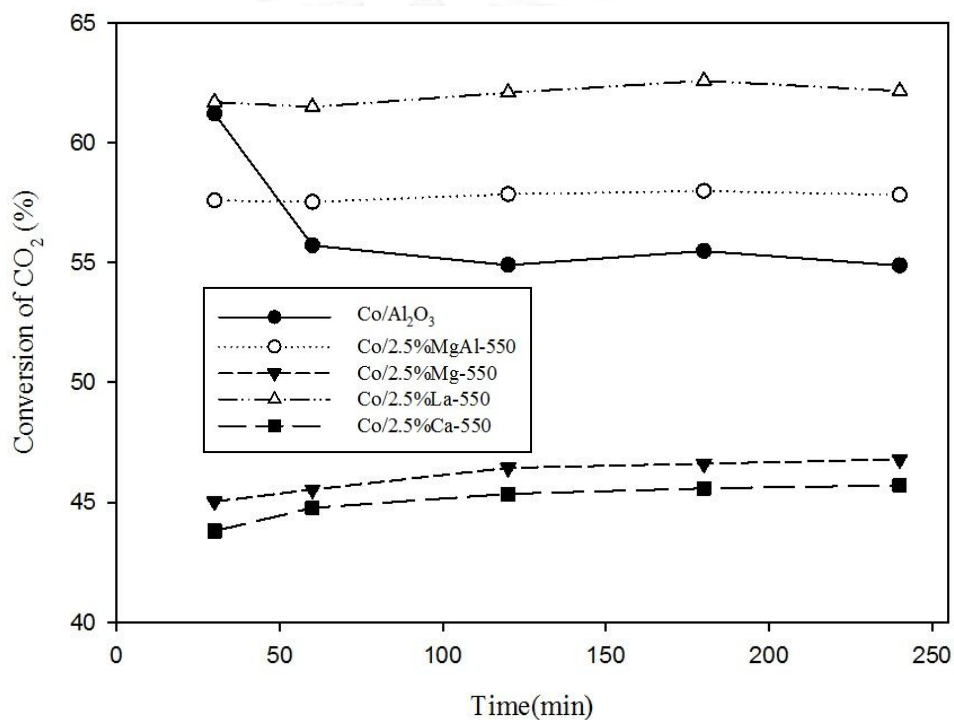
catalytic activity on  $\text{Co}/\text{Al}_2\text{O}_3$  catalyst. However, the addition of 2.5% MgAl (calcinations temperature of support at 900 °C) exhibited higher catalytic activity than 2.5%MgAl-modified  $\text{Co}/\text{Al}_2\text{O}_3$  catalyst (calcinations temperature of support at 550 °C).

It is well known that the strong interaction between cobalt and alumina support bring about the formation of inactive  $\text{CoAl}_2\text{O}_4$  species relative to the low reducibility and low catalytic activity. It was found that the addition of La- modified  $\text{Co}/\text{Al}_2\text{O}_3$  catalyst could suppress the interaction between cobalt metal and alumina support. The TPR result also indicated that the addition of La resulted in a shift of reduction peaks to lower temperature, meaning that the interaction between reducible species (cobalt) and alumina support were weaker, suggesting that in this case, the quantity of reducible cobalt species is higher than other supported cobalt catalysts although the amount Co active site of 2.5%La and 2.5%MgAl determined from  $\text{H}_2$ -chemisorption were no significant different from the non-modified  $\text{Co}/\text{Al}_2\text{O}_3$  catalyst.

On the other hand, addition of Ca- and Mg-modified  $\text{Co}/\text{Al}_2\text{O}_3$  catalysts showed an opposite trend in which the activity for  $\text{CO}_2$  hydrogenation decrease, which similar to the result from the addition of Ca- and Mg- into  $\text{Co}/\text{Al}_2\text{O}_3$  catalysts with calcinations of support at 900 °C. From TPR results, the addition of 2.5%Mg and 2.5%Ca with calcinations of support at 550 °C resulted in the formation of more difficult to reduce cobalt species (inactive  $\text{CoAl}_2\text{O}_4$  species). As can be seen from TPR result, the addition of 2.5% Mg result in the shift of reduction peaks to higher temperature, meaning that the interaction between reducible species (cobalt) and alumina support were stronger, suggesting that in this case, the quantity of reducible cobalt species is lower than other supported cobalt catalysts. According to XRD analyses, although the XRD peaks were also similar to the  $\gamma\text{-Al}_2\text{O}_3$  pattern and there was no indication of the  $\text{MgAl}_2\text{O}_4$  formation due probably to a strong interaction between magnesium and gamma alumina support related to the high calcinations temperature but the TPR results also presented the strong interaction between reducible species (cobalt) and alumina support bring about the lower reducibility of the modified catalysts, compared to the other supported catalysts.



For Ca-modified  $\text{Co}/\text{Al}_2\text{O}_3$  catalysts although the sharp peak at low temperature zone shifted to lower temperature, but the second peak presented a broad reduction zone with lower intensity. In this case, the quantity of reducible cobalt species may be lower and/or the interaction with the support was stronger. Moreover,  $\text{Co}/\text{Al}_2\text{O}_3\text{-2.5\%Ca}$  catalyst had lowest  $\text{H}_2$  consumption, hence the lower activity were obtained. Therefore, the Mg and Ca modification decreased not only the reducibility of cobalt catalysts but also the catalytic activity in carbon dioxide hydrogenation.



CHULALONGKORN UNIVERSITY

Figure 5. 19 Performances of catalysts with the various modified support in  $\text{CO}_2$  hydrogenation.

Table 5. 15 The conversion and product selectivity during CO<sub>2</sub> hydrogenation on basic oxide modified alumina supported cobalt catalysts

Samples	Conversion		Product Selectivity (%)	
	Initial	Steady state	CH <sub>4</sub>	CO
2.5%Ca-550	43.8	45.6	100	0
2.5%La-550	61.7	62.4	100	0
2.5%Mg-550	45.0	46.7	100	0
2.5%MgAl-550	57.6	57.9	100	0
Al <sub>2</sub> O <sub>3</sub>	61.2	55.2	100	0

## CHAPTER VI

### CONCLUSIONS AND RECOMMENDATIONS

#### 6.1 Conclusions

The present work revealed the effect of the basic oxides (MgO, CaO, La<sub>2</sub>O<sub>3</sub> and mixed Mg-Al oxides) modification on the physicochemical properties of Co/Al<sub>2</sub>O<sub>3</sub> catalysts. The carbon dioxide hydrogenation was chosen as a test reaction for evaluating catalytic activity. The results can be concluded as follows:

Modification of  $\gamma$ -Al<sub>2</sub>O<sub>3</sub> supported cobalt catalysts by 2.5%La and 2.5%MgAl resulted in higher reducibility of the catalysts and higher cobalt dispersion on the alumina supports by probably suppression the formation of inactive CoAl<sub>2</sub>O<sub>4</sub> species hence the higher catalytic activity in CO<sub>2</sub> hydrogenation were obtained. However, the optimum calcination temperatures for 2.5%La and 2.5%MgAl were 550 and 900 °C, respectively.

The addition of excessive amount of Mg with high calcination temperature of the magnesium modified alumina support brought about the formation of magnesium aluminate spinel (MgAl<sub>2</sub>O<sub>4</sub>), which resulted in lower reducibility and catalytic activity for CO<sub>2</sub> hydrogenation.

## 6.2 Recommendations

- 1) The carbon dioxide hydrogenation reaction is highly exothermic reaction hence an important issue of carbon dioxide hydrogenation reactor is the removed of heat from reactor.
- 2) Production of methane in carbon dioxide hydrogenation should be studied under various conditions including pressures, the ratios of carbon dioxide/hydrogen and the mixture gas (carbon monoxide/carbon dioxide) in feed gas.
- 3) Among the three types of basic oxide modified alumina support cobalt catalysts including MgO, CaO and La<sub>2</sub>O<sub>3</sub> oxides used in this study, the use of lanthanum and calcium should be varied in content of La and Ca loading, due to the basic oxide content affected the reducibility of catalysts

## REFERENCES

- [1] E.N. Alvar, M. Rezaei, H.N. Alvar, Synthesis of mesoporous nanocrystalline  $\text{MgAl}_2\text{O}_4$  spinel via surfactant assisted precipitation route, *Powder Technology* 198 (2010) 275-278.
- [2] H. Arakawa, J.L. Dubois, K. Sayama, Selective conversion of  $\text{CO}_2$  to methanol by catalytic hydrogenation over promoted copper catalyst, *Energy Conversion and Management* 33 (1992) 521-528.
- [3] A. Bao, K. Liew, J. Li, Fischer–Tropsch synthesis on CaO-promoted  $\text{Co}/\text{Al}_2\text{O}_3$  catalysts, *Journal of Molecular Catalysis A: Chemical* 304 (2009) 47-51.
- [4] R. Bechara, D. Balloy, D. Vanhove, Catalytic properties of  $\text{Co}/\text{Al}_2\text{O}_3$  system for hydrocarbon synthesis, *Applied Catalysis A: General* 207 (2001) 343-353.
- [5] S.A. Bocanegra, A.D. Ballarini, O.A. Scelza, S.R. de Miguel, The influence of the synthesis routes of  $\text{MgAl}_2\text{O}_4$  on its properties and behavior as support of dehydrogenation catalysts, *Materials Chemistry and Physics* 111 (2008) 534-541.
- [6] Ø. Borg, S. Eri, E.A. Blekkan, S. Storsæter, H. Wigum, E. Rytter, A. Holmen, Fischer–Tropsch synthesis over  $\gamma$ -alumina-supported cobalt catalysts: Effect of support variables, *Journal of Catalysis* 248 (2007) 89-100.
- [7] Z. Cai, J. Li, K. Liew, J. Hu, Effect of  $\text{La}_2\text{O}_3$ -dopping on the  $\text{Al}_2\text{O}_3$  supported cobalt catalyst for Fischer-Tropsch synthesis, *Journal of Molecular Catalysis A: Chemical* 330 (2010) 10-17.
- [8] Y. Cui, H. Zhang, H. Xu, W. Li, The  $\text{CO}_2$  reforming of  $\text{CH}_4$  over  $\text{Ni}/\text{La}_2\text{O}_3/\alpha\text{-Al}_2\text{O}_3$  catalysts: The effect of  $\text{La}_2\text{O}_3$  contents on the kinetic performance, *Applied Catalysis A: General* 331 (2007) 60-69.
- [9] J.A.C. Dias, J.M. Assaf, Influence of calcium content in  $\text{Ni}/\text{CaO}/\gamma\text{-Al}_2\text{O}_3$  catalysts for  $\text{CO}_2$ -reforming of methane, *Catalysis Today* 85 (2003) 59-68.
- [10] M.L. Dieuzeide, V. Iannibelli, M. Jobbagy, N. Amadeo, Steam reforming of glycerol over  $\text{Ni}/\text{Mg}/\gamma\text{-Al}_2\text{O}_3$  catalysts. Effect of calcination temperatures, *International Journal of Hydrogen Energy* 37 (2012) 14926-14930.
- [11] M.L. Dieuzeide, M. Jobbagy, N. Amadeo, Glycerol steam reforming over  $\text{Ni}/\gamma\text{-Al}_2\text{O}_3$  catalysts, modified with  $\text{Mg}(\text{II})$ . Effect of  $\text{Mg}(\text{II})$  content, *Catalysis Today* 213 (2013) 50-57.
- [12] C. Dueso, A. Abad, F. García-Labiano, L.F. de Diego, P. Gayán, J. Adánez, A. Lyngfelt, Reactivity of a  $\text{NiO}/\text{Al}_2\text{O}_3$  oxygen carrier prepared by impregnation for chemical-looping combustion, *Fuel* 89 (2010) 3399-3409.

- [13] N. Homs, J. Toyir, P.R. de la Piscina, Chapter 1 - Catalytic Processes for Activation of CO<sub>2</sub>, New and Future Developments in Catalysis, Elsevier, Amsterdam, 2013, pp. 1-26.
- [14] X. Hu, G. Lu, Acetic acid steam reforming to hydrogen over Co–Ce/Al<sub>2</sub>O<sub>3</sub> and Co–La/Al<sub>2</sub>O<sub>3</sub> catalysts—The promotion effect of Ce and La addition, Catalysis Communications 12 (2010) 50-53.
- [15] T.A. J. Lahtinen, G. Somorjai, C, CO and CO<sub>2</sub> hydrogenation on cobalt foil model catalysts : evidence for the need of CoO reduction, Catalysis Letters 25 (1994) 241-255.
- [16] R. Jiang, Z. Xie, C. Zhang, Q. Chen, The catalytic performance of gas-phase amination over Pd–La catalysts supported on Al<sub>2</sub>O<sub>3</sub> and MgAl<sub>2</sub>O<sub>4</sub> spinel, Catalysis Today 93–95 (2004) 359-363.
- [17] B. Jongsomjit, J. Panpranot, J.G. Goodwin Jr, Effect of zirconia-modified alumina on the properties of Co/**Y**-Al<sub>2</sub>O<sub>3</sub> catalysts, Journal of Catalysis 215 (2003) 66-77.
- [18] H. Kusama, K. Okabe, H. Arakawa, Characterization of Rh-Co/SiO<sub>2</sub> catalysts for CO<sub>2</sub> hydrogenation with TEM, XPS and FT-IR, Applied Catalysis A: General 207 (2001) 85-94.
- [19] Y. Li, S. Yan, W. Yang, Z. Xie, Q. Chen, B. Yue, H. He, Effects of support modification on Nb<sub>2</sub>O<sub>5</sub>/**α**-Al<sub>2</sub>O<sub>3</sub> catalyst for ethylene oxide hydration, Journal of Molecular Catalysis A: Chemical 226 (2005) 285-290.
- [20] O. Mekasuwandumrong, P. Tantichuwet, C. Chaisuk, P. Praserthdam, Impact of concentration and Si doping on the properties and phase transformation behavior of nanocrystalline alumina prepared via solvothermal synthesis, Materials Chemistry and Physics 107 (2008) 208-214.
- [21] O. Mekasuwandumrong, N. Wongwaranon, J. Panpranot, P. Praserthdam, Effect of Ni-modified **α**-Al<sub>2</sub>O<sub>3</sub> prepared by sol–gel and solvothermal methods on the characteristics and catalytic properties of Pd/**α**-Al<sub>2</sub>O<sub>3</sub> catalysts, Materials Chemistry and Physics 111 (2008) 431-437.
- [22] G.D.B. Nuernberg, E.L. Foletto, L.F.D. Probst, C.E.M. Campos, N.L.V. Carreño, M.A. Moreira, A novel synthetic route for magnesium aluminate (MgAl<sub>2</sub>O<sub>4</sub>) particles using metal–chitosan complexation method, Chemical Engineering Journal 193–194 (2012) 211-214.
- [23] K. Othmer, Encyclopedia of chemical technology, A Wiley Interscience Publication, New York, 1991.

- [24] Y.-x. Pan, C.-j. Liu, Q. Ge, Effect of surface hydroxyls on selective CO<sub>2</sub> hydrogenation over Ni<sub>4</sub>/Y-Al<sub>2</sub>O<sub>3</sub>: A density functional theory study, *Journal of Catalysis* 272 (2010) 227-234.
- [25] A. Penkova, L. Bobadilla, S. Ivanova, M.I. Domínguez, F. Romero-Sarria, A.C. Roger, M.A. Centeno, J.A. Odriozola, Hydrogen production by methanol steam reforming on NiSn/MgO-Al<sub>2</sub>O<sub>3</sub> catalysts: The role of MgO addition, *Applied Catalysis A: General* 392 (2011) 184-191.
- [26] C.E. Quincoces, S. Dicundo, A.M. Alvarez, M.G. González, Effect of addition of CaO on Ni/Al<sub>2</sub>O<sub>3</sub> catalysts over CO<sub>2</sub> reforming of methane, *Materials Letters* 50 (2001) 21-27.
- [27] S.H.S. S.P. Santos, S.P. Toledo, Standard transition aluminas. Electron microscopy studies,, *Materials Research* 4 (2000) 104-114.
- [28] X. Sun, X. Zhang, Y. Zhang, N. Tsubaki, Reversible promotional effect of SiO<sub>2</sub> modification to Co/Al<sub>2</sub>O<sub>3</sub> catalyst for Fischer-Tropsch synthesis, *Applied Catalysis A: General* 377 (2010) 134-139.
- [29] S. Tada, T. Shimizu, H. Kameyama, T. Haneda, R. Kikuchi, Ni/CeO<sub>2</sub> catalysts with high CO<sub>2</sub> methanation activity and high CH<sub>4</sub> selectivity at low temperatures, *International Journal of Hydrogen Energy* 37 (2012) 5527-5531.
- [30] R.D.H. W.R. Dorner, R.D. Williams, W.F. Davis, D.H. Willauer, Influence of gas feed composition and pressure on the catalytic conversion of CO<sub>2</sub> to hydrocarbons using a traditional cobalt-based Fischer-Tropsch catalyst, *Energy & Fuels* 23 (2009) 4190-4195.
- [31] W.A. Wan Abu Bakar, R. Ali, A.A.A. Kadir, S.J.M. Rosid, N.S. Mohammad, Catalytic methanation reaction over alumina supported cobalt oxide doped noble metal oxides for the purification of simulated natural gas, *Journal of Fuel Chemistry and Technology* 40 (2012) 822-830.
- [32] R.S. Young, COBALT: Its Chemistry, Metallurgy and Uses, Reinhold Publishing Corporation, 1960.
- [33] J. Yu, Q. Ge, W. Fang, H. Xu, Influences of calcination temperature on the efficiency of CaO promotion over CaO modified Pt/Y-Al<sub>2</sub>O<sub>3</sub> catalyst, *Applied Catalysis A: General* 395 (2011) 114-119.
- [34] Y. Zhang, H. Xiong, K. Liew, J. Li, Effect of magnesia on alumina-supported cobalt Fischer-Tropsch synthesis catalysts, *Journal of Molecular Catalysis A: Chemical* 237 (2005) 172-181.

- [35] G. Zhi, X. Guo, Y. Wang, G. Jin, X. Guo, Effect of  $\text{La}_2\text{O}_3$  modification on the catalytic performance of Ni/SiC for methanation of carbon dioxide, *Catalysis Communications* 16 (2011) 56-59.
- [36] G. Zhou, T. Wu, H. Xie, X. Zheng, Effects of structure on the carbon dioxide methanation performance of Co-based catalysts, *International Journal of Hydrogen Energy* 38 (2013) 10012-10018.







APPENDIX

จุฬาลงกรณ์มหาวิทยาลัย  
**CHULALONGKORN UNIVERSITY**

## APPENDIX A

### CALCULATION FOR CATALYST PREPARATION

#### 1. Preparation of MgAl-modified alumina support

Preparation of magnesium and aluminium modified  $\text{Al}_2\text{O}_3$  supported  $\text{Co}/\text{Al}_2\text{O}_3$  catalysts with different loading (1, 2.5, 3.55 and 10 wt.%) of magnesium and aluminium nitrate in  $\gamma\text{-Al}_2\text{O}_3$  support are shown as follows:

<b>Element:</b>	Mg	Molecular weight	=	24.31	g/mol
	Al	Molecular weight	=	26.98	g/mol

Example calculation for the preparation of the 10%  $\text{MgAl}_2\text{O}_4$ -modified  $\text{Al}_2\text{O}_3$  support

$$\text{For using 1 g of } \text{Al}_2\text{O}_3; \text{ 10\%MgAl}_2\text{O}_4/\text{Al}_2\text{O}_3 = \frac{0.1 \text{ g of MgAl}_2\text{O}_4}{1 \text{ g of Al}_2\text{O}_3}$$

Based on 100 g of supports used, the composition of the modified support will be as follow:

$$\begin{aligned} \text{Magnesium required} &= \frac{(\text{MW of Mg})(\text{MgAl}_2\text{O}_4 \text{ required})}{(\text{MW of MgAl}_2\text{O}_4)} \\ &= \frac{(24.31 \text{ g/mol})(0.1\text{g})}{(142.27 \text{ g/mol})} \end{aligned}$$

$$= 0.01709 \text{ g of Mg required}$$

$$\text{Aluminium required} = \frac{(\text{MW of Al})(\text{MgAl}_2\text{O}_4 \text{ required})}{(\text{MW of MgAl}_2\text{O}_4)}$$

$$= \frac{(53.96 \text{ g/mol})(0.1\text{g})}{(142.27 \text{ g/mol})}$$

$$= 0.0379 \text{ g of Al required}$$

The amount of magnesium and aluminium required 0.01709 g and 0.0379 g, respectively, which prepared from the magnesium and aluminium precursor as  $\text{Mg}(\text{NO}_3)_2 \cdot 6\text{H}_2\text{O}$  and  $\text{Al}(\text{NO}_3)_3 \cdot 9\text{H}_2\text{O}$  which had the molecular weight of 256.41 g/mol and the molecular weight of  $\text{Al}(\text{NO}_3)_3 \cdot 9\text{H}_2\text{O}$  is 375.13 g/mol. Therefore, the amount of magnesium and aluminium precursor required can be calculated as follows:

Magnesium 0.01709 g was prepared from  $(\text{Mg}(\text{NO}_3)_2 \cdot 6\text{H}_2\text{O})$  in an aqueous solution

$$\text{Mg}(\text{NO}_3)_2 \cdot 6\text{H}_2\text{O} \text{ required} = \frac{(\text{MW of Mg}(\text{NO}_3)_2 \cdot 6\text{H}_2\text{O}) (\text{Mg required})}{(\text{MW of Mg})}$$

$$(256.41 \text{ g/mol})(0.01709\text{g})$$

$$(24.31 \text{ g/mol})$$

=

$$= 0.1803 \text{ g of Mg}(\text{NO}_3)_2 \cdot 6\text{H}_2\text{O}$$

Aluminium 0.0379 g was prepared from  $\text{Al}(\text{NO}_3)_3 \cdot 9\text{H}_2\text{O}$  in an aqueous solution

$$\begin{aligned} \text{Al}(\text{NO}_3)_3 \cdot 9\text{H}_2\text{O} \text{ required} &= \frac{(\text{MW of Al}(\text{NO}_3)_3 \cdot 9\text{H}_2\text{O})(\text{Al required})}{(\text{MW of Al})} \\ &= \frac{(375.13 \text{ g/mol})(0.0379\text{g})}{(26.98 \text{ g/mol})} \\ &= 0.527 \text{ g of Al}(\text{NO}_3)_3 \cdot 9\text{H}_2\text{O} \end{aligned}$$

## 2. Preparation of Mg-modified alumina support

Example calculation for the preparation of 2.5%Mg/ $\text{Al}_2\text{O}_3$

Based on 1 g of alumina support used, the composition of the support will be as follows:

$$\begin{aligned} \text{Magnesium} &= 0.025 \text{ g} \\ \text{Al}_2\text{O}_3 &= 1 - 0.025 \text{ g} = 0.975 \text{ g} \end{aligned}$$

Magnesium 0.025 g was prepared from  $\text{Mg}(\text{NO}_3)_2 \cdot 6\text{H}_2\text{O}$  and molecular weight of Mg is 24.31

$$\begin{aligned} \text{Mg}(\text{NO}_3)_2 \cdot 6\text{H}_2\text{O} \text{ required} &= \frac{(\text{MW of Mg}(\text{NO}_3)_2 \cdot 6\text{H}_2\text{O})(\text{Mg required})}{(\text{MW of Mg})} \\ &= \frac{(256.41 \text{ g/mol})(0.025\text{g})}{(24.31 \text{ g/mol})} \\ &= 0.2637 \text{ g of Mg}(\text{NO}_3)_2 \cdot 6\text{H}_2\text{O} \end{aligned}$$

### 3. Preparation of La-modified alumina support

Example calculation for the preparation of 2.5%La/Al<sub>2</sub>O<sub>3</sub>

Based on 1 g of alumina support used, the composition of the support will be as follows:

$$\begin{aligned} \text{Lanthanum} &= 0.025 \text{ g} \\ \text{Al}_2\text{O}_3 &= 1 - 0.025 \text{ g} = 0.975 \text{ g} \end{aligned}$$

Lanthanum 0.025 g was prepared from La(NO<sub>3</sub>)<sub>3</sub>·6H<sub>2</sub>O and molecular weight of La is 138.9

$$\begin{aligned} \text{La(NO}_3)_3 \cdot 6\text{H}_2\text{O required} &= \frac{(\text{MW of La(NO}_3)_3 \cdot 6\text{H}_2\text{O})(\text{La required})}{(\text{MW of La})} \\ &= \frac{(433.01 \text{ g/mol})(0.025\text{g})}{(138.9 \text{ g/mol})} \\ &= 0.07794 \text{ g of La(NO}_3)_3 \cdot 6\text{H}_2\text{O} \end{aligned}$$

### 4. Preparation of Ca-modified alumina support

Example calculation for the preparation of 2.5%Ca/Al<sub>2</sub>O<sub>3</sub>

Based on 1 g of alumina support used, the composition of the support will be as follows:

$$\begin{aligned} \text{Calcium} &= 0.025 \text{ g} \\ \text{Al}_2\text{O}_3 &= 1 - 0.025 \text{ g} = 0.975 \text{ g} \end{aligned}$$

Calcium 0.025 g was prepared from  $\text{Ca}(\text{NO}_3)_2 \cdot 4\text{H}_2\text{O}$  and molecular weight of Ca is 40.078

$$\begin{aligned} \text{Ca}(\text{NO}_3)_2 \cdot 4\text{H}_2\text{O} \text{ required} &= \frac{(\text{MW of Ca}(\text{NO}_3)_2 \cdot 4\text{H}_2\text{O})(\text{Ca required})}{(\text{MW of Ca})} \\ &= \frac{(236.15 \text{ g/mol})(0.025\text{g})}{(40.078 \text{ g/mol})} \\ &= 0.1473 \text{ g of Ca}(\text{NO}_3)_2 \cdot 4\text{H}_2\text{O} \end{aligned}$$

### 5. Preparation of $\text{Co}/\text{Al}_2\text{O}_3$ catalysts by incipient wetness impregnation

Example calculation for the preparation of 15% $\text{Co}/\text{Al}_2\text{O}_3$

Based on 1 g of alumina support used, the composition of the support will be as follows:

$$\begin{aligned} \text{Cobalt} &= 0.15 \text{ g} \\ \text{Al}_2\text{O}_3 &= 1 - 0.15 \text{ g} = 0.85 \text{ g} \end{aligned}$$

Cobalt 0.15 g was prepared from  $\text{Co}(\text{NO}_3)_2 \cdot 6\text{H}_2\text{O}$  and molecular weight of Co is 59

$$\begin{aligned} \text{Co}(\text{NO}_3)_2 \cdot 6\text{H}_2\text{O} \text{ required} &= \frac{(\text{MW of Co}(\text{NO}_3)_2 \cdot 6\text{H}_2\text{O})(\text{Co required})}{(\text{MW of Co})} \\ &= \frac{(292 \text{ g/mol})(0.15\text{g})}{(59 \text{ g/mol})} \\ &= 0.7424 \text{ g of Co}(\text{NO}_3)_2 \cdot 6\text{H}_2\text{O} \end{aligned}$$

## APPENDIX B

### CALCULATION OF THE CRYSTALLITE SIZE

Calculation of crystallite size was obtained from Scherrer equation

The average crystallite size of  $\text{Co}_3\text{O}_4$ , calculated from line broadening of  $\text{Co}_3\text{O}_4$  at  $2\theta = 37^\circ$  diffraction peak using the Scherrer's equation.

From Scherrer equation:

$$D = \frac{K\lambda}{\beta \cos \theta}$$

Where

- $D$  = Crystallite size, Å
- $K$  = Crystallite-shape factor = 0.9
- $\lambda$  = X-ray wavelength, 1.54056 Å for  $\text{CuK}\alpha$
- $\theta$  = Observed peak angle, degree
- $\beta$  = X-ray diffraction broadening, radian

The X-ray diffraction broadening ( $\beta$ ) is the pure width of powder diffraction free of all broadening due to the experimental equipment. Standard  $\alpha$ -alumina is used to observe the instrumental broadening since its crystallite size is larger than 2000 Å.

The X-ray diffraction broadening ( $\beta$ ) can be obtained by using Warren's formula.

From Warren's formula:

$$\beta^2 = B_M^2 - B_S^2$$

$$\beta = \sqrt{B_M^2 - B_S^2}$$

Where  $B_M$  = The measured peak width in radians at half peak height.

$B_S$  = The corresponding width of a standard material.

Example: The average crystallite size calculation of  $\text{Co}_3\text{O}_4$  on alumina support

$$\begin{aligned} \text{The half-height width of peak} &= A-B = 0.72^\circ \text{ (from Figure B.1)} \\ &= (0.017444 \times 0.72) \\ &= 0.01256 \text{ radian} \end{aligned}$$

The corresponding half-height width of peak of  $\alpha$ -alumina = 0.00074 radian

$$\begin{aligned} \text{The pure width} &= \sqrt{B_M^2 - B_S^2} \\ &= \sqrt{0.01256^2 + 0.00074^2} \\ &= 0.012538 \text{ radian} \end{aligned}$$

$$\begin{aligned} B &= 0.012538 \\ 2\theta &= 37.0^\circ \\ \theta &= 18.5^\circ = 0.3227 \text{ radian} \end{aligned}$$

$$\begin{aligned} \lambda &= 1.54056 \text{ \AA} \\ \text{The crystallite size} &= \frac{0.9 \times 1.54056}{(0.012538) \cos 0.3227} \\ &= 116.6029 \text{ \AA} \\ &= 11.7 \text{ nm} \end{aligned}$$



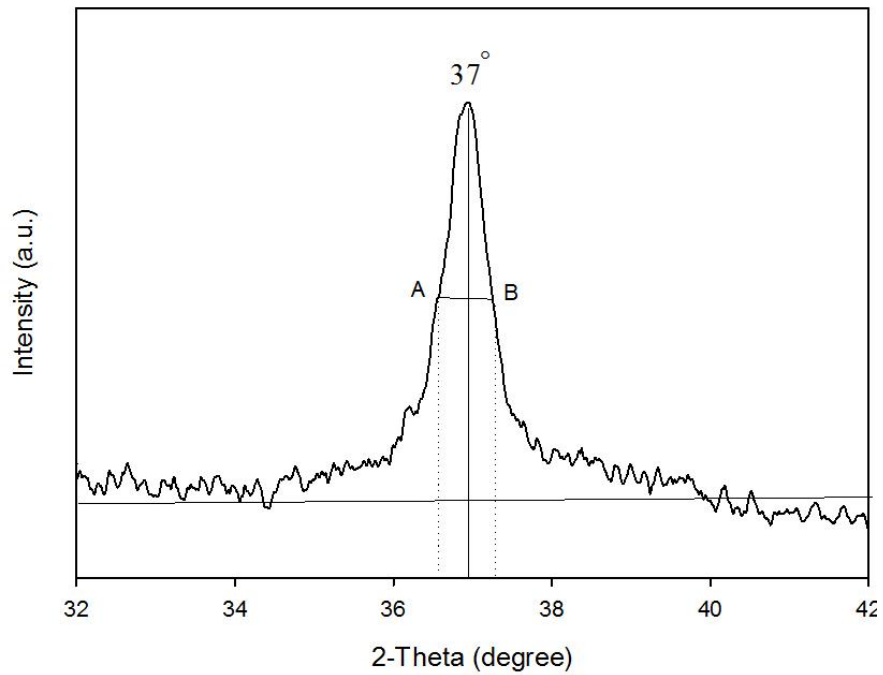


Figure B.1 The measured peak of Co/Al<sub>2</sub>O<sub>3</sub> to calculate the crystallite size.

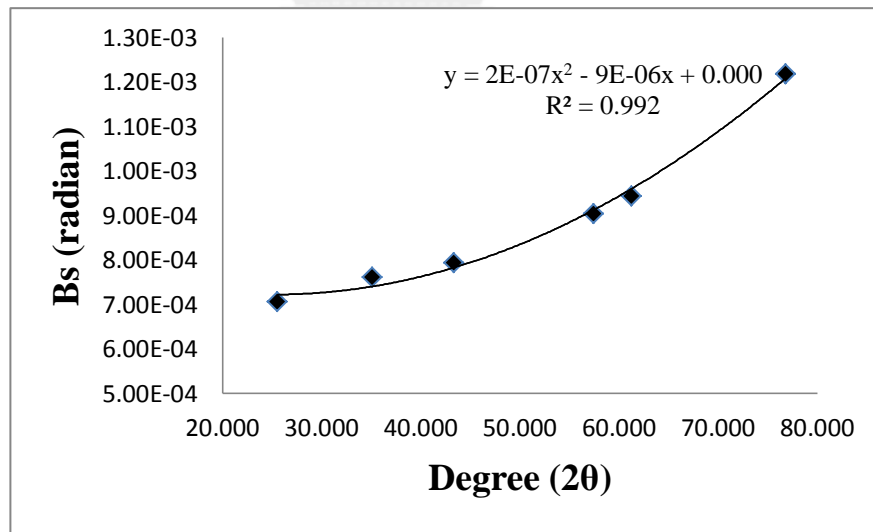


Figure B.2 The plot indicating the value of line broadening due to the equipment. The data were obtained by using  $\alpha$ -alumina as standard.

## APPENDIX C

### CALCULATION FOR TOTAL H<sub>2</sub> CHEMISSORPTION

Calculation of the total H<sub>2</sub> chemisorption and metal dispersion on the surface of catalysts, which a stoichiometry of H/Co = 1, measured by H<sub>2</sub> chemisorption is as follows:

Let the weight of catalyst used	=	W	g
Loop volume dosed	=	V <sub>loop</sub>	μL
Area of H <sub>2</sub> peak after adsorption	=	A <sub>i</sub>	unit
Area of 100 μL of standard H <sub>2</sub> peak	=	A <sub>f</sub>	unit
Molar volume of gas at STP	=	22414	cm <sup>3</sup> /mol
%Metal	=	%M	%
Molecular weight of the metal	=	m.w.	a.m.u.
Avogadro's number	=	6.023 × 10 <sup>23</sup>	molecules/mol
Amount of H <sub>2</sub> adsorbed on catalyst	=	$\frac{V_{loop} \times \sum(A_f - A_i)}{(W \times A_f)}$	= A μL/g <sub>cat</sub>
Amount of H <sub>2</sub> adsorbed on catalyst	=	A/1000	= B cm <sup>3</sup> /g <sub>cat</sub>
Mole of H <sub>2</sub> adsorbed on catalyst	=	B/V <sub>g</sub>	mol/ g <sub>cat</sub>
Molecule of H <sub>2</sub> adsorbed on catalyst	=	2 × moleH <sub>2</sub> × 6.023 × 10 <sup>23</sup>	
Mole of cobalt	=	(W × %M/100)/ m.w.	
%Dispersion	=	(S <sub>f</sub> × mole <sub>H<sub>2</sub></sub> /mole <sub>cobalt</sub> ) × 100	%

## APPENDIX D

### CALIBRATION CURVES

This appendix presented the calibration curves for calculation of composition of reactant and products in the carbon dioxide hydrogenation reaction. The reactant in carbon dioxide hydrogenation reaction is  $\text{CO}_2$  while the main product is methane and the by-product is carbon monoxide. Furthermore, the other products are linear hydrocarbons of heavier molecular weight including ethane propane, butane. However, there are present in little quantity.

The composition of gas in the product stream from the reactor were analyzed by gas chromatograph equipped with a thermal conductivity detector (TCD)

Mole of reagent presented in y-axis and x-axis showed the area, which reported by gas chromatography. The calibration curves for calculation of composition of  $\text{CO}_2$ ,  $\text{CH}_4$  and  $\text{CO}$  are presented in following figures.

Table D.1 Conditions used in shimadzu model GC-8A.

Parameters	Condition
	Shimadzu GC-8A
Width	5
Slope	50
Drift	0
Min. area	10
T.DBL	0
Stop time	12
Atten	5
Speed	3
Method	1
Format	1
SPL.WT	100
IS.WT	1

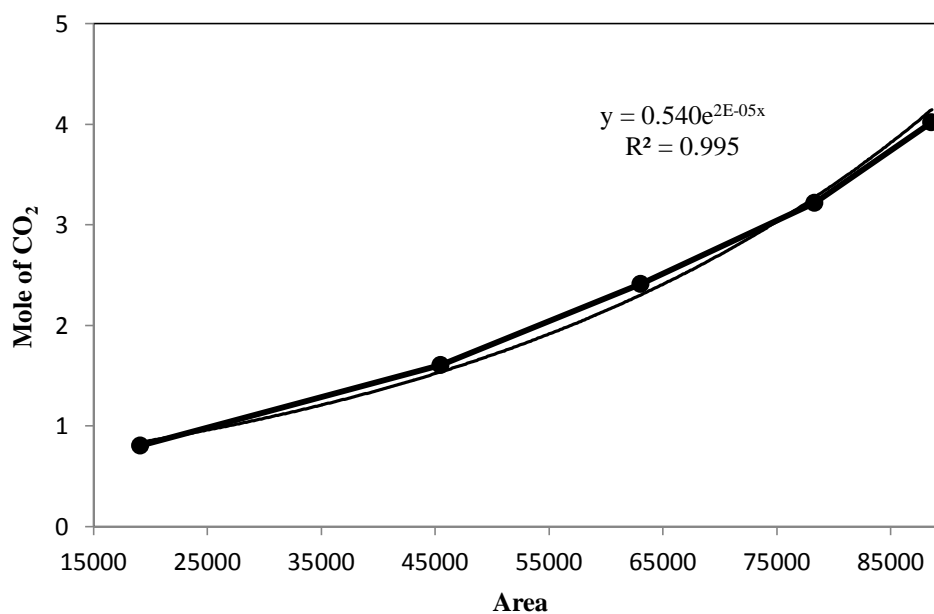


Figure D.1 The calibration curves of carbon dioxide.

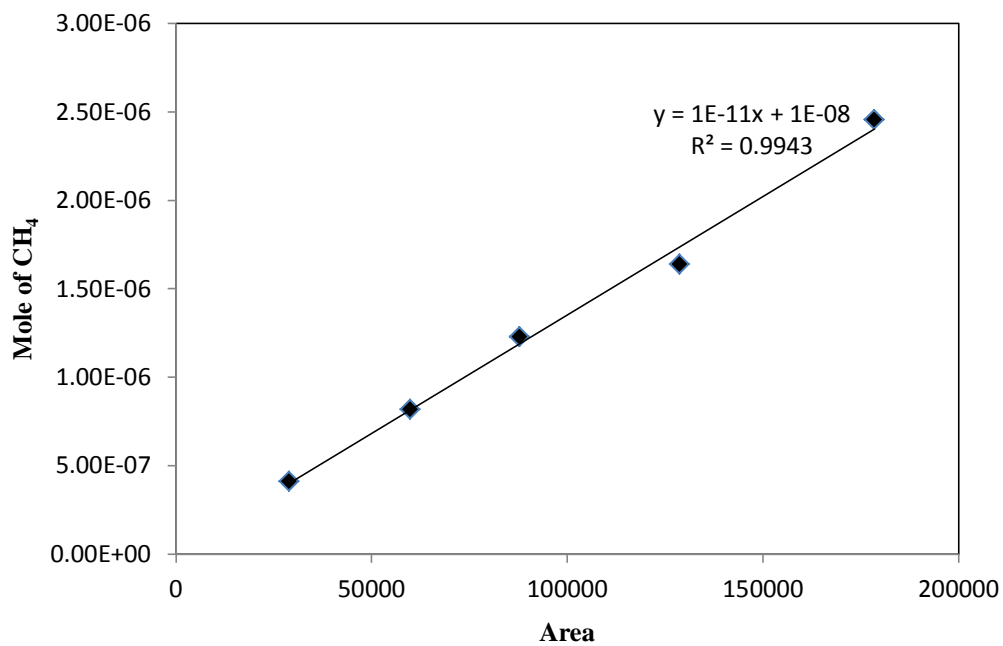


Figure D.2 The calibration curves of methane.

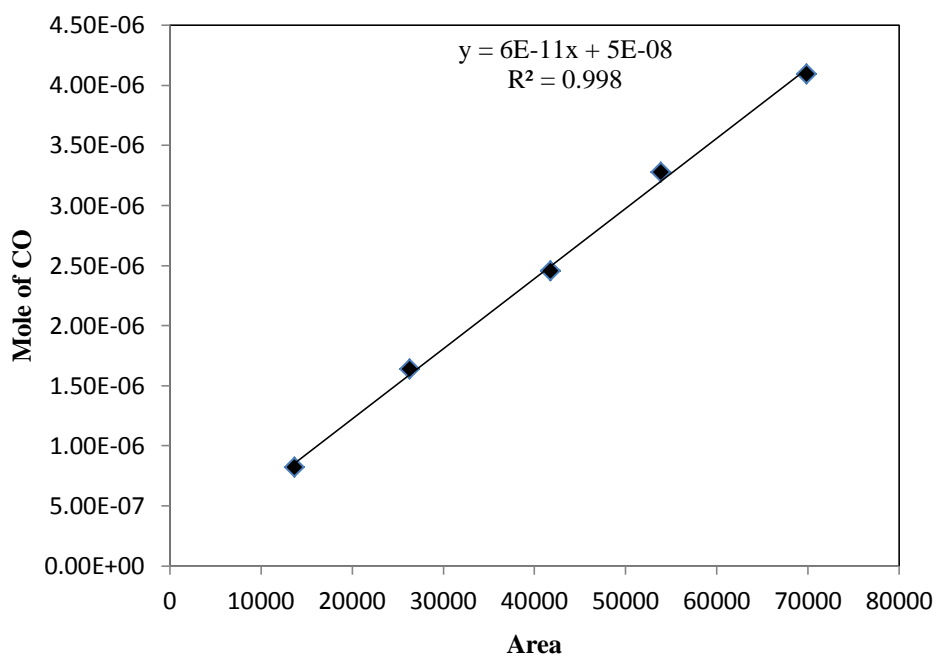


Figure D.3 The calibration curves of carbon monoxide.

## APPENDIX E

### CALCULATION OF CO<sub>2</sub> CONVERSION AND SELECTIVITY

The catalysts performance for the carbon dioxide hydrogenation reaction was evaluated in terms of activity for carbon dioxide conversion and selectivity.

Catalytic activity of catalyst was performed in term of conversion of CO<sub>2</sub>, which is defined as moles of carbon dioxide converted with respect to carbon dioxide in feed.

$$\text{CO}_2 \text{ conversion (\%)} = \frac{\text{Mole of CO}_2 \text{ in feed} - \text{mole of CO}_2 \text{ in product}}{\text{Mole of CO}_2 \text{ in feed}} \times 100$$

Selectivity of product (B) is defined as mole of product (B) formed with related to mole of carbon dioxide converted:

$$\text{CO}_2 \text{ conversion (\%)} = \frac{\text{Mole of product B formed}}{\text{Mole of total products}} \times 100$$

Where

B = product

Mole of product (B) can be measured employing from calibration curve of products including methane and carbon monoxide.

## VITA

Ms. Pornrawee Somkua was born on 13 March 1988, in Suratthani, Thailand. She received her Bachelor degree of Chemical Engineering from Rajamangala University of Technology Thanyaburi, Thailand in March 2011. Since May 22, 2012, she has been studying for her Master degree of Engineering from the department of Chemical Engineering, Chulalongkorn University.

List of publication:

Pornrawee Somkua and Joongjai Panpranot, "CO<sub>2</sub> HYDROGENATION OVER BASIC OXIDE-MODIFIED Al<sub>2</sub>O<sub>3</sub> SUPPORTED COBALT CATALYSTS", Proceeding of the 3rd International Thai Chemical Engineering and Applied Chemistry Conference, Khon Kaen, Thailand, October 17-18, 2013.